A thesis on

Point defects in some body-centred cubic transition metals

by D. E. Peacock

submitted for the Degree of Doctor of Philosophy in the University of London.

Department of Metallurgy,
Imperial College of Science and Technology,
Prince Consort Road,
London S.W.7.

August, 1961.

ABSTRACT

The electrical resistivity of some irradiated and cold-worked body-centred cubic transition metals has been investigated. Data on the increase in resistivity, $\Delta\rho$, of molybdenum irradiated in BEPO at 40°C can be fitted to the equation

$$\Delta\rho = 0.071\ t^{0.54}\ \mu\Omega\,\text{cm.},$$

where t is the irradiation time in months. About 55 per cent of the extra resistivity due to irradiation was found to anneal out in a well-defined recovery stage between 100 and 200°C with an activation energy of 1.25 ±0.08 eV. These results are in agreement with earlier observations by Kinchin and Thompson[17]. New results have been obtained on the magnitude of the recovery, $\Delta\rho$, which passes through a maximum when considered as a function of irradiation time.

On annealing niobium irradiated under the same conditions, a major recovery stage was observed between 80 and 160°C with an activation energy of 1.22 ±0.02 eV. The resistivity recovery during this process also passes through a maximum.

Experiments on niobium and tantalum plastically deformed in tension at room temperature have also revealed a recovery process between 80 and 180°C, with an activation energy of 1.22 ±0.02 eV in niobium and 1.25 ±0.02 eV in tantalum. The relationship between the resistivity recovery, $\Delta\rho$, and the fractional tensile strain, ε , was found to be

$$\Delta\rho = 0.77\,\varepsilon^{1.46}\ \mu\Omega\,\text{cm.} \quad \text{for niobium}$$

and $$\Delta\rho = 2.01\,\varepsilon^{1.41}\ \mu\Omega\,\text{cm.} \quad \text{for tantalum.}$$

The recovery of niobium with a higher initial dislocation density was much greater for comparable strains but tended to become constant after heavy deformation, the corresponding relationship being

$$\Delta\rho = 0.45\,\varepsilon^{0.66}\ \mu\Omega\,\text{cm.}$$

All these results are discussed in terms of current point defect theories and it is concluded that the major recovery process observed in all these materials is due to the migration of vacant lattice sites created during irradiation or plastic deformation and that the process corresponds to Stage III recovery in the face-centred cubic metals.

TABLE OF CONTENTS

Page No.

Title Page . . . . . 1.
Abstract . . . . . 2.
Table of Contents . . . . . 4.
List of Figures . . . . . 6.
List of Tables . . . . . 8.

1 INTRODUCTION

1.1 Equilibrium Concentrations of Point Defects in Metals . . . . . 9.
1.2 Non-Equilibrium Concentrations of Point Defects . . . . . 12.
1.2.1 The introduction of point defects by quenching . . . . . 12.
1.2.2 The generation of point defects by plastic deformation . . . 13.
1.2.3 The generation of point defects by irradiation . . . . . 23.
1.3 The Migration of Point Defects . . . . . 32.
1.4 The Annihilation of Point Defects . . . . . 37.
1.4.1 The disappearance of point defects at fixed sinks . . . . . 38.
1.4.2 The disappearance of point defects by mutual annihilation and aggregation . . . . . 40.
1.5 Previous Work on Point Defects in the Body-Centred Cubic Transition Metals . . . . . 48.
1.5.1 Experiments on irradiated materials . . . . . 48.
1.5.2 Experiments on plastically deformed materials . . . . . 54.
1.5.3 Theoretical studies . . . . . 56.
1.6 Selection of Experiments . . . . . 59.

2 EXPERIMENTAL PROCEDURE

2.1 Preparation of Specimens . . . . . 65.
2.2 Measurement of Resistance . . . . . 71.
2.3 Methods of Annealing . . . . . 76.
2.3.1 Isochronal annealing procedure . . . . . 78.
2.3.2 Isothermal annealing procedure . . . . . 78.

3 RESULTS

3.1 Irradiated Molybdenum . . . . . 81.
3.2 Irradiated Niobium . . . . . 83.
3.3 Cold-Worked Niobium . . . . . 84.
3.4 Cold-Worked Tantalum . . . . . 86.

4 DISCUSSION

Page. No.

4.1 The Increase in Resistivity of Molybdenum on Irradiation . . . 120.

4.2 The Resistivity Recovery of Irradiated Molybdenum and Niobium . . . . . 122.

4.3 The Resistivity Recovery of Cold-Worked Niobium and Tantalum . . . . . 127.

Conclusions . . . . . 131.

Suggestions for Future Work . . . . . 136.

Acknowledgements . . . . . 139.

References . . . . . 140.

LIST OF FIGURES

		Page No.
1.	A schematic representation of the free energy of a solid as a function of the fraction of vacant lattice sites	11.
2.	The generation of point defects by the intersection of two screw dislocations	14.
3.	The formation of a row of vacancies by the combination of two edge dislocations of opposite sign on neighbouring slip planes . .	17.
4.	Jogs on a dislocation line	18.
5.	A schematic representation of collision types for atoms of a metal moving in their own lattice	27.
6.	A cascade of displacements produced by a primary and secondary knock-ons after a fast neutron collision	29.
7.	The unstable intermediate stage in the formation of a displacement spike according to Brinkman	30.
8.	An edge dislocation with a bound vacancy and a jog	38.
9.	Stages in the absorption of a point defect by a screw dislocation	39.
10.	The vacancy or coilion configuration in a body-centred cubic transition metal	58.
11.	Circuit used for resistance measurements	71.
12.	Circuit diagram of the Diesselhorst potentiometer	73.
13.	Increase in resistivity as a function of irradiation time for molybdenum irradiated in BEPO at 40°C	96.
14.	Graph showing the linear relationship between log.$\Delta\rho$ and log.t for irradiated molybdenum using the data of Fig. 13	97.
15.	Isochronal annealing curves for irradiated molybdenum	98.
16.	$\frac{\Delta R_f}{\Delta T}$ plotted against T for irradiated molybdenum using the data of Fig. 15	99.
17.	Resistivity recovery between 40 and 180°C as a function of irradiation time for molybdenum and niobium irradiated in BEPO at 40°C	100.
18.	Isothermal annealing curves for irradiated molybdenum	101.
19.	The relationship between R_f and log. $\frac{\Delta R_f}{\Delta t}$ for irradiated molybdenum using the data of Fig. 18	102.
20.	Isochronal annealing curves for irradiated niobium	103.

Page No.

21. $\frac{\Delta R_f}{\Delta T}$ plotted against T for irradiated niobium using the data of Fig. 20 . . . . . 104.

22. Isothermal annealing curves for irradiated niobium . . . . . 105.

23. Isothermal annealing curves for irradiated niobium . . . . . 106.

24. The relationship between R_f and log. $\frac{\Delta R_f}{\Delta t}$ for irradiated niobium using the data of Fig. 22 . . . . . 107.

25. The relationship between R_f and log. $\frac{\Delta R_f}{\Delta t}$ for irradiated niobium using the data of Fig. 23 . . . . . 108.

26. Isochronal annealing curves for cold-worked niobium . . . . . 109.

27. $\frac{\Delta R_f}{\Delta T}$ plotted against T for cold-worked niobium and tantalum using data from Figs. 26 & 33 . . . . . 110.

28. Resistivity recovery between 20 and 180°C as a function of tensile strain for niobium and tantalum deformed at 20°C . . . . 111.

29. Graph showing the linear relationship between log.$\Delta\rho$ and log.ε for cold-worked niobium and tantalum using the data of Fig. 28. . . . . 112.

30. Isothermal annealing curves for cold-worked niobium . . . . . 113.

31. The relationship between R_f and log. $\frac{\Delta R_f}{\Delta t}$ for cold-worked niobium using the data of Fig. 30 . . . . . 114.

32. 100°C isothermal annealing curves for niobium showing the difference in initial recovery behaviour between irradiated and cold-worked specimens . . . . . 115.

33. Isochronal annealing curves for cold-worked tantalum . . . . . 116.

34. Isothermal annealing curves for cold-worked tantalum . . . . . 117.

35. The relationship between R_f and log. $\frac{\Delta R_f}{\Delta t}$ for cold-worked tantalum using the data of Fig. 34 . . . . . 118.

36. Activation energies for self-diffusion and vacancy migration as functions of melting temperature for some metallic elements . 119.

LIST OF TABLES

Page No.

1. Concentrations of point defects expected as a result of plastic deformation . . . . . 22.
2. Recovery stages observed in molybdenum and tungsten after neutron irradiation at -196°C. (After Kinchin and Thompson[17].) . . . 49.
3. Recovery stages observed in tungsten after neutron irradiation at 4°K. (After Thompson[39].) . . . . . 50.
4. Recovery stages observed in pure and impure tungsten after plastic deformation at room temperature. (After Neimark and Swalin[50].) 55.
5. The formation and migration energies of a vacancy in α-iron and tungsten. (After Brooks[52].) . . . . . 57.
6. The formation and migration energies of the self-ions in several body-centred cubic transition metals. (After Shaw[53].) . . . . . 59.
7. The body-centred cubic transition metals and some of their physical properties . . . . . 60.
8. Nominal chemical analyses of the molybdenum, niobium and tantalum used in the investigation . . . . . 65.
9. List of irradiated specimens prepared and their subsequent annealing treatments . . . . . 68.
10. List of cold-worked specimens prepared and their subsequent annealing treatments . . . . . 69.
11. Data on the increase in resistivity of molybdenum on irradiation . 88.
12. Data on the resistivity recovery of irradiated molybdenum . . . . . 89.
13. Data on the resistivity recovery of irradiated niobium . . . . . 90.
14. Resistivity recovery on annealing cold-worked niobium and tantalum between 20 and 180°C . . . . . 91.
15. Activation energies and numbers of jumps to annihilation associated with the recovery processes observed in the temperature range 80 to 180°C in irradiated molybdenum and niobium . . . . . 92.
16. Activation energies and numbers of jumps to annihilation associated with the recovery processes observed in the temperature range 80 to 180°C in cold-worked niobium and tantalum . . . . . 93.
17. Experimental self-diffusion activation energies for some metallic elements . . . . . 94.
18. Measured vacancy formation and migration energies for some f.c.c. and b.c.c. metals . . . . . 95.

1 INTRODUCTION

1.1 Equilibrium Concentrations of Point Defects in Metals

Imperfections in metallic crystals are usually classified according to their dimensions, that is, as surface, line and point defects. Examples of surface defects are high and low angle grain boundaries, twin boundaries and stacking faults. The most common type of line defect is the dislocation, examples of which are edge, screw and partial dislocations. Point defects include vacant lattice sites or vacancies, interstitial atoms, impurity atoms and combinations of these such as divacancies, trivacancies and vacancy-impurity atom pairs. Surface and line defects always tend to anneal out with increasing temperature but point defects, apart from impurity atoms, are unusual in that they can exist in thermodynamic equilibrium in a crystal.

According to thermodynamics, the equilibrium state of a solid, under low external pressure and at an absolute temperature T, is determined by the minimum value of the Helmholtz free energy F, given by

$$F = E - TS \quad , \qquad (1)$$

where E is the internal energy and S the total entropy of the solid. It can be shown that this condition leads necessarily to the existence of a certain amount of disorder in a crystal lattice at all temperatures above absolute zero. Suppose, for example, that in a perfect metallic crystal a number of vacancies are produced by transferring atoms from the interior to the surface of the crystal. This requires a certain

amount of energy, that is, both E and F increase. On the other hand, the presence of vacancies introduces disorder into the lattice, which increases the configurational entropy of the crystal from zero to a value determined by the number of vacancies present, and this reduces F. The configurational entropy S_c is given by the Boltzmann relationship

$$S_c = k \ln W_c , \tag{2}$$

where k is Boltzmann's constant and W_c is the number of ways in which N atoms and n vacancies can be arranged over (N + n) lattice sites. Hence,

$$W_c = \frac{(N + n)!}{N!\, n!} \tag{3}$$

and

$$S_c = k \ln \left[\frac{(N + n)!}{N!\, n!} \right] . \tag{4}$$

In addition, the presence of vacancies increases the thermal entropy of the crystal, since the vibrational frequency of the atoms in the vicinity of a vacancy is reduced. The result of this competition between energy and entropy is that, under equilibrium conditions, that is, with F a minimum, the crystal contains a certain number of vacant lattice sites at all temperatures $T > 0$. A schematic representation of F as a function of the fraction n/N is shown in Figure 1. For the sake of simplicity it has been assumed that the thermal entropy is independent of n/N.

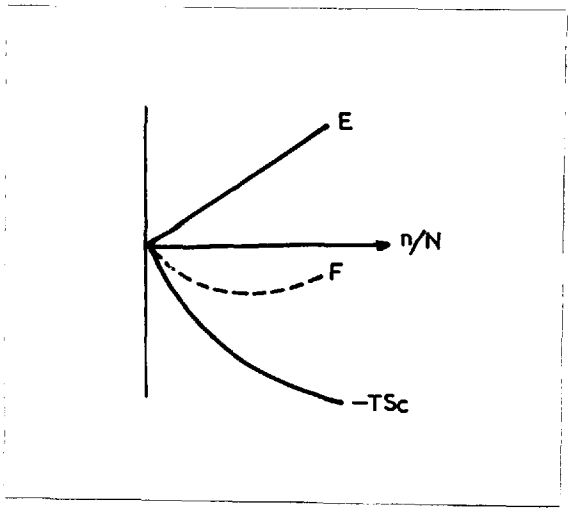


Fig. 1 A schematic representation of the energy E and the configurational entropy term $-TS_c$ as functions of the fraction of vacant lattice sites n/N. The minimum value of the free energy F determines the equilibrium value of n/N. (After Dekker1)

In order to calculate the number of vacancies n present at any particular temperature T, an expression is required for the free energy of the crystal at that temperature. This is given by

$$F(n,T) = F(\text{perfect},T) + nE_f - nT\Delta S_t - kT\ln\left[\frac{(N+n)!}{N!\,n!}\right], \qquad (5)$$

where F(perfect, T) is the free energy of the crystal at temperature T with no vacancies present, E_f is the energy required to create a vacancy and ΔS_t is the increase in thermal entropy due to the presence of a vacancy. In equilibrium, $(\partial F/\partial n)_T = 0$ and employing Stirling's formula in the form $\ln x! \simeq x \ln x$ for $x \gg 1$, we find from (5)

$$n / (N+n) = e^{\Delta S_t / k} \; e^{-E_f/kT} \quad . \qquad (6)$$

Hence the concentration of vacancies at any temperature can be calculated if ΔS_t and E_f are known. Other types of point defects can be treated similarly and it is possible to obtain similar expressions for their equilibrium concentrations.

1.2 Non-Equilibrium Concentrations of Point Defects.

Although it is possible to study point defects by following changes in properties with temperature, most information has been obtained by producing non-equilibrium concentrations of point defects and then carrying out annealing experiments in which the concentrations of defects fall towards their equilibrium values. The three methods most extensively used to introduce non-equilibrium concentrations of point defects are those of quenching, plastic deformation and irradiation and these will now be considered separately.

1.2.1 The introduction of point defects by quenching

In the quenching method use is made of the fact that near its melting temperature a metal contains a relatively high concentration of point defects compared with that at room temperature, the actual concentration of any species depending on the formation energy E_f, the entropy ΔS_t and the temperature T, as described in the previous section. If the metal is cooled sufficiently rapidly from this high temperature to a low one, in practice usually room temperature, it is possible that defects present at the high temperature will be retained

in the lattice and their presence can be detected by measuring a suitable property of the metal before and after quenching. If only one species of point defect is present and if the relationship between the change in the property measured and the number of defects n present is known, it is possible to determine E_f by quenching from a series of temperatures and measuring the slope of the graph obtained by plotting log n as a function of 1/T, where T is the quenching temperature. This will almost certainly be a straight line for the possible experimental range of quenching temperatures. For the noble face-centred cubic metals it is almost certain that the lattice vacancy is the only species of point defect present in thermal equilibrium in any appreciable quantity and hence for these metals E_f found by the above method will almost certainly refer to the formation energy of that type of defect. This is probably also true for the body-centred cubic transition metals.

1.2.2 The generation of point defects by plastic deformation

Many mechanisms have been proposed by which point defects may be produced by plastic deformation or, more specifically, by the movement of dislocations during plastic flow, but at the present time the relative importance of these methods and the types and numbers of defects produced are not known with any certainty. Seitz [2] has listed and discussed in some detail four possible causes of point defect formation during plastic flow. These are:

(i) Local heating of the lattice in the immediate vicinity of a dislocation as it moves through the lattice and absorbs energy from the applied stress field.

(ii) Instability in the in-phase motion of atoms during the passage of a dislocation. For example, it is possible that incipient vacancies are occasionally torn loose from a jog in a dislocation line because of a local disturbance in the lattice.

(iii) Large transient thermal pulses in regions where dislocations annihilate one another and produce large lattice disturbances.

(iv) Purely geometric interaction of dislocations.

The last method appears to have received the greatest attention. For example, the idea that the intersection of two screw dislocations may produce point defects is now fairly well agreed on and is shown schematically in Figure 2.

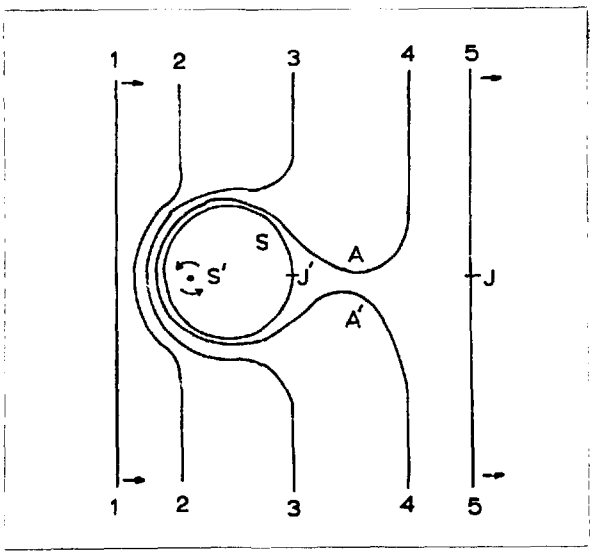


Fig. 2 The generation of point defects by the intersection of two screw dislocations. (After Seitz [2])

S' represents the intersection of a stationary screw dislocation with the slip plane in which another screw dislocation is moving. The line of the moving screw is indicated at successive positions during motion by 1, 2, 3, 4 and 5. Initially, the moving line lies entirely in a single slip plane. However, after looping around the stationary dislocation and leaving a closed segment behind, it possesses a jog J, on either side of which it lies on different slip planes. The ring left behind will also have a jog J'. The segments A and A', which are shown just before combining, move on neighbouring slip planes and have the character of edge dislocations. Hence a row of interstitial atoms or vacant lattice sites will be produced when A and A' meet, the type of defect produced depending on the sign of the intersected dislocation. The distribution of point defects produced in this way is not clear but the usual argument is that the dislocation line is held back by the jog, forming a cusp which keeps the jog moving along a straight line, so that the point defects are deposited in a row. However, both Hasiguti[3] and Damask and Dienes[4] suggest that a row of vacancies is unstable and will tend to break up into clusters and isolated defects.

Taking the crystal as a whole it is not certain whether vacancies or interstitials will be produced preferentially or whether they will arise in roughly equal numbers. It has been suggested that few interstitials are formed because of their large formation energy but Seeger[5] considers this argument to be invalid because, by the same argument, the total dislocation length of a crystal would not increase

during cold-work, contrary to well-known experimental facts. Cottrell[6] has pointed out that when two systems of moving dislocations meet and intersect, that is, under multiple slip conditions, the screw-screw intersections are more likely to produce interstitials than they are vacancies. This is because a dislocation which creates a jog which produces vacancies tends to move in the same direction as the intersecting dislocation whereas that which creates a jog which produces interstitials tends to move in the opposite direction. This favours the creation of interstitials. When one set of dislocations is anchored, for example, under single slip conditions, this argument does not apply and Seeger[5] suggests that in this case the jogs creating interstitials will lag behind those creating vacancies, on account of the larger formation energy of the former, but that this will not change the order of magnitude of the number of interstitials created. Friedel[7] takes the extreme view that there is no reason why the jog, whether interstitial or vacancy producing, should not glide along the screw without creating point defects and attach itself to an edge component of the dislocation line. Recently Mott[8] reported on work done by Hirsch who, by examining the geometry of large jogs and extrapolating their properties to those of atomic dimensions, was led to the conclusion that a vacancy producing jog will move with the creation of a row of vacancies more easily than it will move sideways along the screw, since the latter has a large stress-independent activation energy. On the other hand, an interstitial producing jog will normally move sideways because this process requires a smaller, stress-dependent activation energy.

It has also been proposed that the coalescence of two edge dislocations of opposite sign on neighbouring slip planes will produce a row of point defects, either vacancies or interstitials. The mechanism is shown schematically in Figure 3 for the case where vacancies are produced.

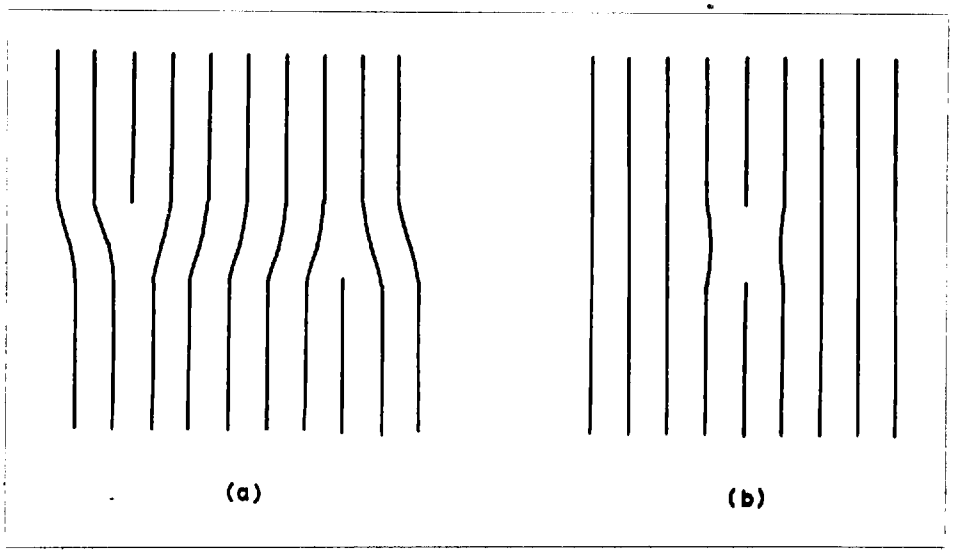


Fig. 3 (a) Two edge dislocations of opposite sign on neighbouring slip planes. (b) These have combined to form a row of vacancies.

Friedel[7] favours this coalescence method of point defect production. He suggests that the two arms of a Frank-Read source may often lie on neighbouring slip planes and that when they coalesce at the end of each cycle of operation of the source a line of point defects is produced. Cottrell[9] has proposed a similar mechanism whereby a closed dislocation ring containing jogs contracts to form a line of point defects. This is shown schematically in Figure 4.

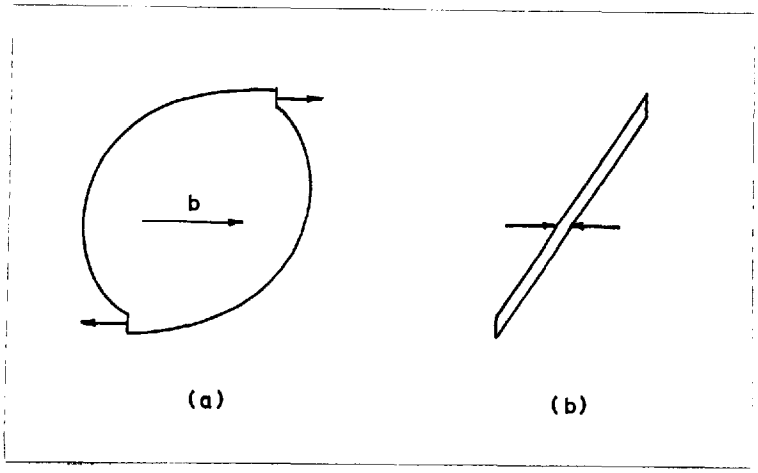


Fig. 4 Jogs on a dislocation line of Burgers vector b. (After Cottrell.[9])

If the ring is expanding, as in (a), the jogs can glide in the directions shown without producing point defects. If the ring is contracting, as in (b), as far as possible the jogs glide backwards without producing point defects but when the ring finally disappears a line of point defects must form between the residual jogs.

Quantitative predictions regarding the production of point defects during plastic flow are in a very unsatisfactory state, partly because the mechanism of their formation is so uncertain and partly because any quantity arrived at depends on the validity of the model of dislocation generation and movement used to describe plastic flow.

Van Bueren[10] has proposed an "energy barrier" model in which he considers a number of independent Frank-Read sources emitting concentric, circular dislocation loops. As long as the influence of the surface can be neglected, each loop contributes to the strain in proportion to its area whereas the dislocation length increases in proportion to its radius. Therefore, per loop,

$$D \quad \alpha \quad \varepsilon^{1/2}, \qquad (7)$$

where D is the newly generated dislocation density and ε is the plastic strain due to each loop. Since the number of loops increases with time and the expansion does not go on indefinitely, this relationship does not apply to the material as a whole. Taking this and also the production of point defects into account and balancing the strain energy gained by expanding against the energy stored in the form of an ever increasing number of lattice imperfections, van Bueren finds the relationship between the overall dislocation density and plastic strain, under single slip conditions, to be

$$D \quad \alpha \quad \varepsilon^{3/4} . \qquad (8)$$

When multiple slip occurs and the newly formed dislocations interact with each other the relationship becomes

$$D \quad \alpha \quad \varepsilon . \qquad (9)$$

For each expanding loop the number of jogs produced is proportional to the number of intersected dislocations and thus to the area of the loop. The number of vacancies and interstitials left in the wake of these jogs is again proportional to the radius of the loop. Therefore, per loop,

$$n \quad \alpha \quad \varepsilon^{3/2} , \qquad (10)$$

where n is the number of defects formed. By again taking into account the formation of new loops and the energy balance van Bueren finds the relationship between the number of defects produced and the strain, for

the material as a whole and under single slip conditions, to be

$$n \quad \alpha \quad \varepsilon^{5/4} \quad . \qquad (11)$$

For multiple slip conditions the relationship becomes

$$n \quad \alpha \quad \varepsilon^{2} \qquad (12)$$

Van Bueren[10] reports that Haasen and Leibfried and Friedel have considered the presence of "fixed barriers" in the material which confine the expansion of the loops to a certain maximum radius. The number of loops per source is then also limited because the back stress exerted by the emitted loops ultimately stops the source. This "fixed barrier" model leads to a dependence of dislocation density on strain such that

$$D \quad \alpha \quad \varepsilon \quad . \qquad (13)$$

On this model both the moving jog and dislocation coalescence mechanisms of point defect generation lead to a dependence of point defect production on strain such that

$$n \quad \alpha \quad \varepsilon \quad . \qquad (14)$$

Both Seitz[2] and Mott[11] have also proposed this relationship.

Seeger[12] has considered the case where the limiting distance a loop may expand depends on the dislocation density. He argues that as the barriers are formed by the mutual interaction of dislocations

they become more numerous as the deformation proceeds. This "growing barrier" model gives the following relationship between dislocation density and strain :

$$D \quad \alpha \quad a(\varepsilon - \varepsilon^*) + b(\varepsilon - \varepsilon^*)^2, \qquad (15)$$

where a and b are constants and $\varepsilon \gg \varepsilon^*$. Van Bueren[10] considers that the number of point defects produced on this model depends very sensitively on the mechanism of production. Briefly, the moving jog mechanism leads to the relationship

$$n \quad \alpha \quad \log(\varepsilon - \varepsilon^*) \qquad (16)$$

and the coalescence mechanism leads to the relationship

$$n \quad \alpha \quad (\varepsilon - \varepsilon^*)^2. \qquad (17)$$

The actual number of defects produced on any of the above theories will depend upon the initial dislocation density of the material and, in practice, the deformation must be carried out at a temperature at which all the defects produced are immobile and retained unchanged in the lattice, if a comparison between theory and experiment is to be possible. Further, these theories ignore the possibility that defects might be removed from the lattice by dislocations moving over slip planes containing them. In addition, since it is well known that at high strains the dislocation density tends to saturate, it is to be expected that the number of defects produced will tend to saturate also. Only Seeger's model of plastic flow, when used in

conjunction with the moving jog mechanism of point defect production, predicts this. Finally, it should be emphasised that although the mechanisms of point defect production discussed above should apply to any material in which dislocation movement takes place, the quantitative theories of van Buren[10], Haasen and Leibfried[10], Friedel[10] and Seeger[12] all refer to face-centred cubic metals, in most cases copper. It is perhaps hazardous to suggest that these theories also describe conditions in body-centred cubic material. However, in order to give some idea of the quantities involved, Table 1 gives the concentrations of point defects expected in copper for various amounts of plastic tensile strain on the energy balance and the fixed and growing barrier theories. An initial dislocation density of 10^8 lines cm^{-2} has been assumed.

Fractional Plastic Tensile Strain	Energy Balance Model	Fixed Barrier Model		Growing Barrier Model	
	Moving Jog Mechanism	Moving Jog Mechanism	Coalescence Mechanism	Moving Jog Mechanism	Coalescence Mechanism
0.01	5×10^{-7}	10^{-5}	10^{-10}	10^{-6}	10^{-9}
0.10	10^{-5}	10^{-4}	10^{-9}	10^{-5}	10^{-7}
1.00	10^{-3}	10^{-3}	10^{-8}	10^{-5}	10^{-5}

Table 1 Concentrations of point defects expected as a result of plastic deformation. (After van Bueren [10].)

1.2.3 The generation of point defects by irradiation

The formation of point defects is thought to be a major result of the bombardment of metals with high energy nuclear particles. In recent years many review articles have been published on this subject and among the most comprehensive have been those of Kinchin and Pease[13], Seitz and Koehler[14] and Dienes and Vineyard[15]. The types, numbers and distributions of defects produced vary greatly with the nature of the bombarding particles. The experiments described in chapter 2 are concerned with pile irradiation so that the present discussion will be confined to neutrons since these are ultimately responsible for all the damage produced in a metal placed in a nuclear reactor.

A neutron, when it collides with an atom, may do one of three things; it may undergo a collision with one or more of the orbital electrons; it may produce some change in the nucleus, either raising it to an excited state or transmuting it; or it may collide elastically with the nucleus.

In an elastic collision with an electron the electron will usually be given enough energy for it to escape from its parent atom. However, such displacements will produce no observable changes in a metal since each electron can return to its lowest energy state by passing its extra energy to other electrons and the lattice as thermal movement.

The new nucleus formed by the capture of a neutron may simply give rise to γ-radiation and the formation of a new isotope, or it

may cause transmutation, that is, the formation of a chemically new atom by the emission of various forms of charged radiation. Sometimes the new nuclei are created with sufficient kinetic energy to cause structural damage to the lattice but this only occurs with elements of low atomic mass or with elements which undergo fission, materials with which the present investigation is not directly concerned.

In an elastic collision with a nucleus a fraction of the incident energy of the neutron will be transferred to the nucleus and if this is sufficient it will cause the atom, with or without its orbital electrons, to escape from its lattice site. The struck atom will usually be given enough energy for it to undergo further collisions with other atoms in the lattice with sufficient energy transfer to cause these to leave their lattice sites and in this way a cascade of defects is produced. The energy given to a nucleus by a scattered neutron can be calculated from elementary mechanics using the principles of conservation of energy and momentum. Hence, the maximum amount of energy that a neutron of mass M_1 and initial energy E can give to a nucleus of mass M_2 is

$$E_{max} = \frac{4 M_1 M_2}{(M_1 + M_2)^2} \cdot E \quad . \qquad (18)$$

The actual distribution of energies imparted during neutron irradiation is related to the distribution of angular deflections of the neutrons. The simplest approximation is that the neutrons are scattered isotropically and in this case all recoil energies between zero and

E_{max} are equally probable and the mean energy transferred per collision is then

$$\bar{E} = 0.5\, E_{max} . \qquad (19)$$

It has been found, however, that neutrons are scattered preferentially in the forward direction and allowing for this behaviour it is found that

$$\bar{E} = 0.3\, E_{max} . \qquad (20)$$

In pile irradiations the average energy of the bombarding neutrons is very roughly 1 MeV. Neutrons with energies of this order are usually termed fast neutrons. E_{max} for a collision between a neutron with this energy and a nucleus of mass A is given by

$$E_{max} = \frac{4A}{(1+A)^2} \text{ MeV} \qquad (21)$$

and $\bar{E}$ is given by

$$\bar{E} = \frac{1.2A}{(1+A)^2} \text{ MeV} \qquad (22)$$

Thus $\bar{E}$ for a struck molybdenum nucleus, mass 96, is about 12 KeV and that for a struck niobium nucleus, mass 93, is about 13 KeV.

Until quite recently copper was the only metal for which the energy required to remove an atom from its lattice site and place it in an interstitial position was known with any certainty. Both theory and experiment agree upon a value for this displacement energy of about 22 eV. Recently, however, Lucasson and Walker[16] have published

experimental data on several metals, including body-centred cubic iron, for which they quote a value of 24 eV. Kinchin and Thompson[17] suggest a value of 50 eV for molybdenum. Thus, typically, a struck atom will receive energy far in excess of that required to displace it from its lattice site. On its subsequent passage through the lattice the struck atom, termed a primary knock-on, will almost certainly cause the displacement of further atoms. The way in which a primary knock-on loses its energy in collisions with other atoms depends largely on its velocity. If it is given a very high velocity the atom will leave behind some or all of its orbital electrons. The ion thus produced is capable of losing energy by Coulomb interaction with the orbital electrons of other atoms in the lattice. It is also capable of losing energy by penetrating the electron cloud of an atom and causing an elastic collision between the two unscreened nuclei. A collision of this type can be treated using the Rutherford scattering laws. As its velocity decreases, the primary knock-on will acquire electrons and the collisions that occur will be between partially screened nuclei at first and finally they will be between completely screened nuclei, when the collisions can be considered as those between hard spheres. For the heavier metals, such as molybdenum and niobium, it is expected that the primary knock-ons and, of course, any secondary knock-ons, will only have sufficient energy for them to undergo hard sphere collisions with other atoms in the lattice. The reason for this is shown schematically in Figure 4.

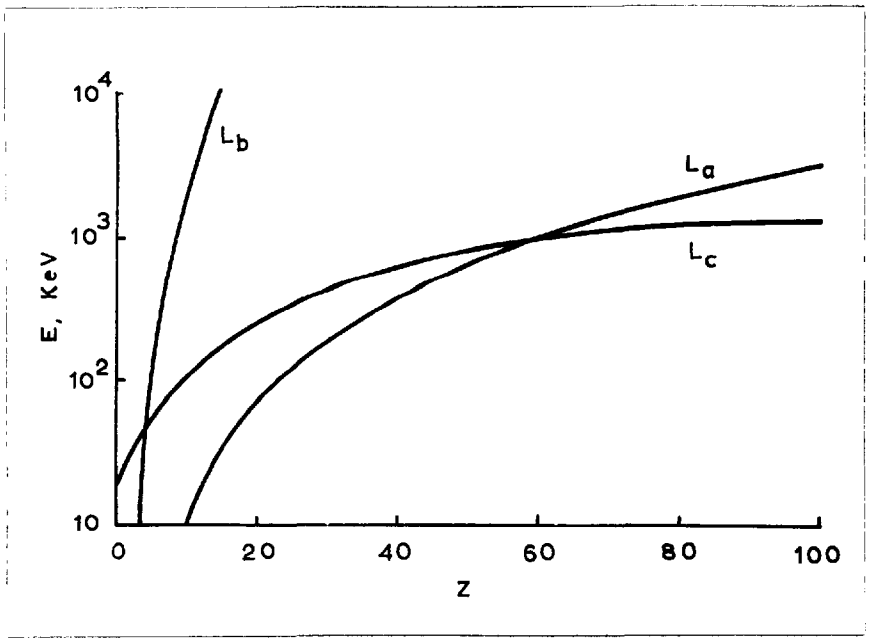


Fig. 5 A schematic representation of collision types for atoms of a metal, atomic number Z, moving in their own lattice. (After Lomer [18].)

The lines L_a, L_b and L_c represent limiting energies separating regions in which different collision types dominate when atoms of a metal atomic number Z and energy E, move through their own lattice. Below L_c the incident particle has too little energy to excite the electrons of the solid. Above L_c energy losses due to ionization rapidly dominate. Below L_a atomic collisions are essentially of the hard sphere type. Between L_a and L_b all the Rutherford collisions give displacements but above L_b only a fraction do so. In molybdenum and niobium, therefore, with atomic numbers 42 and 41 respectively, and with primary knock-ons having energies in the region of 12 KeV, it is expected that there will be little energy loss due to electron excitation and most of the collisions will be of the hard sphere type.

The target area or cross-section that a nucleus presents for an elastic collision with a neutron will vary with the type of nucleus, the type of collision and the energy of the neutron. For a head-on collision with a 1 MeV neutron the scattering cross-section σ_s for molybdenum and niobium is about 5×10^{-24} cm.^{2} or 5 barns. For an irradiation time t of one year in a neutron flux ϕ of 10^{11} fast neutrons cm.$^{-2}$ sec.$^{-1}$, the integrated neutron flux or neutron dose ϕt is about 3×10^{18} fast neutrons cm.$^{-2}$ Thus the fraction of atoms struck in this period, $\phi t \sigma_s$, is 1.5×10^{-5}. This means that one atom in about every 7×10^4 will be displaced from its lattice site. The scattering cross-section for hard sphere collisions is large, of the order of the ionic cross-section. The size of the ion in a metal depends on whether the metal can be considered as "full" or "open". In a full metal the ions interact strongly and the interatomic distance is comparable with the ionic diameter. This is not the case with open metals. The noble metals typify the first class and the alkalis the second. It is not clear in which class the late transition metals, which include molybdenum and niobium, should be placed but Lomer[18] suggests that they can be considered as full. If this is the case the primary and secondary knock-ons in niobium and molybdenum will undergo hard sphere collisions with nearly every atom they meet and the density of displacements in the cascade will be very high. The cascade will grow until no atom has sufficient energy to displace another and retain enough energy for itself to leave the lattice site. Kinchin and Pease[13]

propose that the minimum energy required is twice the displacement energy or $2E_d$. On this model it can be shown that the average number of displacements in a cascade is $E/2E_d$, where E is the energy of the primary knock-on. Thus half of the available energy of the primary knock-on is lost in collisions which do not produce displacements. Assuming a primary knock-on energy of 12KeV and a displacement energy of 50 eV, the average number of vacancy-interstitial pairs produced in a cascade in niobium or molybdenum is roughly 120. The cascade is pear-shaped with vacancies grouped preferentially towards the centre and interstitials towards the rim. A typical cross-section is shown schematically in Figure 6.

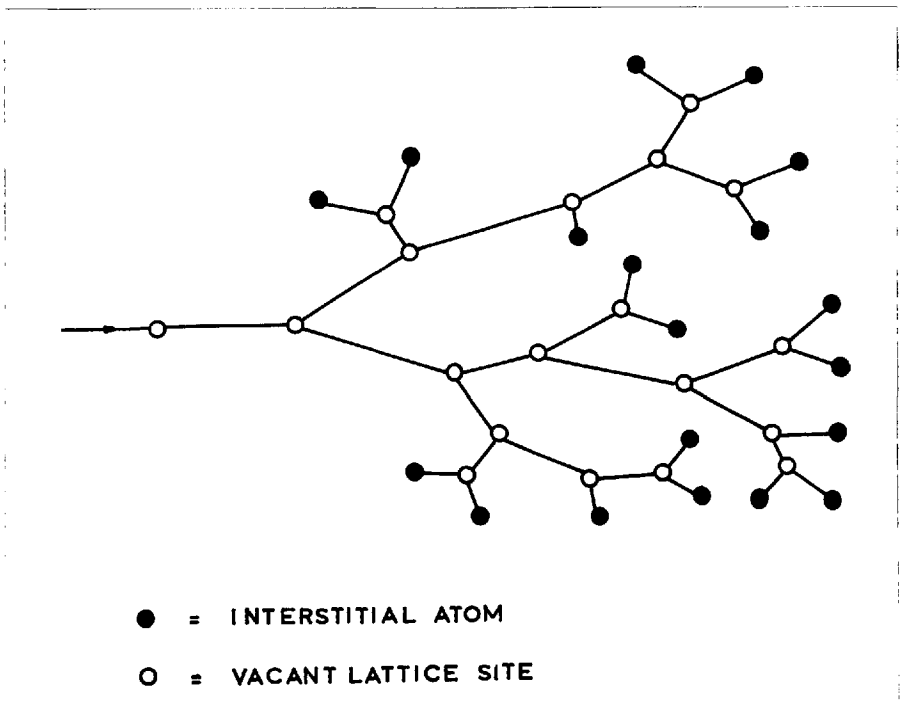


Fig. 6 A cascade of displacements produced by a primary and secondary knock-ons after a fast neutron collision. (After Cottrell [19].)

The stored energy of a vacancy-interstitial pair is only about 5 eV so that over 95 per cent of the energy of the primary knock-on is expended in producing enhanced atomic vibration. This large injection of energy occurs in a relatively small volume and it has been considered as equivalent to raising the temperature of the material in the cascade, or displacement spike as it is usually called, many thousands of degrees when it behaves more as a liquid than as a solid. Under these conditions it is probable that a large proportion of the point defects created by the simple cascade process described above are annihilated. Several models of the displacement spike have been proposed. Brinkman takes the extreme view that at first a multiple vacancy or hole is produced, surrounded by a shell of material containing interstitial atoms. This is shown schematically in Figure 7.

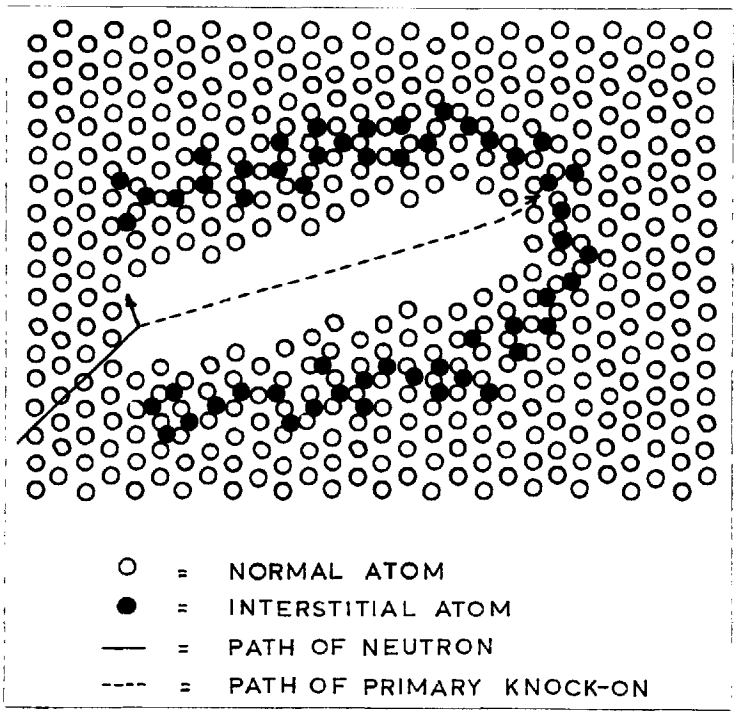


Fig. 7 The unstable intermediate stage in the formation of a displacement spike according to Brinkman. (After Dienes and Vineyard [15].)

Under the pressure exerted by the interstitials the hole collapses and the whole region resolidifies. Since freezing is expected to commence at the outside, the resolidified material is expected to be largely in register with the original lattice. Most of the vacancies and interstitials are annihilated but an undetermined number of these remain, together with small misoriented regions and dislocation loops created by the stress produced at the interface between low and high temperature regions. Other, less radical pictures of the displacement spike have been proposed by Seitz and Koehler[14], Cottrell[19] and Seeger[20], in which more of the original point defects are expected to survive. These theories have been introduced to account for the fact that the amount of damage observed experimentally is always less than that expected on the simple cascade theory but probably more than that expected on the Brinkman model. Lomer[21] recently reviewed the advances made in displacement theory during the last two years and brought to notice the growing realization of the importance of focussing collisions. These explain in a more elegant way than the Brinkman and similar models the discrepancy between the cascade theory and experiment. In a hard sphere collision an atom must receive its energy from an atom which was initially a neighbour in a special crystallographic direction and it therefore has a considerable tendency to move off along that particular direction. There is thus a tendency for the momentum to be transmitted along the nearest neighbour directions. Since all the atoms are of the same mass, each one is stopped completely when it

passes its energy to its neighbour and it may stop in its own lattice position or in the neighbouring one. Neither is of importance as far as the total number of displacements is concerned. Once the energy has been trapped into such a focussing mode, it can only produce one displacement. Thus, compared with the cascade theory, the number of displacements caused by a fast neutron collision is much less and the geometrical arrangement of displacements is more widely dispersed and is not so symmetrical.

1.3 The Migration of Point Defects

Non-equilibrium concentrations of point defects fall towards the appropriate equilibrium values as the temperature of the material is raised. The time taken to reach the equilibrium concentration of any particular species of defect depends on the temperature, the mechanism by which the defect disappears from the lattice and the energy required for its migration, if this is necessary for its removal. The migration of a defect is assumed to occur by a series of jumps from one lattice position to another. The frequency of these jumps is given by

$$f = Z\alpha\nu e^{-\Delta F/kT}, \qquad (23)$$

where Z is the number of adjacent sites to which the defect may go, which, at least for a vacancy, is the co-ordination number of the lattice, $\alpha\nu$ is the frequency of attempts by the defects to move to each adjacent site and $e^{-\Delta F/kT}$ is the fraction of time that a defect

has sufficient free energy to jump. ν is the frequency of the resultant vibration containing the total vibrational energy of the atom making the jump, usually taken as the Debye frequency, and α is the fraction of the resultant vibrations in each jump direction. On the assumption that the resultant vibration of an atom adjacent to a vacancy is always in the direction of the vacancy, $\alpha = 1$ but Piercy[22] has suggested that this is unlikely since each atom vibrates in phase with its neighbours and the wavelength of vibration is usually greater than three to four atoms. A more appropriate value of α is Z^{-1}, since there are Z possible jump directions and the fraction of the resultant vibrations in any one jump direction is about Z^{-1}. The free energy required by the defect to jump is given by

$$F = E_m - T \Delta S, \qquad (24)$$

where E_m is the activation energy required to move the defect and ΔS is the entropy change produced by the defect moving from one site to the saddle point midway between sites. Lomer[18] reports that the factor $e^{\Delta S/k}$ is seldom greater than 10.

The simplest interpretation of an experiment in which some property which indicates the presence of point defects, such as electrical resistivity, recovers in a certain temperature range is that the defects responsible for the observed change in property are mobile at these temperatures and are able to migrate to sinks, where they disappear. Possible sinks for the defects are free surfaces, grain boundaries, dislocations and other point defects. The average

number of jumps required by the defects to reach a sink can be calculated from the rate of recovery of electrical resistivity at a constant temperature T. If the defect concentration is assumed to be proportional to the additional resistivity $\Delta\rho$ above that for the fully recovered sample, the recovery rate can be expressed as

$$\frac{d\Delta\rho}{dt} = -\Delta\rho f p, \tag{25}$$

where t is the time and p is the probability per jump that a defect reaches a sink. p is equal to the fraction of lattice sites from which the defect is directly attracted to the sink. This depends on the concentration of sink sites, their distribution and the maximum distance of attraction between the defect and sink. Thus

$$p = j^{-1} = \beta C_s , \tag{26}$$

where j is the average number of jumps required by the defect to reach a sink, C_s is the concentration of sink sites and β is a term depending on the sink distribution and the maximum distance of attraction between a defect and a sink. Piercy[22] calls the term βC_s the effective sink concentration. From equations (23), (24), (25) and (26) it can easily be shown that

$$j = Z\alpha\nu S^{-1} e^{\Delta S/k} e^{-Em/kT} , \tag{27}$$

where S is equal to $(1/\Delta\rho)/(d\Delta\rho/dt)$, which can be estimated from the slope of the graph obtained by plotting the logarithm of the fraction of the resistivity increase remaining as a function of time

at temperature T. E_m can be obtained from the change in recovery rate for small temperature changes, as described in 2.3.2. The other parameters, Z, α , ν and $e^{\Delta S/k}$, can be estimated as described previously.

An independent estimate of j may be made if the initial distributions of the defects and sinks are known and if this agrees with the experimental value an identification of the observed recovery process is possible. If there is no agreement either the assumed distributions are incorrect or a simple migration of defects is not occuring. For example, if a random distribution of vacancies or interstitials in a fully annealed crystal are assumed to disappear on the 10^8 dislocation lines cm^{-2} usually present, the typical defects are 10^3 to 10^4 lattice spacings from any sink. j is then expected on a random walk basis to be between 10^6 and 10^8 and independent of the concentration of defects. This will be altered somewhat if the defects are attracted towards the sinks by dislocation stress fields and if the distribution of the sinks is not uniform. However, many observed processes give values of j very much smaller than this which implies either that the defects are all very near sinks or that the above analysis is incomplete. Lomer and Cottrell[23] take the latter view and suggest that impurity atoms, which are present in appreciable quantities in nearly all materials, can interact with point defects and modify the value of j appreciably. Lomer[18] has made a detailed analysis of this effect. He considers a concentration c of impurity

atoms or traps which attract the point defects with an energy B. The concentration of the defects in the lattice is denoted by n and that in the traps by n'. If each trap can accommodate only one defect then

$$n' = n e^{B/kT} / (1 + n e^{B/kT}). \qquad (28)$$

A typical defect spends a proportion $n/(n + cn')$ of its time migrating through the lattice and a proportion $cn'/(n + cn')$ trapped. The number of jumps made in time S^{-1} is thus

$$j = Z \alpha \nu S^{-1} e^{\Delta S/k} e^{-E_m/kT} (n + e^{-B/kT})/(n + e^{-B/kT} + c). \qquad (29)$$

If c is negligible this becomes identical, with equation (27) since the last fraction is unity. If c is small compared with $e^{-B/kT}$ the fraction is unity for large n and a little less than unity for small n and the defect spends only a very small proportion of its time trapped, whatever the defect concentration. When c is greater than $e^{-B/kT}$ there are three ranges of n to consider. Firstly, $n > c > e^{-B/kT}$; for this the correction factor is again unity, since the traps are saturated, and the annealing kinetics of the defects are unaltered. Secondly, $c > n > e^{-B/kT}$; for this the correction factor is approximately $n/(c + n)$ and a gradual emptying of the traps occurs which appreciably modifies the annealing kinetics of the defects. Thirdly, $c > e^{-B/kT} > n$; for this the correction factor is $c^{-1} e^{-B/kT}$ which is independent of n but has a marked temperature dependence. In addition the observed value of E_m includes the

binding energy, B. Thus, if experimental data is analysed on the basis of equation (27), which makes no allowance for trapping, the relationship between the true and apparent values of j is

$$j_{app} = j\,(c + n) / n, \quad \text{for} \quad n \gg e^{-B/kT} \qquad (30)$$

and

$$j_{app} = j\,c, \quad \text{for } n \ll e^{-B/kT}. \qquad (31)$$

Since the impurity concentration may lie in the region 10^{-3} to 10^{-5} and the defect concentration in the range 10^{-3} to 10^{-7}, j app may differ considerably from j. In many cases, however, c and $e^{-B/kT}$ may be too nearly equal to allow the limiting forms, equations (30) and (31), to be used and the full formula should be employed when analysing experimental data. If the observed value of j is anomalously large it may be accounted for by considering that a defect makes many jumps but does not sample a new site each time, thus reducing the frequency of disappearance. For example, the migration of a crowdion may well be restricted to a single atomic row, in which case in j jumps it samples only $j^{1/2}$ new sites whereas in three dimensional diffusion it would sample nearly j new sites.

1.4 The Annihilation of Point Defects.

The processes which may lead to the annihilation of point defects fall naturally into two main classes. The first involves disappearance at essentially inexhaustible sinks such as free surfaces, grain boundaries and dislocations and the second involves disappearance by aggregation or mutual annihilation.

1.4.1 The disappearance of point defects at fixed sinks

(i) Free surfaces and grain boundaries

If the average number of jumps a point defect makes before annihilation is about 10^9, the thickness of the surface layer which can feed a substantial number of point defects to the surface is about 10^{-3}cm. and the surface is unimportant in specimens having a diameter greater than about 10^{-2}cm. If the number of jumps is 10^4 the corresponding specimen diameter is about 10^{-5}cm. Since most experiments are carried out on specimens with diameters greater than 10^{-2}cm. the surface is usually considered as unimportant as a sink for point defects. A similar argument can be applied to grain boundaries and it can be seen that they will become important if the grain diameter is less than 100μ if 10^9 jumps to annihilation are involved or less than 0.1μ if 10^4 jumps are involved.

(ii) Dislocations

A vacancy V may arrive at a part of an edge dislocation which is atomically smooth, as indicated in Figure 8.

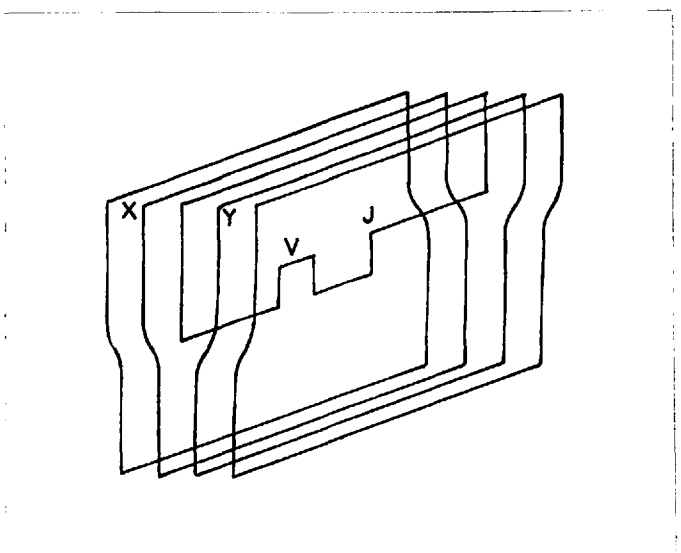


Fig. 8 An edge dislocation with a bound vacancy V and a jog J. (After Lomer.[18])

A vacancy in this state is referred to as a bound vacancy because the elastic stresses at the dislocation cause it to be energetically stable there, whilst the neighbouring planes X and Y cannot close in to hide its vacancy character. In general a dislocation line is not atomically smooth and a vacancy may arrive at a jog, such as J, where the dislocation line steps from one plane to an adjacent one. In this case the vacancy can be completely absorbed by moving the jog one atomic spacing along the dislocation line. Similarly, it is possible for an interstitial to be completely absorbed at J by moving the jog one atomic distance in the opposite direction.

Cottrell[9] has shown that it is geometrically possible to absorb point defects on screw dislocations also. The mechanism is shown schematically in Figure 9.

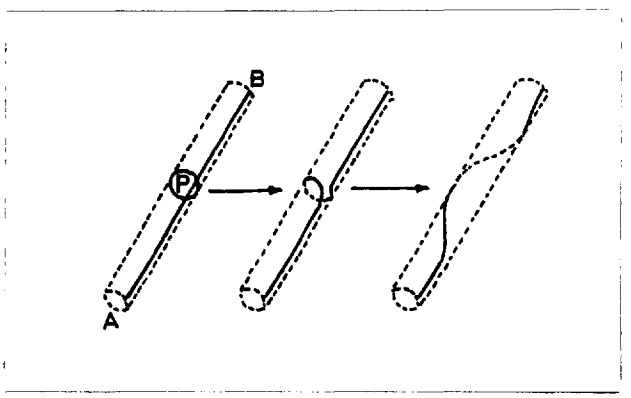


Fig. 9 Stages in the absorption of a point defect P by a screw dislocation AB. (After Cottrell[9].)

He suggests, however, that the absorption occurs in practice only if P represents several point defects. This mechanism is closely related to the formation of spiral prismatic dislocations, the possibility of

which was first suggested by Seitz[2].

If both the point defects and the dislocations are randomly distributed and the defects are considered to move independently of each other, a constant value of j, the number of jumps to annihilation, should be obtained. In this case the recovery process is referred to as first order. Disappearance at dislocations may not always be simple, however. In a heavily damaged material produced by quenching or irradiation the concentration of defects may be as high as 10^{-3} and the dislocation density only 10^{8} lines $cm.^{-2}$ In this case the absorption of all the defects on the dislocation lines requires the movement of the dislocations over many thousands of atomic spacings. In practice such movement may be restricted in the same way as movement under stress is restricted in work-hardened material, or it may even amount to considerable annealing by allowing many of the dislocations to disappear. The annealing of point defects produced by cold-working may deviate even more from first order kinetics since they may be deposited in special positions relative to the dislocations, as mentioned in 1.2.2.

1.4.2 The disappearance of point defects by mutual annihilation and aggregation

Vacancies and interstitial atoms may disappear by mutual annihilation. It is thought that there is no appreciable long range attraction between the two types of defect so that combination occurs by random migration of the defects to neighbouring positions. If both are initially independently and randomly distributed the combination rate depends on the product of their concentrations. If, in addition,

the initial concentrations are equal, they will remain equal throughout the recovery process and the rate of combination may be written as proportional to the square of either concentration, giving second order kinetics with a continuous increase in j. These simple kinetics can easily be lost, however, for any one of the following reasons.

(i) If the initial concentrations of vacancies and interstitials are not equal.

(ii) If the initial distribution of either vacancies or interstitials is not uniform.

(iii) If the vacancy and interstitial distributions are correlated. For example, if the defects are present as randomly distributed close pairs.

(iv) If either vacancies or interstitials are able to disappear by another competing process.

In fact, no known method of damage can produce the conditions necessary for mutual annihilation to give simple second order kinetics and in practice an increase in j as annealing proceeds may indicate that some process involving the destruction of sinks is occuring, or that the initial distribution of either sinks or defects is not uniform, or that trapping at impurities is occuring.

Vacancies, at least in the face-centred cubic lattice, may also disappear by combining together to form vacancy pairs which, because of their high mobility compared with single vacancies, first proposed by Seitz[2], migrate very quickly to sinks. Little appears to be known about the possibility of a similar process for interstitials although

Vineyard[24] has suggested that an interstitial pair in copper has quite a high binding energy. The rate of combination of single vacancies depends on the number of jumps one vacancy has to make before meeting another. This rate is proportional to the square of the concentration of single vacancies, which gives rise to second order kinetics. These kinetics will only be observed in a situation where the only point defects initially present are randomly distributed single vacancies and where the formation of larger clusters than vacancy pairs does not occur. In practice, these conditions are unlikely to occur together, although the formation of divacancies probably plays an important role as an intermediate step in many annealing processes.

The difficulty, mentioned earlier, in explaining the disappearance of a large number of point defects on a relatively small number of dislocations, when the latter are considered to be the only sinks available, can be overcome if it is assumed that large clusters of like defects can form during annealing. The theory of vacancy or interstitial interaction cannot provide a reliable estimate of the amount of clustering to be expected, because so little is known about the mobilities and binding energies of clusters of defects. However, some progress has been made in the case of copper, notably by Damask, Dienes and Weizer[25] and Vineyard[24], who have made considerable use of computer calculations. On the other hand, a considerable amount of both direct and indirect experimental evidence now exists which suggests that clustering, at least in some face-centred cubic metals, plays an extremely important role in the annealing of materials containing high concentrations of

point defects.

The particularly careful experiments of Bauerle and Koehler[26], who measured the electrical resistivity of gold before and after quenching and on subsequent annealing, suggest that although the increase in resistivity found on quenching can be satisfactorily explained in terms of the formation and retention of predominantly single vacancies, only after quenches from low temperatures can the recovery of resistivity be explained in terms of single vacancies migrating to and being annihilated at fixed sinks, such as might be provided by the dislocation network of the material. For quenches from high temperatures Bauerle and Koehler explain their more complicated results in terms of the migration of divacancies produced during the quench. The ratio of the number of divacancies produced from single vacancies to the number of single vacancies left is expected to increase with increase in quenching temperature, because the concentration of single vacancies increases and the rate of formation of divacancies depends on this concentration, as explained above. Kimura, Maddin and Kuhlmann-Wilsdorf[27] have re-analysed these results and suggest that this is too simple a picture and introduce the idea of variable sinks in the form of sessile dislocation rings created by the collapse of discs of vacancies, formed by the aggregation of single vacancies, during the quench or immediately on annealing. The possibility of the formation of dislocation rings from the collapse of discs of vacancies was first proposed by Frank[28]. Kuhlmann-Wilsdorf[29] has considered the mechanism in some detail for different crystal structures and for metals with

different stacking fault energies. She considers that vacancies which accidentally meet during their thermal motion form loosely bound groups containing up to perhaps seven defects. The energy of such groups is lowest if they form discs parallel to the most densely packed lattice planes. If two or more such groups meet on the same plane they form a disc-shaped hole which is large enough to collapse, thus forming a stacking fault bounded by a Frank sessile dislocation. This model of dislocation loop formation and its application to the annealing kinetics of quenched gold is supported, but requires slight modification, by the presence of stacking fault tetrahedra reported by Silcox and Hirsch[30] in transmission electron micrographs of quenched gold foils annealed at a temperature at which most of the resistivity recovery occurs. The tetrahedra are thought to be formed by the dissociation of the Frank partial, which has a large Burgers vector, into a stair rod dislocation and a Shockley partial, according to the vector equation

$$a/3 \quad [111] \longrightarrow a/6 \quad [101] + a/6 \quad [121] .$$

In a face-centred cubic metal with a high stacking fault energy the stacking fault can be eliminated by the nucleation of a Shockley partial which reacts with the Frank partial to form a prismatic dislocation according to the equation

$$a/3 \quad [111] + a/6 \quad [11\bar{2}] \longrightarrow a/2 \quad [110] .$$

Such prismatic dislocations have been observed in quenched aluminium foils by Hirsch, Silcox, Smallman and Westmacott[31].

Experiments on quenched body-centred cubic metals have yet to be carried out but Kuhlmann-Wilsdorf[29] predicts that because of their

high stacking fault energy the stacking fault produced by the collapse of a disc of vacancies on a [110] plane should be removed by a dislocation reaction of the type

$$a/2\ [110] + a/2\ [001] \longrightarrow a/2\ [111] .$$

Evidence for dislocation loop formation in neutron irradiated metals has also been reported. Smallman and Westmacott[32] bombarded aluminium foils with 10^{18} fast neutrons $cm.^{-2}$ at -196° C and examined the foils in the electron microscope at 20° C, a temperature at which most of the point defects in aluminium should be mobile. As well as loops they found jogged and spiral dislocations, the first direct evidence for the annihilation of point defects at dislocations. Makin, Whapham and Minter[33] recently reported the examination by transmission electron microscopy of neutron irradiated copper. Foils irradiated with 3×10^{17} fast neutrons $cm.^{-2}$ at -196° C and examined at -50° C contained many dislocation loops which, because of the expected immobility of vacancies at this temperature, are thought to be due to the clustering of interstitial atoms. Little change occured in these foils on warming to room temperature. Foils bombarded with 2×10^{18} fast neutrons $cm.^{-2}$ at 27° C also contained loops and on annealing at 306° C, a temperature at which appreciable self-diffusion can occur, the loops began to disappear and a large number of very small defects became visible. These small defects are interpreted as vacancy clusters formed by the re-arrangement of vacancies created in displacement spikes.

In contrast, both Wilsdorf[34] and Silcox[35] have discovered no change in electron micrographs of neutron irradiated nickel foils.

However, Wilsdorf[34] found that if a foil bombarded with 10^{19} fast neutrons $cm.^{-2}$ was deformed about 2 per cent, the resulting dislocation structure was very different from that of an unirradiated foil deformed the same amount. The structure contained many jogged dislocations and small dislocation loops. Wilsdorf interpreted this difference by supposing that the vacancies produced by irradiation, presumably mobile at the irradiation temperature used, exist as clusters of some kind which cannot be resolved in the electron microscope. On plastic deformation the first glide dislocations cause the transformation of these clusters into discs of vacancies which collapse to form dislocation loops. The loops are nucleated either in the neighbourhood of dislocations, in which case they remain as loops, or in direct contact with them, in which case they create kinks in the dislocation lines. In this way an appreciable fraction of the excess vacancies are annihilated, leaving a relatively clear passage for later dislocations, which may originate from suitable loops or kinks. This would explain the unaltered rate of work-hardening observed in nickel, and other metals, after irradiation. Silcox[36] suggests that the absence of loops in his specimens, which were irradiated at room temperature but subsequently annealed at 250° C, a temperature at which all point defects in nickel should be mobile, may be due to point defect-impurity atom interaction which would inhibit clustering and tend to encourage vacancy-interstitial atom mutual annihilation. This explanation would not appear to be applicable in the case of Wilsdorf's experiments since

1.5 Previous Work on Point Defects in the Body-Centred Cubic Transition Metals

As early as 1927 Geiss and van Liempt[38] reported large increases in the electrical resistivity of molybdenum and tungsten that had been heavily deformed by wire-drawing at room temperature but these observations were not discussed in terms of dislocation and point defect theories, which have only come into prominence since about 1945. In fact it was not until 1954 that any comprehensive work was published on point defects in the body-centred cubic transition metals. The increased interest in these metals at that time was brought about mainly by the nuclear power programme and the development of high speed flight, both in this country and elsewhere, and their need for new materials. The data published since that time can be conveniently divided into that provided by (i) experiments on irradiated materials, (ii) experiments on plastically deformed materials and (iii) theoretical studies.

1.5.1 Experiments on irradiated materials

Kinchin and Thompson[17] irradiated specimens of molybdenum and tungsten in BEPO at A.E.R.E., Harwell at 30° C and at -196° C and measured changes in electrical resistivity on irradiation and subsequent annealing. They also measured the stored energy release of molybdenum that had been irradiated at 30° C. Specimens of both molybdenum and tungsten irradiated at 30° C showed an initial sharp rise in resistance but when the neutron dose exceeded about 10^{18} fast neutrons cm.$^{-2}$ the rate of increase decreased and remained constant up to a dose of

2×10^{19} fast neutrons $cm.^{-2}$ At this dose the increase in resistance, measured at 0°C, was 15 per cent for molybdenum and 25 per cent for tungsten. On annealing specimens irradiated at -196°C, two recovery processes were observed for both metals. The temperature T at which each occured, and the activation energy E_m and the number of jumps j associated with the recovery, are given in Table 2.

	Mo		W	
T, °C	-170	+150	-80	+320
E_m, eV	0.25	1.3	0.48	1.7
j	$10^5 \pm 2$	$10^{1.5} \pm 2$	$10^{4.5} \pm 1$	$10^{2.5} \pm 1.5$

Table 2 Recovery stages observed in molybdenum and tungsten after neutron irradiation at -196°C. (After Kinchin and Thompson[17].)

These results were explained in terms of the migration of vacancies and interstitial atoms created during irradiation. The first recovery stage in each metal was attributed to the migration of interstitials, either to vacancies, in which case they were annihilated, or to impurity atoms, in which case they became trapped. The second stage was attributed either to the migration of vacancies to the trapped interstitials, which were present in the form of crowdions, or to the formation of highly mobile vacancy pairs from the interaction of single vacancies. Both these mechanisms accounted for the rather low number of jumps associated with the second stage. The stored energy

measurements suggested that a concentration of 2.6×10^{-5} vacancy-interstitial atom pairs were present after irradiation with 10^{18} fast neutrons $cm.^{-2}$ at 30°C and that the presence of 1 per cent vacancies and 1 per cent interstitials produced an increase in resistivity of 28 $\mu\Omega$ cm.

Thompson[39] later made a detailed study of the electrical resistivity changes in tungsten after irradiation in BEPO at 4°K. A comparison was made between five different types of specimens prepared from cold-drawn wire. Specimens of the first type were irradiated in the cold-worked state and specimens of the second, third and fourth types were annealed, before irradiation, at 2000, 1500 and 500°C, respectively. Specimens of the fifth type were prepared from material with a greater impurity content and these were annealed at 1500°C before irradiation. Four stages of recovery were observed when the irradiated specimens were annealed. The temperature T at which each occured and its associated activation energy Em are shown in Table 3.

Recovery Stage	T, °C	E_m, eV
I	Below -170	
II	-170 to 350	0.25 to 1.7
III	350 to 450	1.7
IV	Above 450	

Table 3 Recovery stages observed in tungsten after neutron irradiation at 4°K. (After Thompson[39].)

The free interstitial was assumed to be mobile below -170°C, giving rise to Stage I recovery. Recovery in Stage II, which was enhanced by the presence of cold-work and impurities and was suppressed in well-annealed specimens given light irradiations, was attributed to the release of interstitials trapped at impurities and dislocations. A comparison with other metals led Thompson to the conclusion that Stage III recovery was due to the migration of vacancies and that this occurs in most metals at an absolute temperature of about $T_m/5$ and with an activation energy of about 5×10^{-4} T_m eV, where T_m is the absolute melting temperature of the metal concerned. The resistance versus neutron dose curve for cold-worked specimens showed acceleration and Thompson considered this as evidence for the action of displacement spikes on the unstable arrays of vacancies produced by plastic deformation.

Adam and Martin[40] measured the lattice parameter and linear dimensions of molybdenum before and after irradiation in BEPO at 30°C. They found that irradiation produced an increase in both length and lattice parameter but that the fractional length change was greater than the fractional lattice parameter change. Since any uniform distribution of point defects should effect both properties to the same degree it was concluded that new lattice sites must have been created during irradiation. This might have occured by the clustering of interstitial atoms that were mobile at the irradiation temperature. On annealing at 180°C a decrease in specimen length was observed which could be attributed to the annihilation of vacant lattice sites.

Gray and Cummings[41] measured changes in the lattice parameter, X-ray line width and micro-hardness of stress-relived molybdenum on irradiation with pile neutrons at 35°C. The lattice parameter versus neutron dose curve reached a maximum after irradiation with 5×10^{19} fast neutrons cm.$^{-2}$ and a net decrease from the pre-irradiation value occured after a neutron dose of 1.2×10^{20} fast neutrons cm.$^{-2}$ Both line width and hardness increased with neutron dose and although the hardness approached a limiting value the line width did not. These results were discussed in terms of the recovery processes that might occur during irradiation and it was concluded that interstitial atoms must be mobile at the irradiation temperature. When the concentration of interstitials was small a considerable number became trapped at impurity atoms but with larger concentrations interstitial cluster formation and growth occured. These authors did not carry out annealing experiments on the irradiated specimens but earlier Gray[42] had observed that about 25 per cent of the increase in lattice parameter due to irradiation with between 6.5×10^{16} and 2.3×10^{19} fast neutrons cm.$^{-2}$ annealed out in the temperature range 100 to 170°C.

Chaudhuri, Mendelssohn and Thompson[43] carried out an interesting experiment on the thermal conductivity of niobium irradiated in BEPO at 30°C. Niobium is a superconductor and in the superconducting state thermal conduction is due only to phonons and consequently it is only affected by defects comparable in size with the phonon wavelength. At the temperatures concerned this was of the order of 100°A. In the presence of a magnetic field, however, the superconductor reverts to its

normal state where heat is carried by electrons whose short wavelength allows them to interact with small defects, such as vacancies and interstitial atoms. After irradiation with 10^{18} fast neutrons $cm.^{-2}$ it was found that both in its normal and superconducting states niobium had suffered a loss of conduction. The loss in the normal state indicated a point defect concentration of about 10^{-4} and in the superconducting state the loss could be accounted for by an increase in dislocation density of about 3×10^{9} lines $cm.^{-2}$ Assuming that the dislocations were in the form of loops formed by the aggregation of point defects this increase could be accounted for by a concentration of 10^{-5} point defects forming loops 100Å in diameter. It was suggested that the isolated defects were vacancies and that the loops were formed by the clustering of interstitial atoms that were mobile at the irradiation temperature.

Makin and Minter[44] investigated the effect of irradiation with up to 10^{20} fast neutrons $cm.^{-2}$ at 16°C on the mechanical properties of niobium. Only a moderate increase in yield stress occured on irradiation but on annealing in the temperature range 125 to 175°C there was a further large, increase and the appearance of a yield drop. An increase in yield stress on annealing irradiated molybdenum in the temperature range 150 to 200°C has also been observed by Makin and Gillies[45] and Wronski[46]. The activation energy of the process in niobium was measured and found to be 1.3 ± 0.1 eV and both this process and those observed in molybdenum have been attributed to the migration

to dislocations of vacancies produced during irradiation.

Dautreppe, Moser and Pauleve[47] looked for magnetic after-effects in iron after pile irradiations at 25°C and -196°C. After irradiation with 4×10^{18} fast neutrons cm.$^{-2}$ at 25°C a region of magnetic after-effect was observed between -20 and 150°C. The activation energy for motion of the defects responsible for this effect was found to be 1.2 eV. After irradiation with 2.5×10^{11} fast neutrons cm.$^{-2}$ at -196°C this region was found to be absent but two other regions were observed at -150 and -60°C, the corresponding activation energies being 0.3 and 0.6 eV, respectively. No attempt was made to attribute these effects to any particular species of defects.

1.5.2 Experiments on plastically deformed materials

Martin[48] carried out annealing experiments on molybdenum that had been wire-drawn at room temperature and found that about 50 per cent of the increase in electrical resistivity due to a 44 per cent reduction in area annealed out in a well-defined recovery process between 100 and 180°C. The recovery proceeded with an activation energy of 1.26 ± 0.04 eV. Martin attributed this to the migration of vacancies created by plastic deformation.

Peiffer[49] investigated changes in the electrical resistivity of molybdenum deformed various amounts in tension at room temperature and found that a linear relationship existed between percentage elongation and the change in resistivity due to prolonged annealing of the cold-worked specimens at 145°C. In this case the recovery represented

about 30 per cent of the increase in resistivity due to plastic deformation. The observed linear relationship would appear to support the predictions of Seitz[2] and Mott[11] and the theories of Haasen and Leibfried[10] and Friedel[10].

Neimark and Swalin[50] performed annealing experiments on pure and impure tungsten wire that had been rolled at room temperature. The impure tungsten contained small amounts of potassium and aluminium. Two resistivity recovery processes were observed, one closely following upon the other, in both types of specimens. The change from the first to the second process occured at 325°C in the pure and at 375°C in the impure material. The measured activation energy E_m for each recovery process is given in Table 4.

Recovery Stage	E_m, eV	
	Pure W	Impure W
1	1.5 ± 0.1	1.2 ± 0.1
2	1.7 ± 0.1	2.3 ± 0.1

Table 4 Recovery stages observed in pure and impure tungsten after plastic deformation at room temperature. (After Neimark and Swalin[50].)

Recovery in the second stage was thought to be due to the migration and annihilation of single vacancies and in the first stage it was attributed to the annihilation of a more mobile defect such as

divacancies. The high activation energy for the second stage in the impure material was thought to include a binding energy of 0.6 eV for a vacancy-impurity atom pair.

Schultz[51] also found a resistivity recovery process in tungsten cold-worked by wire-drawing at room temperature. It occured between 300 and 400°C with an activation energy of 1.73 eV.

1.5.3 Theoretical studies

The lattice vacancy is the only species of point defect in the body-centred cubic transition metals to have received any theoretical attention. Macroscopic concepts such as surface energy and elastic constants have been used in these calculations although there is no real justification for using them on an atomic scale. However, the more rigorous quantum mechanical approach involves such drastic approximations that the cruder estimates would appear to be more reliable.

Brooks[52] considered the formation of a vacancy to be approximately equivalent to the creation of a spherical surface corresponding to one atomic volume. In order to preserve the volume energy of the crystal the missing atom is considered to be spread uniformly over the outer surface of the crystal so that the resultant increase in external surface becomes negligible as the volume of the crystal increases. However, surface tension tends to reduce the size of the hole and this results in elastic distortion of the crystal. Equilibrium is achieved when the strain energy balances the surface energy lost by contraction. On this model Brooks calculated the formation and migration energies, E_f and E_m, of a vacancy in α-iron and tungsten. These are given

in Table 5.

	E_f, eV	E_m, eV
α-Fe	2.54	0.72
W	5.73	1.25

Table 5 The formation and migration energies of a vacancy in α-iron and tungsten. (After Brooks[52].)

Shaw recently carried out a similar calculation in which the surface energy was replaced by a more detailed set of interatomic forces. He chose a suitable central law of force between the atoms and combined this with a volume potential to ensure stability, the relevant parameters being chosen so as to yield the observed elastic constants, lattice parameters and sublimation energies of the metals. He first assumed that the eight nearest neighbour atoms of the vacancy relaxed radially inwards and calculated the change in interatomic bond energy corresponding to this movement. Further investigation showed that this was not the minimum energy configuration. If a nearest neighbour atom was moved towards the vacancy, the rest of the atoms being held in their normal lattice positions, it was found that the potential energy dropped to a minimum at the half-way stage. Consequently, Shaw suggests that the vacancy in the body-centred cubic transition metals exists as a "coilion", which is equivalent to a single vacancy in that it consists of two vacant lattice sites with an atom situated symmetrically between them. This configuration is shown

schematically in Figure 10.

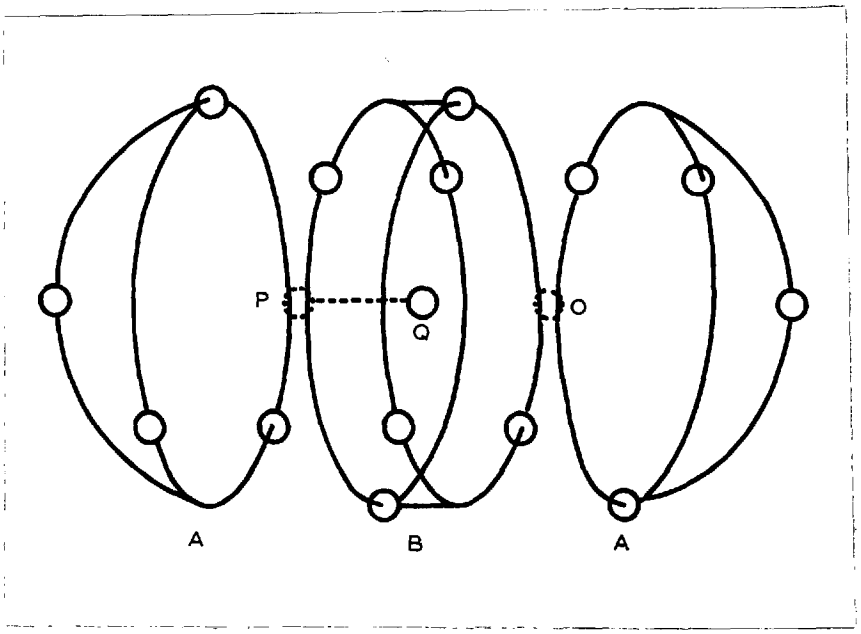


Fig. 10 The vacancy or coilion configuration in a body-centred cubic transition metal. P is the site of a nearest neighbour atom to O, the vacant site in the body-centred cubic lattice. The atom Q has been moved from its natural site at P. The atoms on the cylinder B may be held in their natural positions but the atoms on the hemi-spheres A, centred on the vacant sites O and P, may relax radially. (After Shaw[53])

Shaw calculated the formation and migration energies, E_f and E_m, of the coilion in several metals. These are given in Table 6. Also shown is the sum of E_f and E_m which can be compared with the experimentally determined value of the self-diffusion activation energy, E_d, given in the last column. The significance of this is discussed in later sections.

Metal	E_f , eV	E_m , eV	$E_f + E_m$	E_d , eV
α-Fe	1.69	0.60	2.29	2.92
V	1.29	0.92	2.21	
Nb				4.56
Mo	2.60	1.72	4.32	4.95
Ta				4.77
W	4.01	2.23	6.24	5.89

Table 6 The formation and migration energies, E_f and E_m, of the coilion in several body-centred cubic transition metals. (After Shaw[53]) The experimentally determined value of the self-diffusion activation energy, E_d, is shown in the last column.

Recently, also, Mehl, Swanson and Pound[54] proposed a semi-empirical relationship between the formation energy of a vacancy and the macroscopic properties heat of fusion and solidification shrinkage. This gives a value of 2.12 eV for the formation energy of a vacancy in α-iron.

1.6 Selection of Experiments

At the time this investigation was initiated work was already in progress in the Department on the effect of pile irradiation on the mechanical properties of molybdenum. As the result of such an irradiation is to introduce lattice defects, in particular point defects, such as vacant lattice sites and interstitial atoms, it was thought

necessary to attempt to confirm what little was already known about these defects in molybdenum and to extend the work to cover as many of the other body-centred cubic transition metals as possible. The metals concerned are given in Table 7, together with some of their physical properties. Most of the data are taken from references 116 and 117.

	V	Cr	Fe	Nb	Mo	Ta	W
Atomic Number	23	24	26	41	42	73	74
Atomic Weight	50.9	52.0	55.9	92.9	95.9	180.9	183.9
Lattice Parameter at 25°C, Å	3.04	2.88	2.87	3.30	3.15	3.31	3.16
Melting Temperature, °C	1900±25	1874±40	1537±1	2468±10	2622±10	2996±50	3370
Electrical Resistivity at 25°C μΩcm.	19.9	12.9	9.71	14.5	5.3	13.1	5.3

Table 7 The body-centred cubic transition metals and some of their physical properties.

The metals readily available at the time were iron, niobium, molybdenum, tantalum and tungsten. It was thought that because it so readily oxidises iron would be difficult to handle experimentally and it was also thought that most point defects in this metal would be mobile at room temperature. A research programme on tungsten was already being carried out by Thompson[39] at A.E.R.E., Harwell, and so attention

was focussed on the three remaining metals, niobium, molybdenum and tantalum.

Probably the most attractive method of introducing point defects is that of quenching, because of the quantity of information obtained from such an experiment and the relative ease of interpretation of results. It was decided not to use this method, however, for two reasons. The first was because it was thought that appreciable concentrations of point defects only exist near the melting points of these metals and the difficulty of carrying out efficient quenches from the very high temperatures involved would be considerable. The second was because it was considered that the formation energies of vacancies in the body-centred transition metals were particularly high, thus reducing the concentrations of defects normally to be expected. This conclusion was arrived at on rather scanty experimental evidence but information obtained since would appear to support this view. Unfortunately there was, and still is, no direct experimental information concerning the formation energies of point defects in the body-centred transition metals but if it is assumed that self-diffusion in these metals is by a vacancy mechanism an estimate can be made, since the sum of the vacancy formation and migration energies is then equal to the self-diffusion energy. We thus have

$$E_f + E_m = E_d \qquad (32)$$

Tungsten was the only metal for which E_m and E_d were known. From Kinchin and Thompson's[17] work E_m was estimated to be 1.7 eV and

Vasil'ev and Chernomorchenko[55] had found a value of 5.9 eV for E_d. The deduced value for E_f, 4.2 eV, represents about 70 per cent of the self-diffusion energy compared with 40 to 50 per cent for the face-centred metals, (see Table 18). Since there is a roughly linear relationship between self-diffusion energies and melting temperatures, (see Figure 36), this means that near its melting point tungsten will probably contain a smaller concentration of vacancies than a face-centred metal in the same state. Using equation (6), the concentration of vacancies in tungsten near its melting point of 3600°K should be approximately 10^{-5}, assuming a value of 5 for $e^{\Delta S_f/k}$. This concentration of defects might be expected to produce an increase in electrical resistivity of about 10^{-3} $\mu\Omega$ cm. which is rather close to the expected detectable change of about 10^{-4} $\mu\Omega$ cm.

It was decided, therefore, to concentrate on plastic deformation and irradiation as methods of introducing point defects. Tensile straining was chosen as a convenient method for producing controlled amounts of plastic deformation and pile irradiation was used since this was also convenient and results could be compared directly with those obtained from the investigation on mechanical properties. Since tantalum becomes extremely radio-active irradiation was confined to niobium and molybdenum. A comprehensive study of cold-worked molybdenum had already been published by Martin[48] and it was thought unnecessary to repeat this work as well as that on irradiated molybdenum by Kinchin and Thompson.[17] Plastic deformation was thus confined to

niobium and tantalum. From the previous work on molybdenum it was expected that at least one species of point defects would become mobile well above room temperature so that plastic deformation and irradiation were conveniently carried out at room and normal pile temperatures, about 20 and 40°C respectively.

The obvious choice of a method to detect point defects was to use electrical resistivity measurements since it is well-known that the electrical resistance of a metal specimen, particularly at low temperatures, is sensitive to the presence of lattice defects of all kinds. Comprehensive reviews on this subject have been published by Broom[56] and Broom and Ham[57]. Also, the construction of a suitable resistance measuring apparatus is reasonably simple, since all the components are standard.

A programme was drawn up which included an investigation into the effect of neutron dose on the electrical resistivity of niobium and molybdenum and the effect of various amounts of plastic deformation on the electrical resistivity of niobium and tantalum. The main interest, however, lay in the subsequent annealing behaviour of the damaged materials. It was found later that the resistivity of the niobium and tantalum prior to irradiation and plastic deformation varied from specimen to specimen and since the resistivity of individual specimens was not determined before these treatments were carried out it was only possible to determine the effect of neutron dose on the resistivity of

molybdenum. It is not clear what these variations were due to but possible explanations are large variations in impurity content and in wire-drawing and annealing treatment. However, satisfactory recovery experiments were carried out on all materials. These included the determination of the temperature ranges in which recovery took place and the measurement of activiation energies of recovery processes.

2 EXPERIMENTAL PROCEDURE

2.1 Preparation of Specimens

Specimens were prepared from the purest material commercially available. Nominal chemical analyses supplied by the manufacturers, Murex Limited, are given in Table 8,

	C	O	N	Al	Fe	Si	Mo	Nb	Ta
Mo	0.008%	<0.001%	~0.003%		0.01%	~ 0.002%	~99.98%		
Nb	~ 0.1%	~0.05%	~ 50ppm	~0.03%	~0.03%	~ 0.02%		~99.5%	< 0.3%
Ta	0.01%							<0.1%	~ 99.9%

Table 8 Nominal chemical analyses of the molybdenum, niobium and tantalum used in the investigation. Values in weight per cent.

The molybdenum and niobium to be irradiated were given various swaging, wire-drawing and intermediate annealing treatments to produce a wire 1 mm. in diameter which was finally annealed for 1 hour at a temperature of about 1300°C. The molybdenum wire was loosely coiled after this treatment and specimens 15 cm. in length were cut from this coil. The niobium was cut into specimens 15 cm. in length as it was withdrawn from the annealing furnace. Molybdenum and niobium specimens were placed together in specially constructed aluminium containers which were then evacuated, filled with argon gas at a pressure of 0.5 atmosphere and finally sealed by argon-arc welding. Four containers,

each containing four molybdenum and three niobium specimens, together with other wires and tensile test pieces required for other investigations, were irradiated in BEPO at A.E.R.E., Harwell at a temperature of about 40°C. One was irradiated for 3 months, one for 6 months, one for 9 months and one for 12 months. The irradiations were carried out in a vertical hole in the reactor where the flux was 1.2×10^{12} epithermal neutrons $cm.^{-2}$ $sec.^{-1}$ Probably about 1 epithermal neutron in 10 had an energy greater than 1 MeV. After irradiation the specimens were stored at room temperature until required. During this storage period, which for some specimens was as long as 12 months, the radio-activity of the specimens decreased sufficiently for them to be handled with forceps.

Niobium to be plastically deformed was prepared from two batches of material of the same nominal composition. The first batch, and also the tantalum to be plastically deformed, were treated in a similar manner to that described for molybdenum. The second batch of niobium received the same treatment as the first up to the final annealing treatment, which was carried out at 700°C instead of 1300°C. Prior to this both batches of material had been given a 90 per cent reduction in area by wire-drawing at 20°C. This left the material in a brittle condition which was completely eliminated in the first batch by annealing at a temperature of 1300°C, well above the recrystallization temperature of about 900°C. Annealing the second batch at 700°C was sufficient to cause internal stress-relief, with an accompanying increase in

ductility, but insufficient to cause recrystallization and a substantial decrease in dislocation density.

Plastic deformation of the niobium and tantalum specimens was carried out by tensile straining at room temperature. The wires were mounted in disc wire-grips and a gauge mark of coloured varnish was made on the wire about 0.5 cm. from each grip. The distance between the inside edges of these, about 12 cm., was measured with an accuracy of 0.02 cm. with a travelling vernier microscope. The diameter of the wire was measured at about 2 cm. intervals along the gauge length. A hand micrometer was used for this purpose and the diameter was determined with an accuracy of 0.002 mm. In no case was the diameter found to vary by more than this amount. The specimens were pulled in a Hounsfield tensometer, at a strain rate of about $1.3 \times 10^{-5} sec.^{-1}$, for a time calculated to give the required amount of plastic strain. The load was then released, the distance between the gauge marks was again measured and the actual amount of tensile strain was calculated from the increase in gauge length. The diameter was again measured at 2 cm. intervals along the gauge and if it was found to vary by more than 0.002 mm. the deformation was considered to be inhomogenous and the specimen was discarded. This usually occurred at between 1 and 3 per cent below the estimated elongation to fracture.

In Tables 9 and 10 are shown the number of irradiated and cold-worked specimens prepared, how they were divided into groups and the subsequent annealing treatment each group received. The grain size of all recrystallized sarting material was about 5 . No individual grains could be seen in the stress-relieved niobium, which had a typical cold-worked appearance under the optical microscope at a magnification of X 950.

IRRADIATED MOLYBDENUM 16 Specimens	GROUP 1	One specimen irradiated 3 months " " " 6 " " " " 9 " " " " 12 "	Annealed isochronally in silicone oil between 60 and 200° C
	GROUP 2	" " " 3 " " " " 6 " " " " 9 " " " " 12 "	Annealed isochronally in vacuum between 60 and 900°C
	GROUP 3	" " " 3 " " " " 6 " " " " 9 " " " " 12 "	Annealed isothermally in silicone oil at 140, 160, 180 and 200°C
	GROUP 4	" " " 3 " " " " 6 "	Annealed isothermally in silicone oil at 150 and 180°C
	GROUP 5	" " " 9 " " " " 12 "	Annealed for 24 hours in silicone oil at 200°C
IRRADIATED NIOBIUM 12 Specimens	GROUP 1	" " " 3 " " " " 6 " " " " 9 " " " " 12 "	Annealed isochronally in silicone oil between 60 and 180°C
	GROUP 2	" " " 3 " " " " 6 " " " " 9 " " " " 12 "	Annealed isochronally in vacuum between 60 and 400°C
	GROUP 3	" " " 3 " " " " 6 "	Annealed isothermally in silicone oil at 150 and 180°C
	GROUP 4	" " " 9 " " " " 12 "	Annealed isothermally in silicone oil at 100, 120, 140, 160 and 180°C

Table 9 List of irradiated specimens prepared and their subsequent annealing treatments.

COLD-WORKED NIOBIUM 32 Specimens Batch 1 and 12 Specimens Batch 2	GROUP 1	One specimen Batch 1 with 5.69% El. " " " " " 7.77 " " " " 2 " 4.61 " " " " " " 8.84 "	Annealed isochronally in silicone oil between 40 and 180°C.
	GROUP 2	" " " 1 " 5.41 " " " " " " 7.70 " " " " 2 " 5.45 " " " " " " 7.73 "	Annealed isochronally in vacuum between 40 and 400°C
	GROUP 3	" " " 1 " 12.30 " " " " 2 " 7.54 "	Annealed isothermally in silicone oil at 100, 120, 140, 160 and 180°C.
	GROUP 4	" " " 1 " 7.69 " " " " 2 " 7.61 "	Annealed isothermally in silicone oil at 100°C
	GROUP 5	26 specimens Batch 1 with between 0.82 and 11.58% El. 6 specimens Batch 2 with between 0.57 and 6.38% El.	Annealed in silicone oil for 24 hours at 180°C
COLD-WORKED TANTALUM 28 Specimens	GROUP 1	One specimen with 6.56% El " " " 8.74 " " " " 9.90 " " " 11.14	Annealed isochronally in silicone oil between 40 and 180°C
	GROUP 2	" " " 7.60 " " " " 8.49 " " " " 10.05 " " " " 11.17 "	Annealed isochronally in vacuum between 40 and 400°C
	GROUP 3	" " " 13.74 " " " " 10.03 "	Annealed isothermally in silicone oil at 120, 140, 160 and 180°C
	GROUP 4	18 specimens with between 1.02 and 9.54% El.	Annealed in silicone oil for 24 hours at 180°C

Table 10 List of cold-worked specimens prepared and their subsequent annealing treatments.

The specimens in each group were mounted, together where possible, either in a framework or in an evacuated glass tube. Both were designed to hold four specimens so that the niobium specimens in group 5 and the tantalum specimens in group 4 were mounted in several frames. The procedure for mounting specimens in a framework was as follows. The specimens were first placed in position by passing them through drilled holes in Sindanyo end pieces. Short lengths of recrystallized 1 mm. diameter wire of the same material as the specimens were then spot-welded to the specimens so as to connect them in series. Finally, current and potential leads of recrystallized 0.5mm. diameter wire, again of the same material as the specimens, were spot-welded in position. To prevent any relative movement between the specimens and the leads at the welds, which might cause the resistance of the specimens to change on subsequent handling, both specimens and leads were anchored in position with small screws in one end piece. For mounting specimens in an evacuated glass tube the specimens and leads were passed through holes drilled in two Sindanyo discs. The specimens were connected in series and the leads attached by spot-welding as before. The tube itself was initially in one piece and closed both top and bottom; through the top passed 10 short lengths of 0.5 mm. diameter recrystallized molybdenum wire. To mount the specimens, the tube was broken open near the top and the free ends of the current and potential leads of the specimens were spot-welded to the molybdenum wires. The two parts of the tube were fused together, with the specimens

and leads inside, and the whole was then evacuated through a short glass pumping tube. When the pressure had dropped to about 10^{-3}mm. of mercury the tube was flushed with argon gas. The tube was then pumped down overnight and finally sealed. The final pressure in the tube was considered to be less than 10^{-3}mm. of mercury.

2.2 Measurement of Resistance

The resistance of each specimen was determined by a potentiometric technique. The circuit used is shown in Figure 11.

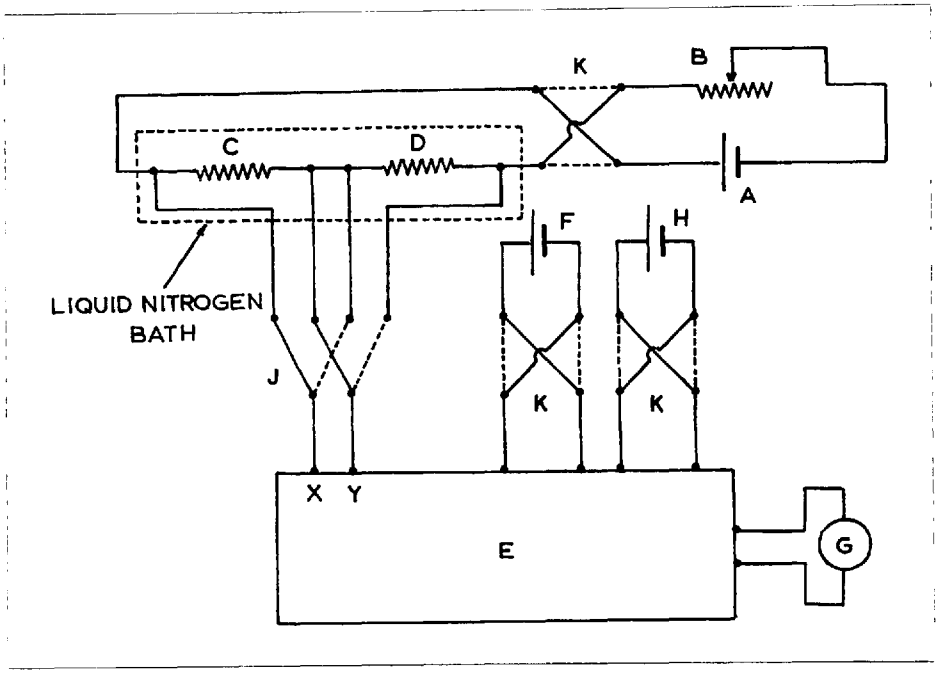


Fig. 11 Circuit used for resistance measurements.

A steady current of about 50 mA supplied by a 2V accumulator A and controlled by a decade resistance box B, was passed through the

specimen C and a standard resistor D, prepared from the same batch of annealed material as the specimen. The potential drop across the specimen P_c and that across the standard P_d were measured on a Diesselhorst potentiometer E, with its associated standard cell F, 2V accumulator H and galvanometer G. Since both specimen and standard carried the same current the relationship between P_c, P_d, the resistance R_c of the specimen and the resistance R_d of the standard was such that

$$P_c/P_d = R_c/R_d \quad . \qquad (33)$$

The value of R_d, and hence R_c, was determined by replacing the specimen with a manganin resistor of known resistance and obtaining the resistance ratio. The resistivity ρ of the specimen was determined by measuring the distance l between the welds connecting the two potential leads to the specimen and the diameter d of the wire, using the microscope and micrometer as described in 2.1, and employing the formula

$$\rho = \frac{R_c \pi d^2}{4} \quad . \qquad (34)$$

The ratio P_c/P_d was determined after every annealing treatment the specimen received. Since R_d remained constant, any change in the ratio was due to a change in R_c and in fact the fractional change in the ratio could be identified as a fractional change in the resistance and also the resistivity of the specimen. Both specimen and standard were immersed in boiling liquid nitrogen whilst measurements were made.

This ensured that all resistance measurements were made at the same temperature and also increased any change observed in the resistance ratio by a factor of about 5 over that observed at room temperature, since the thermal term in the resistance was considerably reduced. Having the specimen and standard of the same material and at the same temperature also reduced the effect of any change in the boiling point of the nitrogen due to dissolved oxygen and variations in atmospheric pressure.

The resistance measuring circuit was designed to eliminate thermo - e.m.f.s, since these effected the reproducibility of the resistance ratio. The Diesselhorst potentiometer is designed to reduce to a minimum the effect of thermo - e.m.f.s generated in the potentiometer itself. The principle of its design is shown in Figure 12.

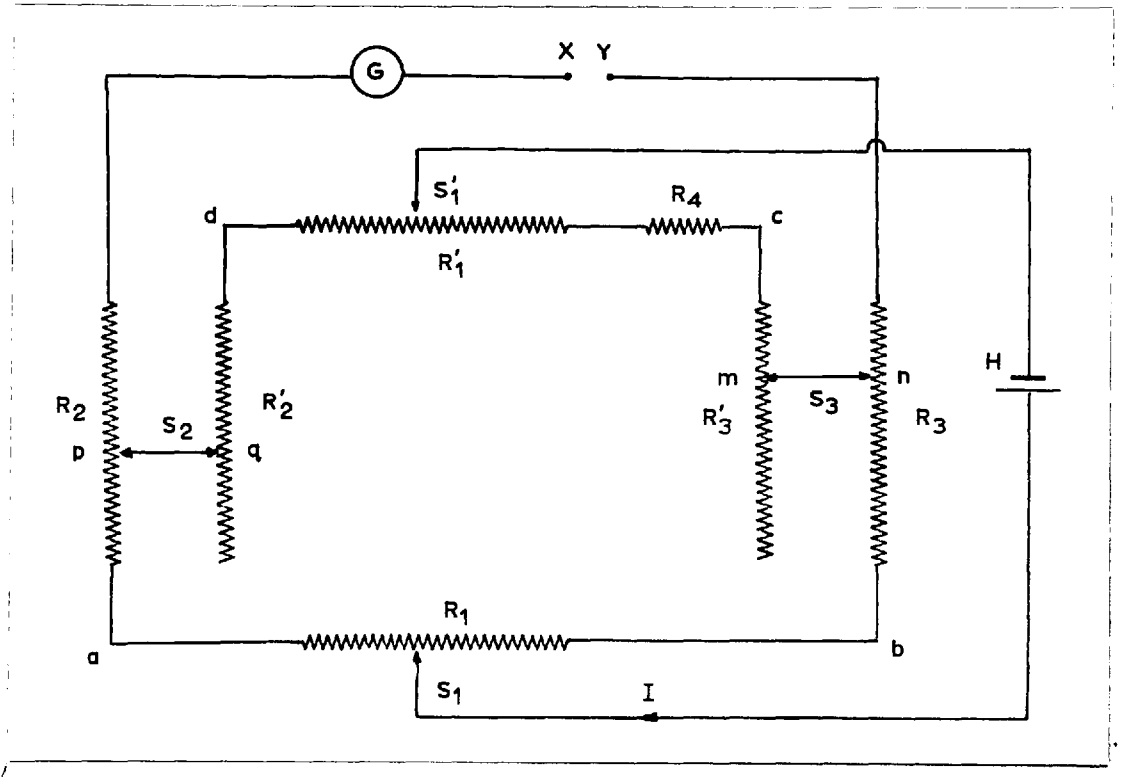


Fig. 12 Circuit diagram of the Diesselhorst potentiometer. (After Chalmers and Quarrel[59].)

The potentiometer network is made up of the resistances shown, the following being identical in pairs; R_1 and R'_1, R_2 and R'_2, and R_3 and R'_3. The resistances are built up of accurately matched resistance coils. The contacts S_1 and S'_1 are mechanically linked so that on turning a rotary switch, S'_1 moves to the right the same amount as S_1 moves to the left, the position being indicated on a dial. By turning another rotary switch, the connecting contact S_2 moves the same amounts over the resistances R_2 and R'_2, the position again being indicated on a dial. S_3 moves in a similar manner over R_3 and R'_3. Thus no matter how the positions of S_1, S'_1, S_2 and S_3 are changed the resistances in the arms S_1 bc S'_1 and S_1 a d S'_1 remain constant. The value of R_4 is so chosen that the resistance in S_1 bc S'_1 is exactly ten times that in S_1 a d S'_1 so that 1/11 of the total current I passes to the right of the network and 10/11 to the left, and the value of I is, of course, independent of the positions of the switches. I is fixed at a standard value by means of the standard cell F in Figure 11. The potential difference to the measured is connected across the points X and Y, so that the potential difference against which it is to be balanced is that between the points p and n. This potential is dependent upon the positions of the switches S_1, S'_1, S_2 and S_3 and the resistance values are so chosen that when the switches are set to give balance the dial readings give the potential difference directly in volts. R_1 and R'_1 are actually more complicated than shown and the potential is indicated on 5 dials covering 5 orders of magnitude. The circuit constants are such that the resistance in the galvanometer circuit is

almost independent of the positions of the switches so that the galvanometer deflection may be used to interpolate between readings on the last decade dial with a high degree of accuracy. The particular value of this circuit lies in its virtual elimination of thermo-electric effects due to the switches. Any e.m.f.s due to manipulation of switches S_1 and S'_1 will simply be added to the battery e.m.f. and be negligible in effect. If an e.m.f. E' is caused by manipulating S_2 the effect can be regarded as superimposing on the existing currents in the circuit p a b n m c d q a current of magnitude

$$\frac{E}{(R_1 + R'_1 + R_2 + R_3 + R_4)} .$$

The change in potential between p and n as a result of this is

$$\frac{ER}{(R_1 + R'_1 + R_2 + R_3 + R_4)} ,$$

where R is the resistance in the branch p a b n. The ratio

$$\frac{R}{(R_1 + R'_1 + R_2 + R_3 + R_4)}$$

is of the order 1/100 so that the error due to the e.m.f. is reduced to about 1 per cent of the actual potential generated. Similar considerations apply to the thermo - e.m.f.s generated at the other switches in the instrument. That part of the resistance measuring circuit outside the potentiometer was constructed of copper where possible. The free ends of the potential leads of the specimen and

standard were connected to small copper terminal blocks which in turn were connected by screened copper wire to an oil-immersed all-copper selector switch J (Fig. 11). The output side of the switch was connected to the XY terminals of the potentiometer. In order to reduce the effect of those thermo - e.m.f.s remaining in the circuit the potentials across the specimen and standard were measured with the current passing in both directions. The average potentials across the specimen and standard were then used to determine the ratio P_c / P_d. The reversing switch K (Fig. 11) used for this purpose was oil-immersed and constructed entirely of copper. It simultaneously reversed the current through the specimen and standard, reversed the currents in the battery and standard cell circuits of the potentiometer, and interrupted the galvanometer circuit.

2.3 Methods of annealing

Annealing treatments up to 260°C were carried out in a well-stirred silicone oil bath, the temperature of which was controlled to within 0.1°C of its nominal value by a modified toluene regulator in which the toluene was replaced by silicone oil so that the regulator could be operated at higher temperatures. The temperature of the bath was measured with an accuracy of 0.1°C with a calibrated mercury-in-glass thermometer. Annealing treatments between 260 and 650°C were carried out in a molten salt bath the temperature of which was controlled to within 0.5°C of its nominal value by an electronic proportional

controller. The temperature of the bath was measured with a calibrated chromel-alumel thermocouple. Annealing treatments between 050 and 900°C were carried out in a kanthal wound tube furnace the temperature of which was controlled to within 2°C of its nominal value. The methods of temperature control and measurement were the same as those for the salt bath. Annealing treatments up to 180°C in the case of niobium and tantalum and 200°C in the case of molybdenum could be carried out with the specimens in direct contact with the silicone oil. Up to these temperatures there was no change in the resistance of control specimens prepared from annealed material. Above these temperatures, however, the resistance of the control specimens rose, presumably due to oxidation, and all specimens had to be annealed in vacuum. The evacuated glass tubes began to soften at 400°C so that this was the maximum annealing temperature normally used. However, group 2 irradiated molybdenum specimens were annealed at temperatures up to 900°C by transferring the specimens to a mullite sheath after the 400° anneal. This was continuously evacuated to a pressure probably below 10^{-3} mm. of mercury.

Both isochronal and isothermal methods of annealing were employed. The isochronal method was used to determine the temperatures at which recovery occured and the isothermal method was used to investigate further the recovery processes revealed by the isochronal method.

2.3.1 Isochronal annealing procedure

In the isochronal method the resistance ratio R_c / R_d was first determined with the specimen in the irradiated or cold-worked condition. The specimen was then annealed for 4 hours at a temperature 20°C above the temperature of irradiation or cold-work. The resistance ratio was again determined, the temperature of the bath was raised 20°C and the specimen was annealed for a further 4 hours. This procedure was repeated over the temperature range of interest. Each resistance ratio was divided by the ratio obtained in the cold-worked or irradiated state which gave the resistance of the specimen as a fraction, R_f, of the resistance in the damaged condition. This fraction was found to be reproducible to about 2 parts in 10^4. An isochronal annealing curve of R_f as a function of annealing temperature was then plotted and this gave an immediate indication of any recovery process that had taken place.

2.3.2 Isothermal annealing procedure

In the isothermal method the specimen was annealed at a temperature at which recovery was known to occur and an isothermal annealing curve of R_f as a function of annealing time was obtained. Measurements were taken until the shape of the curve was well-defined. The temperature of the bath was then raised 20°C and a further curve was obtained. This procedure was repeated until no further recovery occured. The major recovery process in each specimen took place at temperatures below those at which oxidation was expected to occur so

that all the isothermal curves were obtained with specimens in direct contact with the silicone oil in the annealing bath. This eliminated the necessity of having to calculate the "effective" annealing times of specimens that have been heated in vacuum. The specimen was plunged into the bath at the start of each anneal and rapidly withdrawn and quenched in cold silicone oil at the end. The time that the specimen was at the temperature of the bath was estimated to within about 2 seconds. The shortest annealing time used was 3 minutes. From the series of curves obtained it was possible to calculate the activation energy of the recovery process. The method used assumes the validity of the equation

$$d R_f / dt = -f(R_f - R_o) \; e^{-E_m / kT} , \qquad (35)$$

where R_o is the value of R_f with no defects present, R_f is the resistance fraction with n defects present, t is the annealing time, T is the absolute annealing temperature, E_m is the activation energy of the recovery process and k is Boltzmann's constant. If the final rate $(dR_f / dt)_1$ at a temperature T_1 and the initial rate $(dR_f / dt)_2$ at the following temperature T_2 are known then,

$$E_m = \frac{k T_1 T_2}{T_2 - T_1} \ln (dR_f / dt)_2 / (dR_f / dt)_1 , \qquad (36)$$

at a temperature $(T_1 + T_2) / 2$, since $f(R_f - R_o)$ is the same for each annealing curve. To determine the values of the slopes at the point of intersection of two isothermals the following procedure was adopted. The slope at the mid-point of a curve between two adjacent experimental

points was assumed to be equal to the slope of a straight line joining the two points. This slope was plotted on a logarithmic scale against the value of R_f at the mid-point. Two roughly parallel straight lines were obtained, each line representing an isothermal. It was only necessary to extrapolate each line a short distance in order to obtain the values of dR_f/dt at the point of intersection.

The number of jumps to annihilation associated with a recovery process was calculated using the method described in 1.3. The isothermal annealing curves used for this purpose were those obtained for group 3 irradiated molybdenum specimens, group 3 cold-worked niobium and tantalum specimens and groups 3 and 4 irradiated niobium specimens. The resistivity recovery due to each recovery process was calculated and the fraction of this extra resistivity remaining after an anneal was plotted on a logarithmic scale as a function of annealing time. A series of approximately straight lines was obtained for each specimen. The slope S of the line during which 50 per cent recovery occured was measured and inserted in equation 27;

$$j = Z\alpha\nu S^{-1} e^{\Delta S/k} e^{-E_m/kT}. \qquad (27)$$

The other parameters were given the following values; $Z = 8$, $\alpha = 1/8$, $\nu = 10^{13}$, T = temperature of anneal during which 50 per cent recovery occured, E_m = measured activation energy of recovery process, $e^{\Delta S/k} = 5$.

3 RESULTS

3.1 Irradiated Molybdenum

The effect of irradiation on the resistivity of the 16 molybdenum specimens is shown in Table 11. The maximum expected experimental error in any resistivity measurement is about ±0.0035 $\mu\Omega$cm. and that in any change in resistivity is about ±0.00008 $\mu\Omega$cm. or ±0.5%, whichever is the greater. The results are summarized in graphical form in Figure 13, in which the average increase in resistivity for each dose is plotted as a function of irradiation time. There is an almost linear increase up to a time of 3 months but after this the rate of change decreases and there is little difference between specimens irradiated for 9 and 12 months. By plotting the increase in resistivity, $\Delta\rho$, and the irradiation time, t, in months, on logarithmic scales (Figure 14) the equation of the curve was found to be

$$\Delta\rho = 0.071\ t^{0.54}\ \mu\Omega\text{cm.} \qquad (37)$$

The maximum increase in resistivity observed, 0.236$\mu\Omega$cm. for a specimen irradiated for 12 months, represents about 46% of the resistivity of an unirradiated specimen, measured at -196°C.

Isochronal annealing curves are shown in Figure 15 for specimens irradiated for 3, 6, 9 and 12 months and annealed in vacuum at temperatures up to 400°C. The curves obtained by annealing in silicone oil are identical with these up to 200°C and are therefore not reproduced. (This also applies to the curves obtained for irradiated and cold-worked niobium and cold-worked tantalum, except that deviations occurred at 200°C.) A major recovery process occurs between 100 and 200°C and a minor one at 280°C. These processes are shown

more clearly in the annealing spectra of Figure 16. To obtain these the change in R_f due to annealing at a particular temperature was divided by the temperature interval between this anneal and the preceding one and plotted against the mean temperature of the two anneals. The resistivity change during the major recovery process is given in Table 12, which shows that for all specimens about 55% of the extra resistivity due to irradiation anneals out between 40 and 180°C. The average result for each dose is shown graphically in Figure 17, in which the change in resistivity is plotted as a function of irradiation time. This curve appears to pass through a maximum. Table 12 also gives the recovery obtained on annealing at temperatures up to 900°C. This varies from 85 to 95% according to the time of irradiation.

Isothermal annealing curves of R_f as a function of annealing time t are shown in Figure 18 for specimens irradiated for 3, 6, 9 and 12 months and annealed in silicone oil at 140, 160, 180 and 200°C. In Figure 19 R_f has been plotted against log. $\Delta R_f/\Delta t$ and from these curves the values of the slopes at the intersections of the isothermals have been obtained. The activation energies calculated from these slopes by the method described in 2.3.2 are given in Table 15, together with the values obtained for the two specimens of group 4 which were irradiated for 3 and 6 months and annealed in silicone oil at 150 and 180°C. The average value of the 14 determinations is 1.25 eV with an r.m.s. deviation of 0.08 eV. The maximum expected experimental error in any value varies

from ±0.09 and ±0.02 eV according to the magnitude of the values of dR_f/dt at the intersections of the isothermals. Thus the activation energy would appear to be independent of both irradiation time and annealing temperature. The number of jumps to annihilation associated with the recovery of each specimen of group 3 is also given in Table 15. This is of the order of 10^3.

3.2 Irradiated Niobium

Isochronal annealing curves are shown in Figure 20 for niobium specimens irradiated for 3, 6, 9 and 12 months and annealed in vacuum at temperatures up to 400°C. A major recovery process occurs between 80 and 180°C. This is shown more clearly in the annealing spectra of Figure 21 obtained in the same way as those for the irradiated molybdenum. The resistivity change during the recovery process is given in Table 13. The maximum expected experimental error in any resistivity measurement is about ±0.01 $\mu\Omega$cm. and that in any change in resistivity is about ±0.00036 $\mu\Omega$cm. or ±0.5%, whichever is the greater. The average resistivity recoveries are shown graphically in Figure 17 where they can be compared with those obtained for molybdenum. This curve passes through a more pronounced maximum than that for molybdenum and for comparable irradiation times the resistivity recovery of niobium is greater than that of molybdenum by a factor of about 1.5.

Isothermal annealing curves for specimens irradiated for 3 and 6 months and annealed in silicone oil at 150 and 180°C are

shown in Figure 22. Curves for specimens irradiated for 9 and 12 months and annealed in silicone oil at 100, 120, 140, 160 and 180°C are shown in Figure 23. The corresponding plots of R_f as a function of log. $\Delta R_f/\Delta t$ are shown in Figures 24 and 25 and the activation energies calculated from the slopes at the intersections of the isothermals are given in Table 15. The average value of the 10 determinations is 1.22 eV with an r.m.s. deviation of 0.02 eV. The maximum expected experimental error in any value, as in the previous case of molybdenum, varies from ±0.09 to ±0.02 eV so that again the activation energy would appear to be independent of both irradiation time and annealing temperature. The number of jumps to annihilation associated with the recovery of each specimen of groups 3 and 4 is also given in Table 15. This is of the order of 10^2 compared with the 10^3 obtained for molybdenum.

3.3 Cold-Worked Niobium

Isochronal annealing curves are shown in Figure 26 for four cold-worked niobium specimens, two of recrystallized and two of stress-relieved material, annealed in vacuum at temperatures up to 400°C. As in the irradiated specimens, a distinct recovery process occurs between 80 and 180°C. Between 200 and 400°C further, continuous recovery occurs which is quite appreciable in the stress-relieved material. Annealing spectra are shown in Figure 27 for two of these specimens, one recrystallized and one stress-relieved. In Figure 28 the resistivity recovery during the process is plotted as a function of tensile strain, for both types of material.

The data from which these curves were obtained are given in Table 14. The maximum expected experimental error in any resistivity change is the same as that given previously for irradiated niobium. It can be seen that for comparable strains the recovery is far greater in the stress-relieved material and that for this the curve is a decelerating one, compared with an accelerating one for the recrystallized material. The recovery obtained for the most heavily deformed stress-relieved specimens is similar to that obtained for niobium specimens irradiated for 3 months. By plotting both the change in resistivity and tensile strain on logarithmic scales, (Figure 29), the equations of the curves were found to be

$$\Delta = 0.77\,\varepsilon^{1.46}\ \mu\Omega\text{cm}. \qquad (38)$$

and

$$\Delta = 0.45\,\varepsilon^{0.66}\ \mu\Omega\text{cm}. \qquad (39)$$

for the recrystallized and stress-relieved material respectively, where ε is the fractional tensile strain.

Isothermal annealing curves for one recrystallized and one stress-relieved specimen annealed in silicone oil at 100, 120, 140, 160 and 180°C are shown in Figure 30. The corresponding plots of R_f against log. $\Delta R_f/\Delta t$ are shown in Figure 31 and the activation energies calculated from these are given in Table 16. The average value of the 8 determinations is the same as that for the irradiated niobium, that is, 1.22 eV, with an r.m.s. deviation of 0.02 eV. The maximum expected experimental error varies from $\pm$0.6 to $\pm$0.1 eV so that the activation energy would appear to be independent of the

initial dislocation density of the material, the amount of plastic deformation and the annealing temperature. The number of jumps to annihilation associated with the recovery process, given in Table 16, is the same for both types of material and is of the same order as that for the irradiated specimens, that is, 10^3. The initial recovery of both irradiated and cold-worked niobium can be compared in Figure 32. Each irradiated specimen shows an incubation period which is completely absent in the cold-worked material.

3.4 Cold-Worked Tantalum

Isochronal annealing curves for four cold-worked tantalum specimens annealed in vacuum at temperatures up to 400°C are shown in Figure 33. As in the cold-worked niobium specimens, a distinct recovery process occurs between 80 and 180°C. There is also some recovery between 300 and 400°C, similar to that found in niobium, but it is only appreciable in the more heavily deformed specimens. The annealing spectrum for one of these is shown in Figure 27. The resistivity change during the recovery process is plotted as a function of tensile strain in Figure 28. The data from which this curve was obtained are given in Table 14. The maximum expected experimental error in any resistivity change is the same as that given for niobium. The shape of the curve is similar to that obtained for recrystallized niobium and from the log.-log. plot of Figure 29 the equation of the curve was found to be

$$\Delta\rho = 2.01\varepsilon^{1.41}\ \mu\Omega\text{cm}. \qquad (40)$$

It can be seen that for comparable strains the resistivity change in tantalum is greater than that in niobium by a factor of about 3.

Isothermal annealing curves for four specimens annealed in silicone oil at 120, 140, 160 and 180°C are shown in Figure 34. The corresponding plots of R_f against log. $\Delta R_f/\Delta t$ are shown in Figure 35 and the activation energies calculated from these are given in Table 16. The average value of the 10 determinations is 1.25 eV with an r.m.s. deviation of 0.02 eV. The maximum expected experimental error in any value varies from ±0.08 to ±0.05 eV so that again the activation energy would appear to be independent of both amount of plastic deformation and annealing temperature. The number of jumps to annihilation associated with the recovery process was found to be 10^3, the same as that for cold-worked niobium.

Time of Irradiation	Specimen Group Number	Resistivity at -196°C μΩcm.	Average Resistivity at -196°C μΩcm.	Increase in Resistivity μΩcm.	Average Increase in Resistivity μΩcm.	Average Increase in Resistivity %
Nil			0.532 ±0.002 (Average of four Specimens)			
3 Months	1	0.657	0.659 ±0.006	0.125	0.127 ±0.006	24±1
	2	0.663		0.131		
	3	0.665		0.133		
	4	0.650		0.118		
6 Months	1	0.719	0.720 ±0.006	0.187	0.188 ±0.006	35±1
	2	0.719		0.187		
	3	0.712		0.180		
	4	0.730		0.197		
9 Months	1	0.753	0.756 ±0.003	0.221	0.224 ±0.003	42±1
	2	0.762		0.230		
	3	0.754		0.221		
	5	0.755		0.223		
12 Months	1	0.762	0.764 ±0.003	0.230	0.232 ±0.003	46.5±0.5
	2	0.765		0.233		
	3	0.768		0.236		
	5	0.760		0.228		

Table 11 Data on the increase in resistivity of molybdenum on irradiation.

Time of Irradiation	Specimen Group Number	Resistivity Recovery between 40 and 180°C μΩcm.	Average Resistivity Recovery between 40 and 180°C μΩcm.	Average Resistivity Recovery between 40 and 180°C %	Resistivity Recovery between 40 and 900°C %
3 Months	1	0.067	0.069 ±0.002	54±2	84.7
	2	0.071			
	3	0.066			
	4	0.071			
6 Months	1	0.108	0.107 ±0.002	57±1	94.7
	2	0.105			
	3	0.105			
	4	0.108			
9 Months	1	0.126	0.126 ±0.003	56±1	95.2
	2	0.123			
	3	0.124			
	5	0.129			
12 Months	1	0.126	0.123 ±0.003	53±1	94.8
	2	0.121			
	3	0.118			
	5	0.124			

Table 12 Data on the resistivity recovery of irradiated molybdenum.

Time of Irradiation	Specimen Group Number	Resistivity at -196°C μΩcm.	Average Resistivity at -196°C μΩcm.	Resistivity Recovery between 40 and 180°C μΩcm.	Average Resistivity Recovery between 40 and 180°C μΩcm.
Nil			4.85 ±0.18 (Average of five Specimens)		
3 Months	1	4.71	4.80 ±0.08	0.107	0.104 ±0.003
	2	4.90		0.105	
	3	4.79		0.101	
6 Months	1	4.41	4.74 ±0.20	0.191	0.194 ±0.001
	2	5.07		0.193	
	3	4.75		0.194	
9 Months	1	4.71	4.57 ±0.11	0.235	0.229 ±0.005
	2	4.44		0.223	
	4	4.57		0.230	
12 Months	1	4.86	4.88 ±0.02	0.210	0.211 ±0.002
	2	4.91		0.209	
	4	4.87		0.213	

Table 13 Data on the resistivity recovery of irradiated niobium.

NIOBIUM Batch 1 (Recrystallized)		NIOBIUM Batch 2 (Stress-Relieved)		TANTALUM (Recrystallized)	
% El	$\Delta\rho$, $\mu\Omega$cm.	% El	$\Delta\rho$, $\mu\Omega$cm.	% El	$\Delta\rho$, $\mu\Omega$cm.
0.82	0.0008	0.57	0.015	1.02	0.0031
1.52	0.0017	1.34	0.025	1.38	0.0049
2.22	0.0030	2.17	0.036	1.79	0.0066
2.98	0.0042	3.25	0.048	2.12	0.0080
3.65	0.0064	4.15	0.055	2.19	0.0092
4.04	0.0071	4.61	0.060	2.52	0.0104
4.27	0.0079	5.45	0.067	2.66	0.0122
4.33	0.0077	6.38	0.072	3.01	0.0141
4.34	0.0075	7.54	0.083	3.22	0.0171
5.41	0.0109	7.73	0.084	3.50	0.0183
5.69	0.0129	8.84	0.090	3.97	0.0205
5.88	0.0126			4.29	0.0259
5.94	0.0132			4.74	0.0279
6.03	0.0131			5.48	0.0332
6.10	0.0126			5.54	0.0295
6.60	0.0150			5.96	0.0420
6.64	0.0144			6.19	0.0378
7.70	0.0175			6.56	0.0442
7.77	0.0189			7.60	0.0538
7.79	0.0178			8.24	0.0613
8.12	0.0203			8.49	0.0592
8.31	0.0200			9.54	0.0680
9.43	0.0231			9.90	0.0721
9.65	0.0261			10.05	0.0760
9.66	0.0262			11.14	0.0827
9.75	0.0266			11.17	0.0895
10.22	0.0284			13.74	0.1214
10.23	0.0290			16.03	0.1516
10.68	0.0303				
11.58	0.0330				
12.30	0.0385				

Table 14 Resistivity recovery of cold-worked niobium and tantalum in the temperature range 20 to 180°C.

% El = percentage tensile strain; $\Delta\rho$, = change in resistivity

Material	Specimen Group Number	Time of Irradiation, months	Isothermal T_1, °C	Isothermal T_2, °C	$\frac{T_1 + T_2}{2}$, °C	Activation Energy E_m, eV	Number of Jumps j at 50% Recovery
IRRADIATED MOLYBDENUM	3	3	140.1	160.0	150.1	1.25	4×10^3
	"		160.0	180.0	170.0	1.30	
	"		180.0	200.1	190.1	1.27	
	4		150.0	180.0	165.0	1.18	
	3	6	140.1	160.0	150.1	1.32	3×10^3
	"		160.0	180.0	170.0	1.22	
	"		180.0	200.1	190.1	1.30	
	4		150.0	180.0	165.0	1.27	
	3	9	140.1	160.0	150.1	1.10	4×10^3
	"		160.0	180.0	170.0	1.25	
	"		180.0	200.1	190.1	1.37	
	3	12	140.1	160.0	150.1	1.08	3×10^3
	"		160.0	180.0	170.0	1.30	
	"		180.0	200.1	190.1	1.32	
IRRADIATED NIOBIUM	3	3	150.0	180.0	165.0	1.19	3×10^2
	3	6	150.0	180.0	165.0	1.21	3×10^2
	4	9	100.0	120.0	110.0	1.21	3×10^2
	"		120.0	140.0	130.0	1.25	
	"		140.0	160.0	150.0	1.25	
	"		160.0	180.0	170.0	1.25	
	4	12	100.0	120.0	110.0	1.22	3×10^2
	"		120.0	140.0	130.0	1.24	
	"		140.0	160.0	150.0	1.24	
	"		160.0	180.0	170.0	1.19	

Table 15 Activation energies and numbers of jumps to annihilation associated with the recovery processes observed in the temperature range 80 to 180°C in irradiated molybdenum and niobium.

Material	Specimen Group Number	Amount of Cold-Work	Isothermal T_1, °C	Isothermal T_2, °C	$\frac{T_1 + T_2}{2}$, °C	Activation Energy E_m, eV	Number of Jumps j at 50% Recovery
COLD-WORKED NIOBIUM	3	12.30 % El (Batch 1)	100.0	120.0	110.0	1.21	1×10^3
	"		120.0	140.1	130.1	1.24	
	"		140.1	160.1	150.1	1.19	
	"		160.1	180.0	170.1	1.20	
	3	7.54 % El (Batch 2)	100.0	120.0	110.0	1.22	1×10^3
	"		120.0	140.1	130.1	1.23	
	"		140.1	160.1	150.1	1.24	
	"		160.1	180.0	170.1	1.22	
COLD-WORKED TANTALUM	3	13.74 % El	120.1	140.0	130.1	1.27	1×10^3
	"		140.0	160.1	150.1	1.26	
	"		160.1	180.0	170.1	1.25	
	3	16.03 % El	120.1	140.0	130.1	1.27	1×10^3
	"		140.0	160.1	150.1	1.22	
	"		160.1	180.0	170.1	1.26	

Table 16 Activation energies and numbers of jumps to annihilation associated with the recovery processes observed in the temperature range 80 to 180°C in cold-worked niobium and tantalum.

Metal	Crystal Structure	T_m , °K	E_d , eV	$E_d/T_m \times 10^{-3}$	Ref.
Na	b.c.c.	371	0.44	1.2	60, 61, 62, 63.
Li	b.c.c.	459	0.57	1.2	60, 62, 64.
Cd	c.p.h.	594	0.79	1.3	65.
Pb	f.c.c.	600	1.08	1.8	66, 67.
Zn	c.p.h.	693	0.91	1.3	68, 69, 70, 71.
Mg	c.p.h.	924	1.40	1.5	72.
Al	f.c.c.	933	1.40	1.5	73.
Ag	f.c.c.	1234	1.93	1.6	74, 75, 76, 77.
Au	f.c.c.	1336	1.84	1.4	78, 79, 80, 81.
Cu	f.c.c.	1357	2.04	1.5	82, 83.
Ni	f.c.c.	1725	2.82	1.6	84, 85.
Co	f.c.c.	1753	2.93	1.7	86, 87.
Pt	f.c.c.	2047	2.96	1.5	88.
γ-Fe	f.c.c.	1810	2.92	1.6	89, 90, 91.
α-Fe	b.c.c.	1810	2.92	1.6	92.
Cr	b.c.c.	2147	3.00	1.4	93, 94, 119, 120.
Nb	b.c.c.	2741	4.56	1.7	95.
Mo	b.c.c.	2895	4.95	1.7	94.
Ta	b.c.c.	3269	4.77	1.5	96, 97.
W	b.c.c.	3643	5.89	1.6	55.

Table 17 Experimental self-diffusion activation energies for some metallic elements.

Tm = melting temperature; E_d = activation energy for self-diffusion

Metal	E_f , eV	E_m , eV	E_f/E_d	E_m/E_d	Ref.
Al	0.76 Q		0.54		98
	0.76 Q		0.54		99
	0.79 Q	0.65 Q	0.56	0.46	100
		0.55 I		0.39	101
Ag	1.06 Q		0.55		102
		0.65 W		0.34	103
Au	0.95 Q		0.52		104
	0.98 Q	0.82 Q	0.53	0.45	26
		0.69 W		0.38	103
Cu	1.0 Q		0.49		105
		0.67 W		0.33	106
		0.68 I		0.33	107
		0.72 I		0.35	108
		0.60 I		0.29	109
Ni	1.4 Q		0.50		110
		1.0 W		0.35	111
		1.05 W&I		0.37	112
Pt	1.4 Q		0.47		113
	1.23 Q	1.42 Q	0.42	0.48	114
	1.20 Q	1.48 Q	0.41	0.50	115
		1.43 W&I		0.48	22
Nb		1.22 W		0.27	This Work
		1.3 I		0.29	44
		1.22 I		0.27	This Work
Mo		1.26 W		0.24	48
		1.3 I		0.25	17
		1.25 I		0.24	This Work
Ta		1.25 W		0.26	This Work
W		1.7 W		0.29	50
		1.73 W		0.29	51
		1.7 I		0.29	17
		1.7 I		0.29	39

Table 18 Measured vacancy formation and migration energies for some f.c.c. and b.c.c. metals.

Ef = formation energy; Em = migration energy (Stage III recovery);
Q = quenched material; W = cold-worked material;
I = irradiated material.

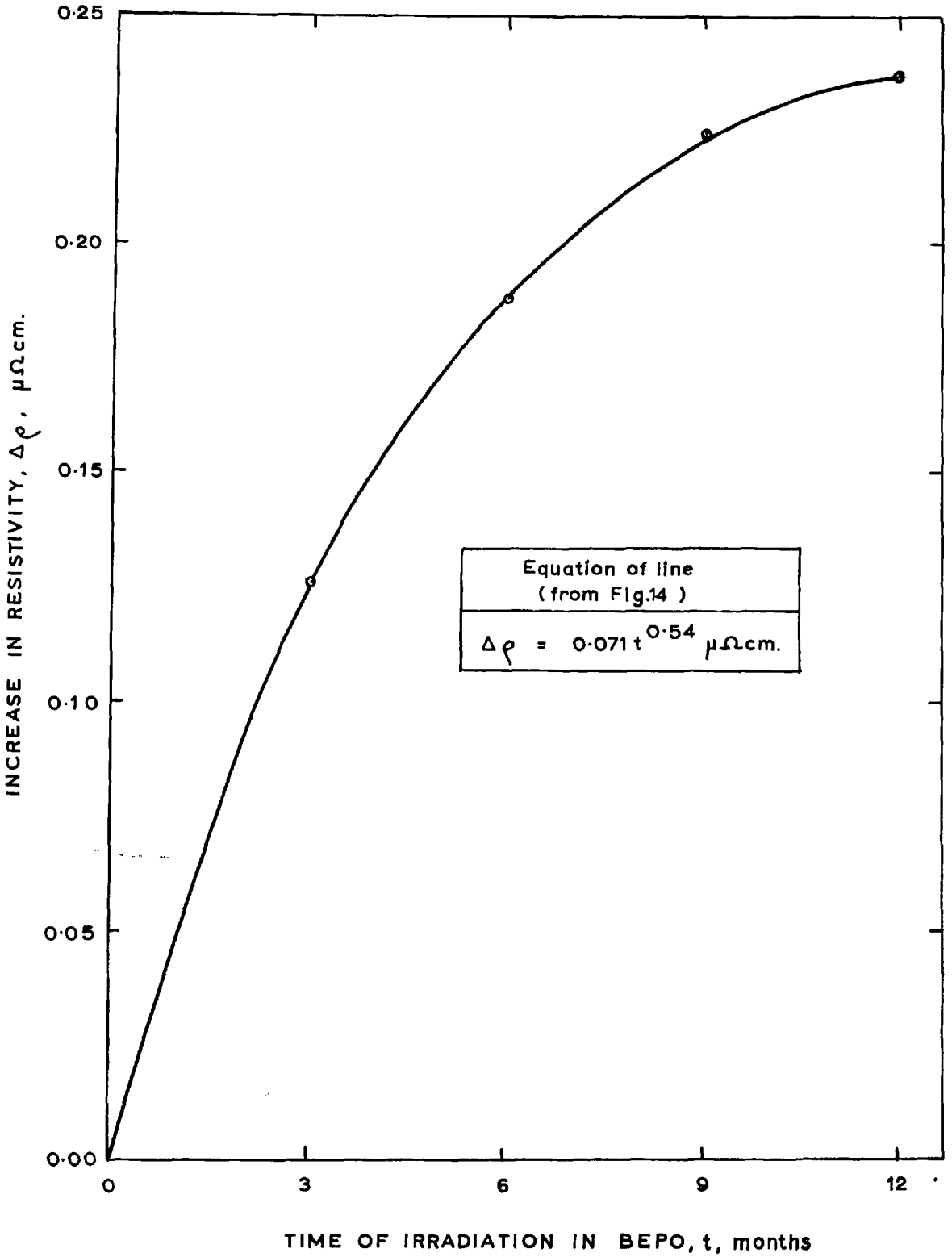


FIG.13 INCREASE IN RESISTIVITY AS A FUNCTION OF IRRADIATION TIME FOR MOLYBDENUM IRRADIATED IN BEPO AT 40°C

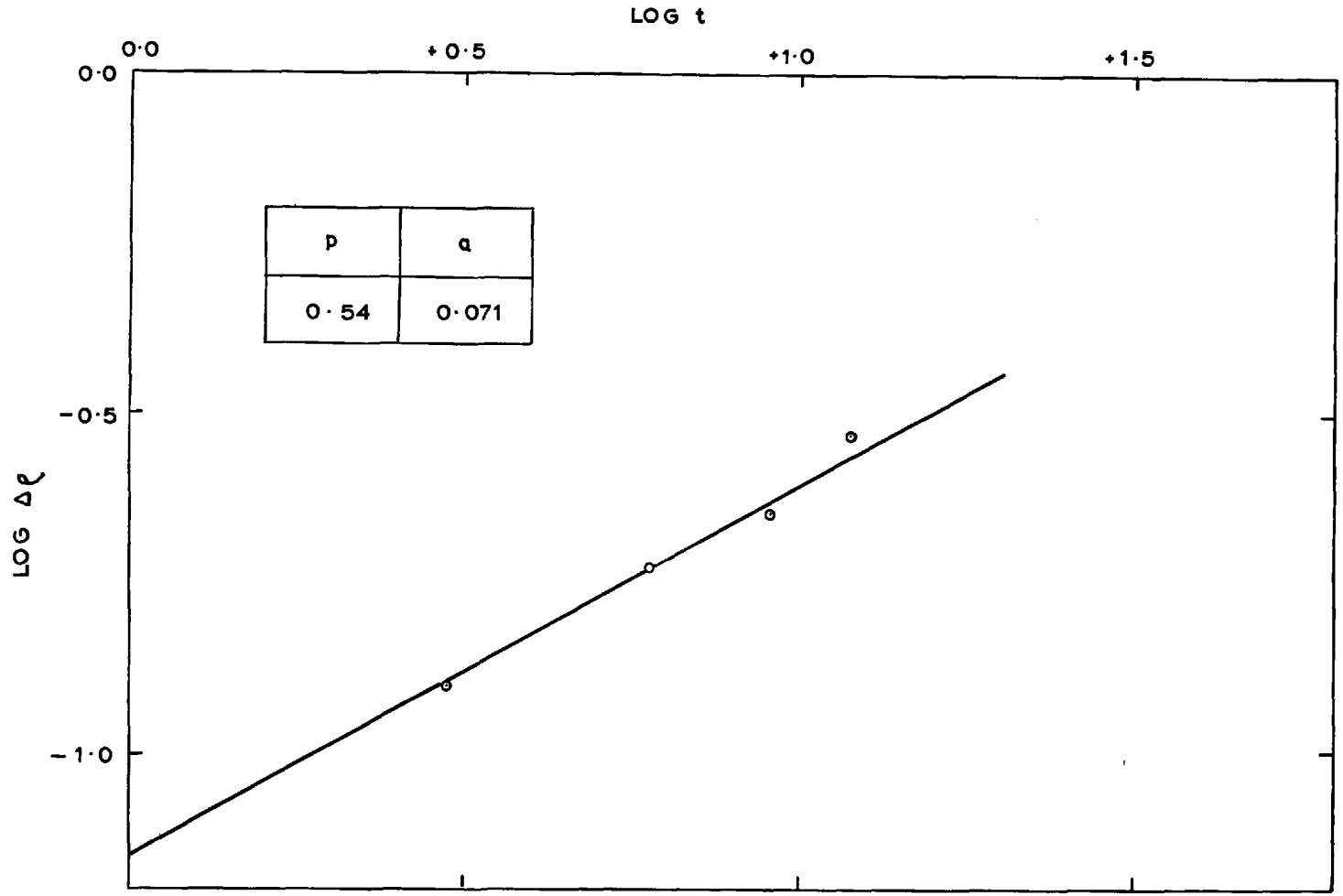


FIG.14 GRAPH SHOWING THE LINEAR RELATIONSHIP BETWEEN LOG $\Delta\rho$ AND LOG t FOR IRRADIATED MOLYBDENUM USING THE DATA OF FIG.13. THE RELATIONSHIP BETWEEN $\Delta\rho$ AND t IS THUS OF THE FORM $\Delta\rho = a t^{p}$

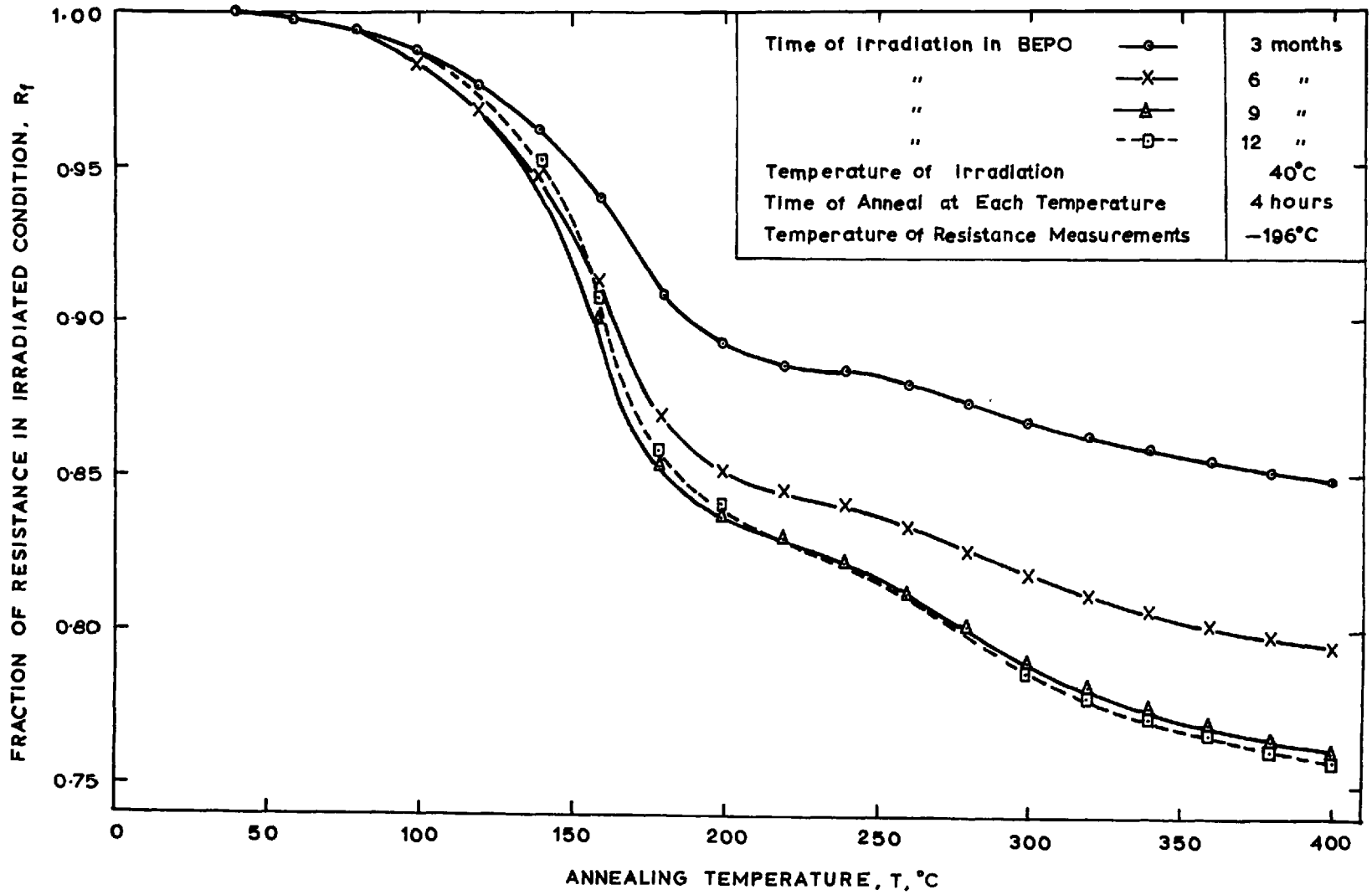


FIG.15 ISOCHRONAL ANNEALING CURVES FOR IRRADIATED MOLYBDENUM

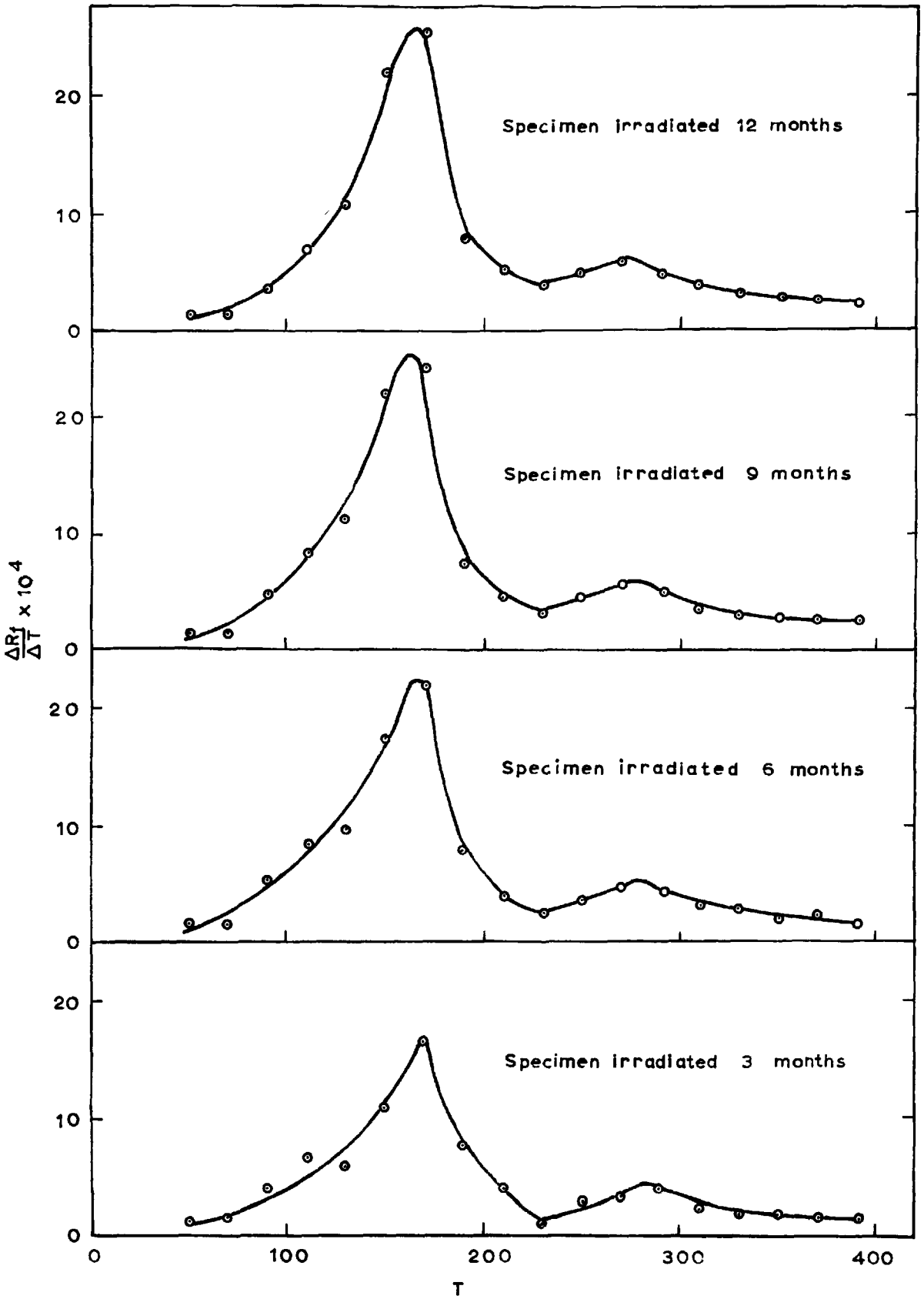


FIG 16 $\frac{\Delta R_f}{\Delta T}$ PLOTTED AGAINST T FOR IRRADIATED MOLYBDENUM USING THE DATA OF FIG.

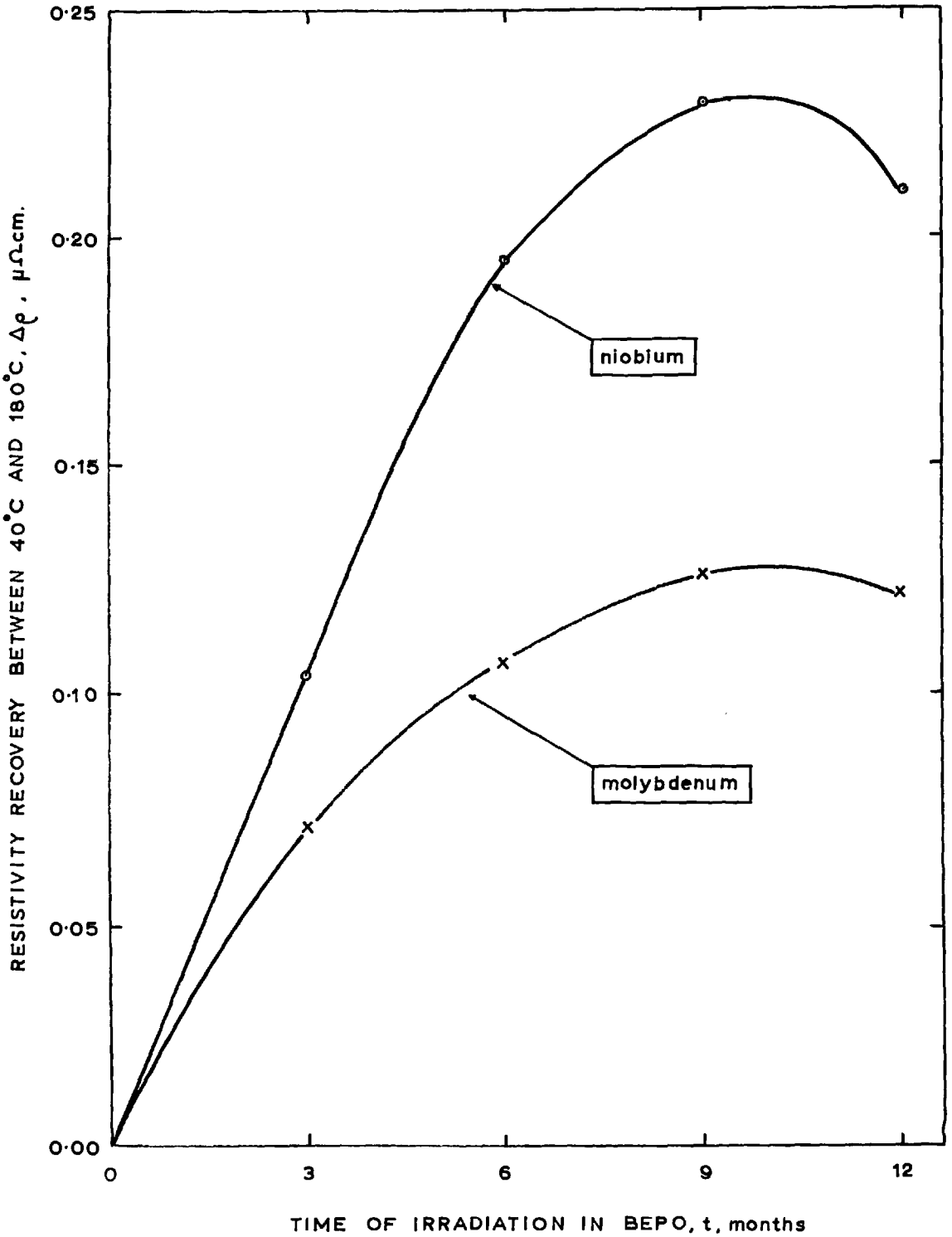


FIG.17 RESISTIVITY RECOVERY BETWEEN 40°C AND 180°C AS A FUNCTION OF IRRADIATION TIME FOR MOLYBDENUM AND NIOBIUM IRRADIATED IN BEPO AT 40°C

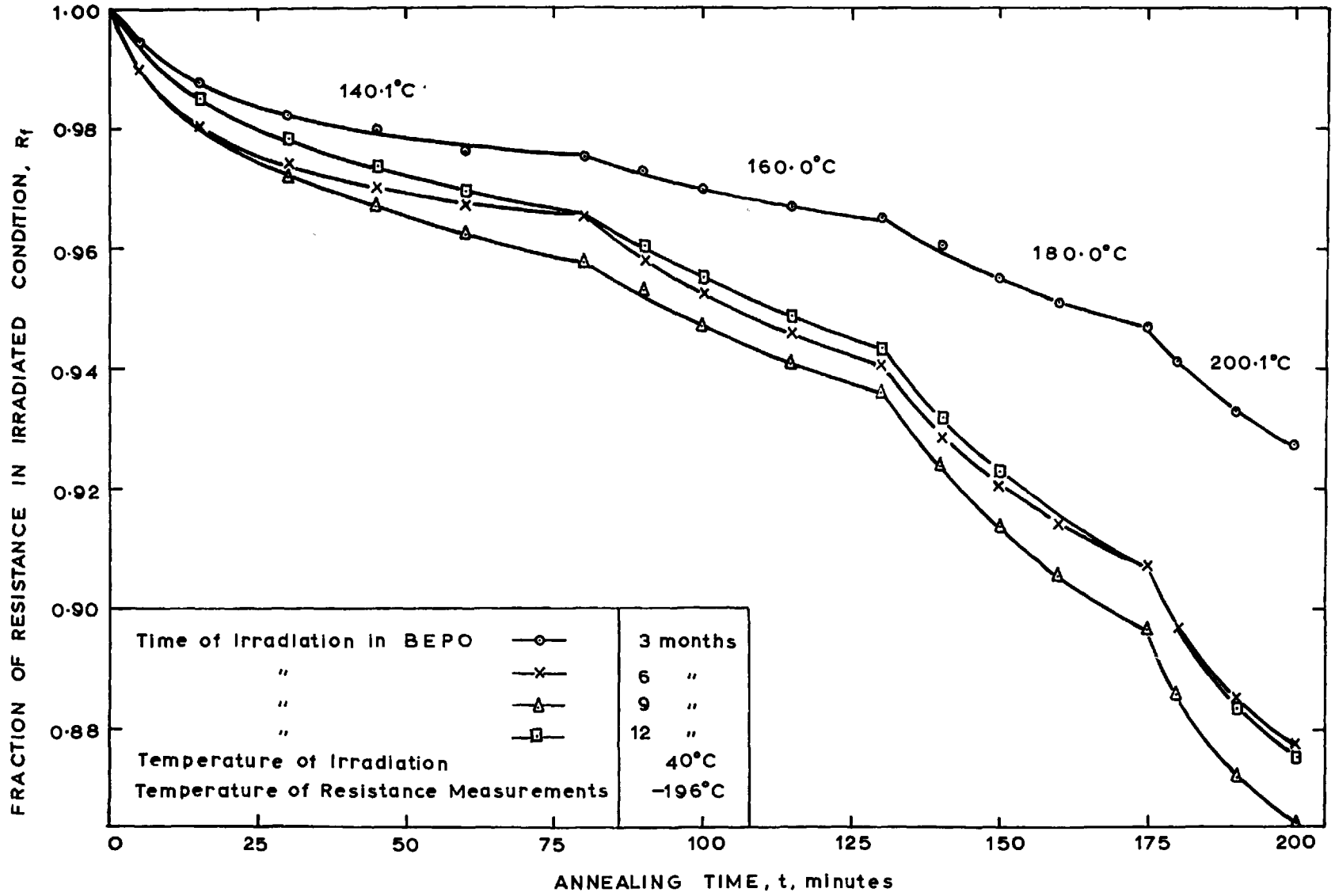


FIG.18 ISOTHERMAL ANNEALING CURVES FOR IRRADIATED MOLYBDENUM

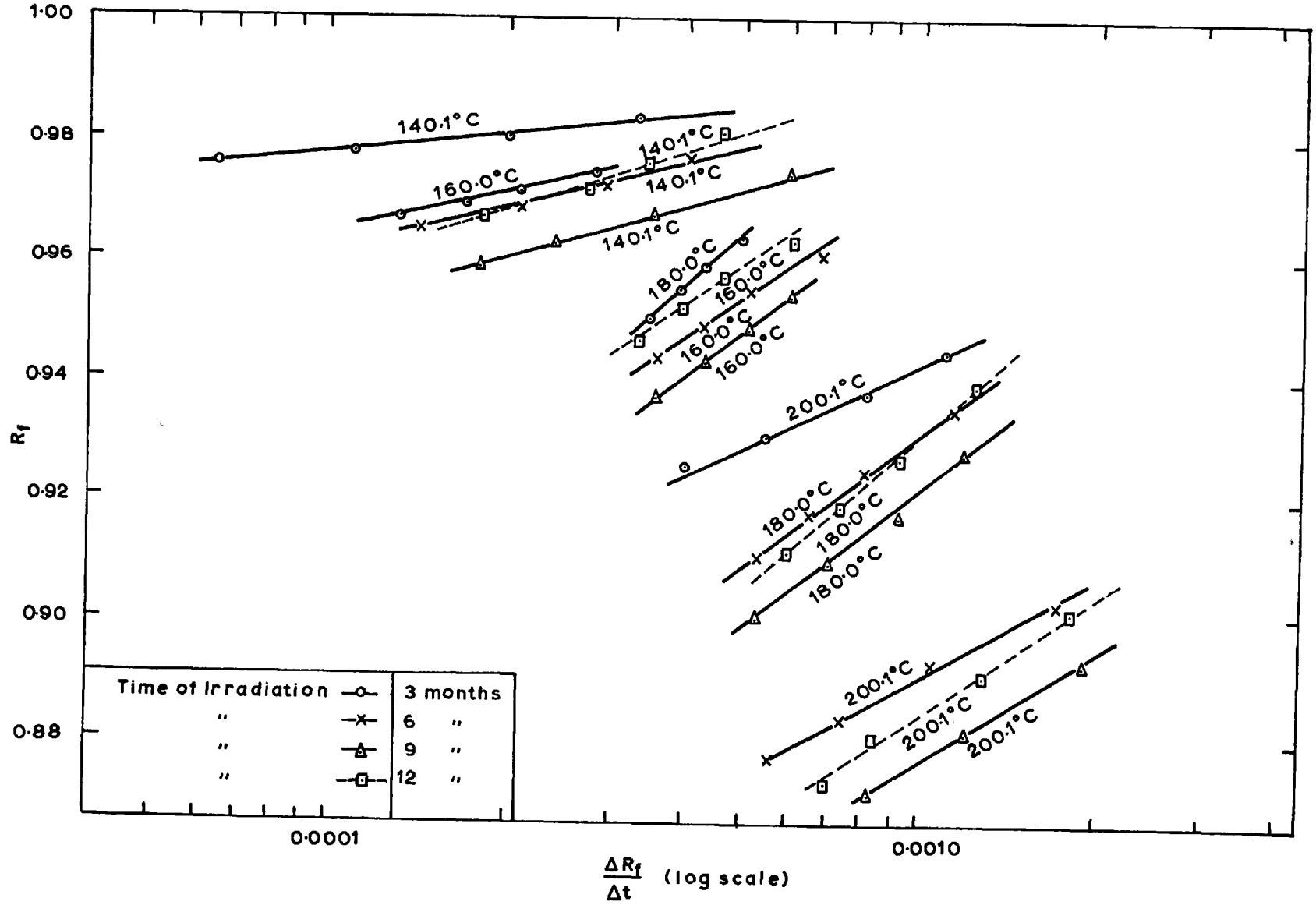


FIG.19 THE RELATIONSHIP BETWEEN R_f AND LOG $\frac{\Delta R_f}{\Delta t}$ FOR IRRADIATED MOLYBDENUM USING THE DATA OF FIG.18

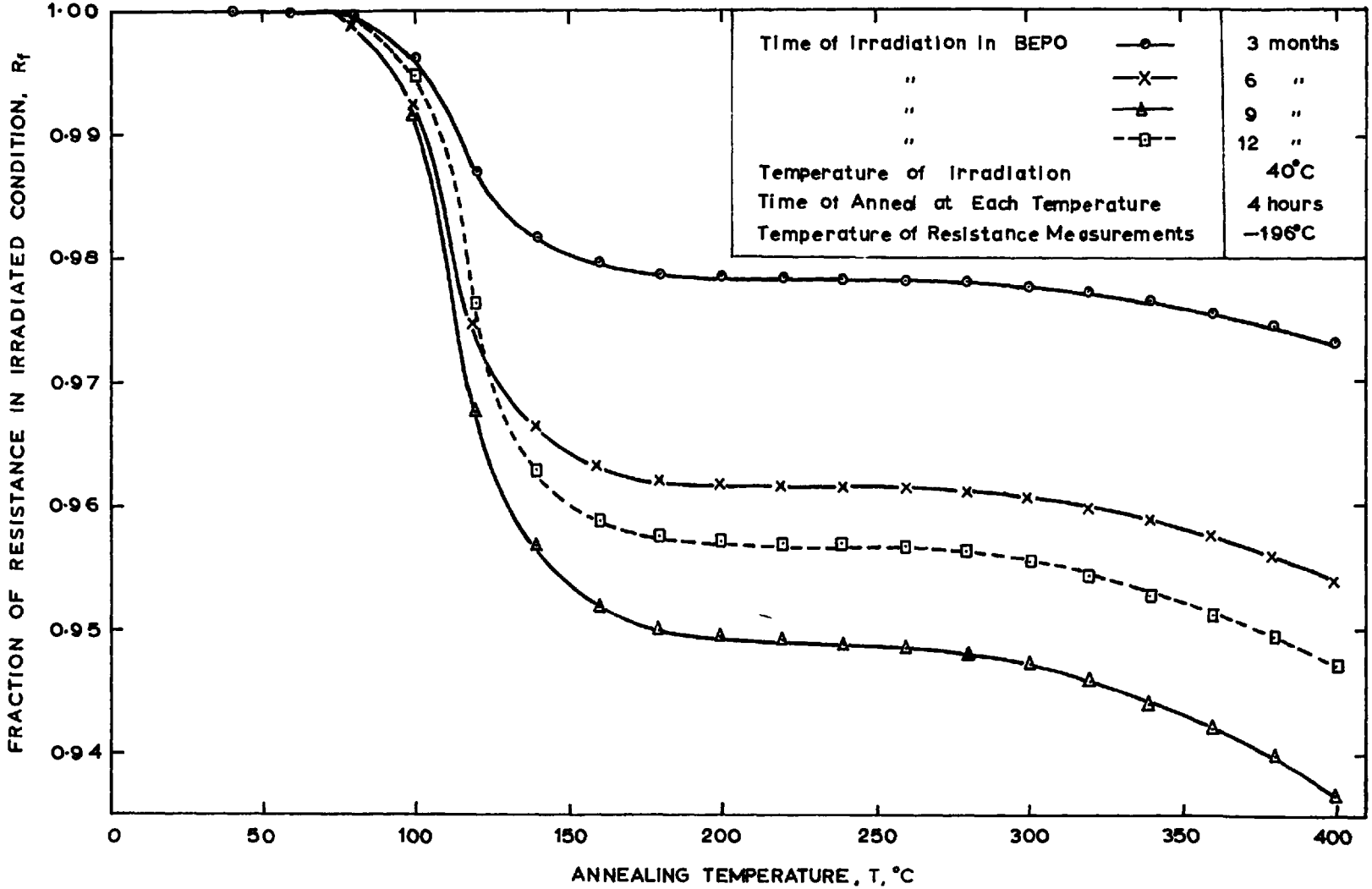


FIG.20 ISOCHRONAL ANNEALING CURVES FOR IRRADIATED NIOBIUM

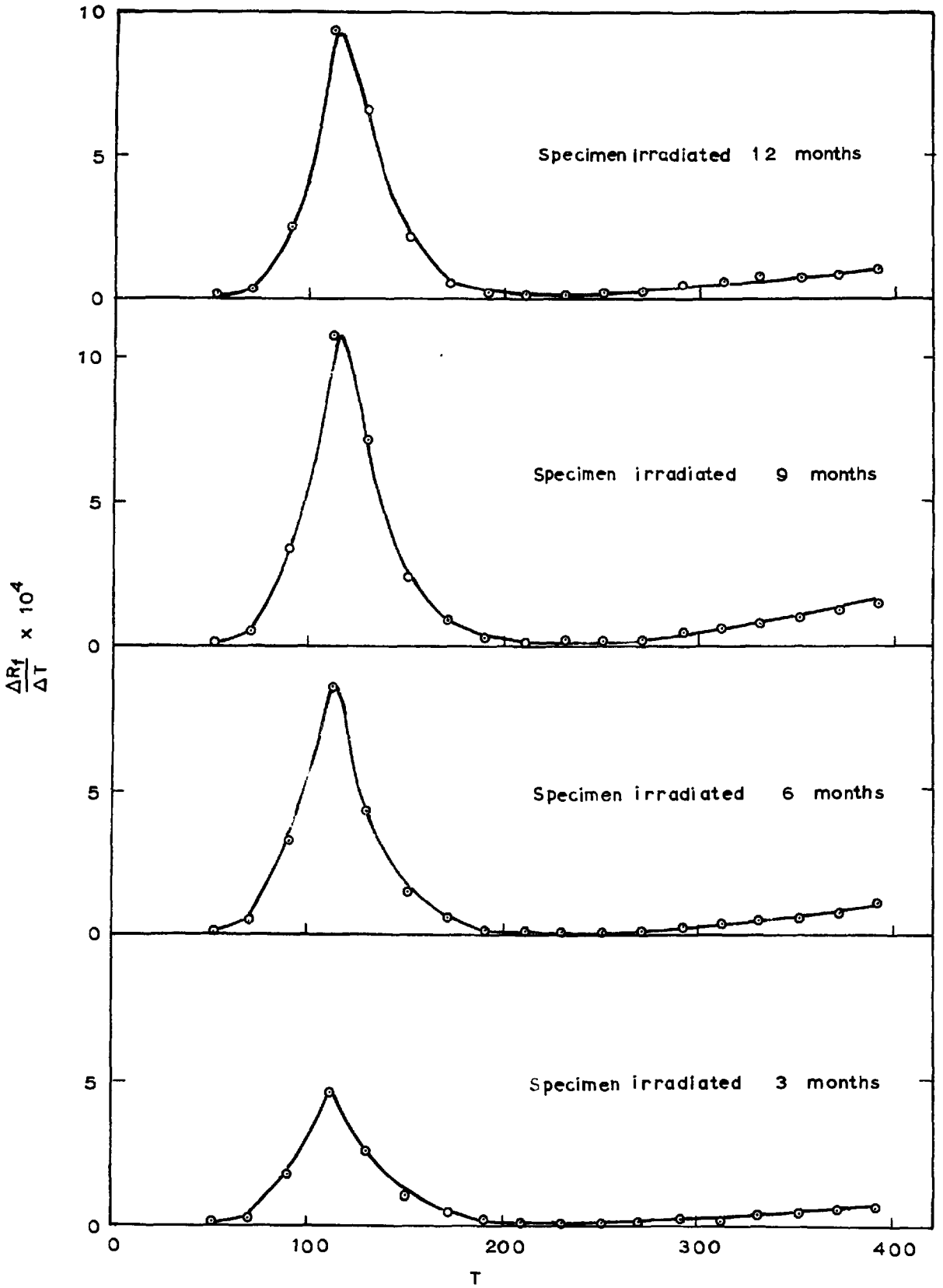


FIG. 21 $\frac{\Delta R_f}{\Delta T}$ PLOTTED AGAINST T FOR IRRADIATED NIOBIUM USING THE DATA OF FIG.

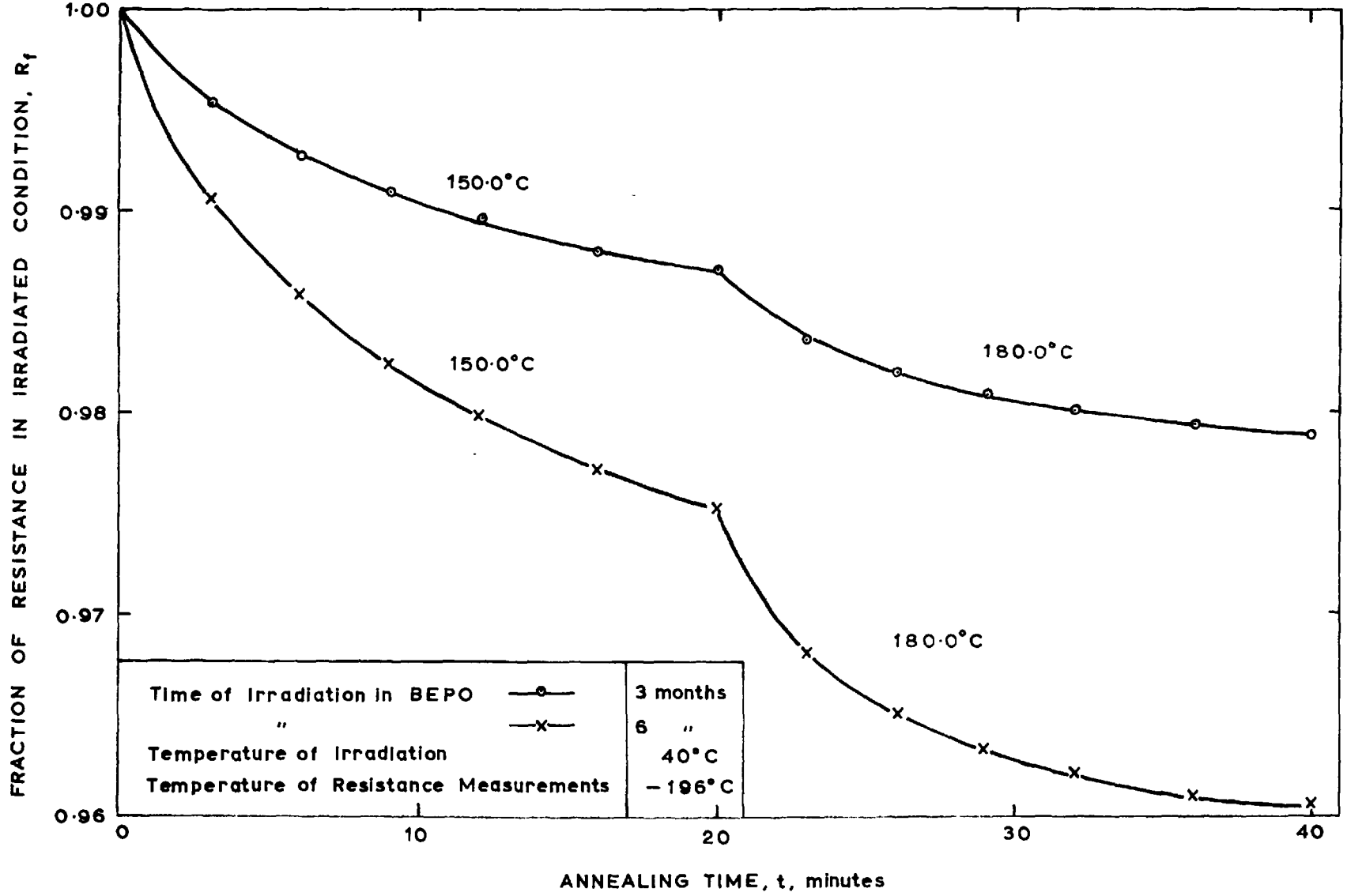


FIG. 22 ISOTHERMAL ANNEALING CURVES FOR IRRADIATED NIOBIUM

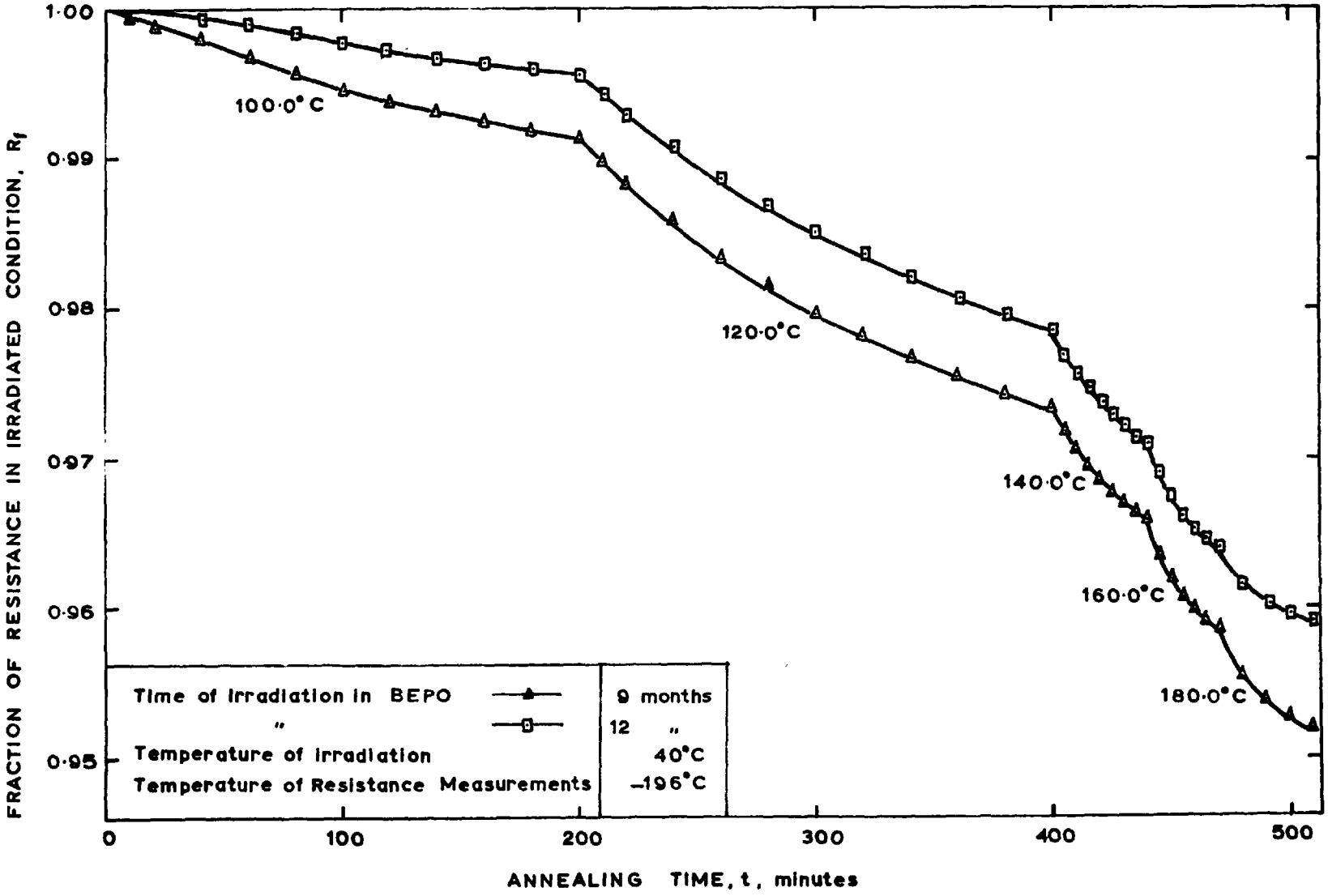


FIG. 23 ISOTHERMAL ANNEALING CURVES FOR IRRADIATED NIOBIUM

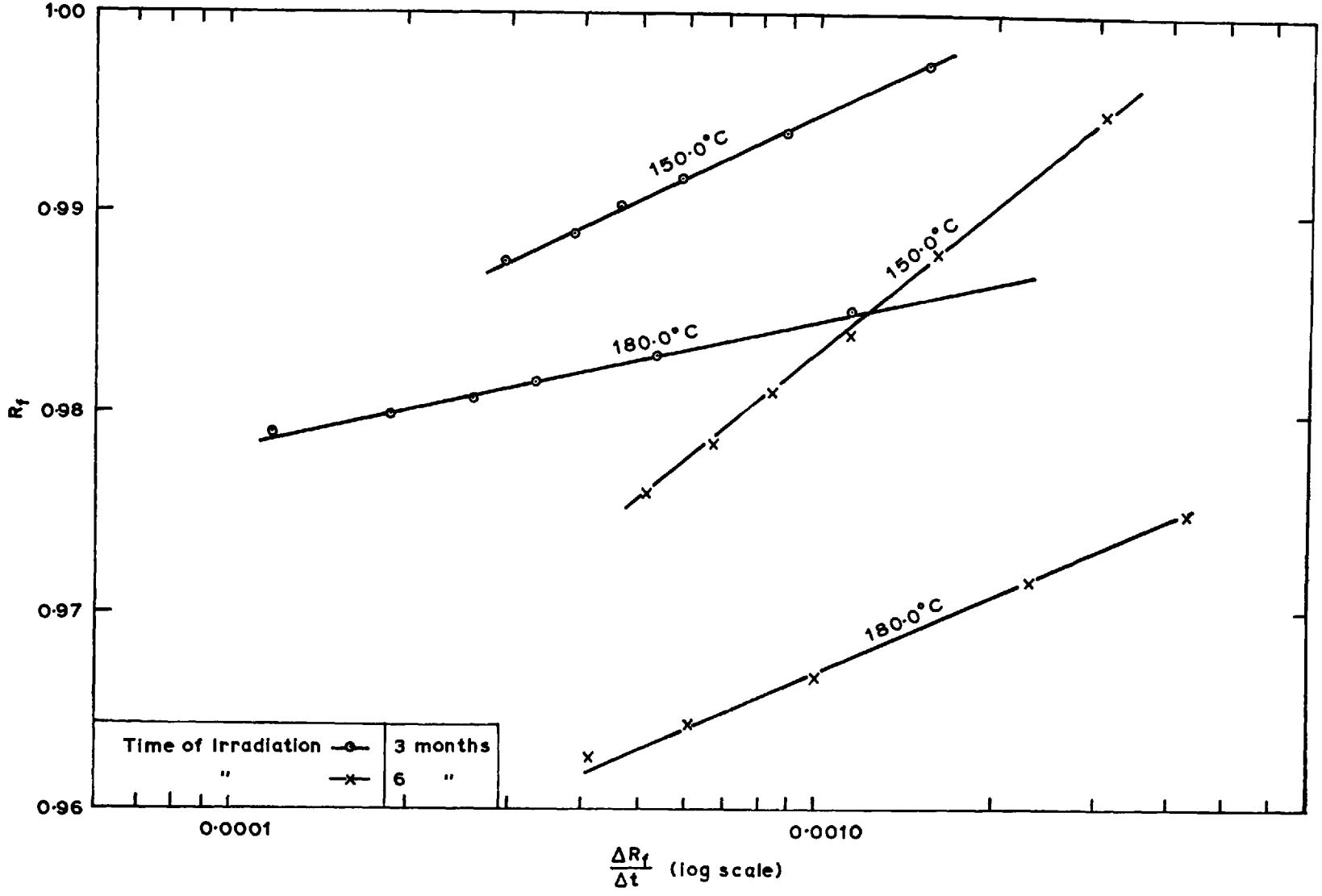


FIG.24 THE RELATIONSHIP BETWEEN R_f AND LOG $\frac{\Delta R_f}{\Delta t}$ FOR IRRADIATED NIOBIUM USING THE DATA OF FIG.22

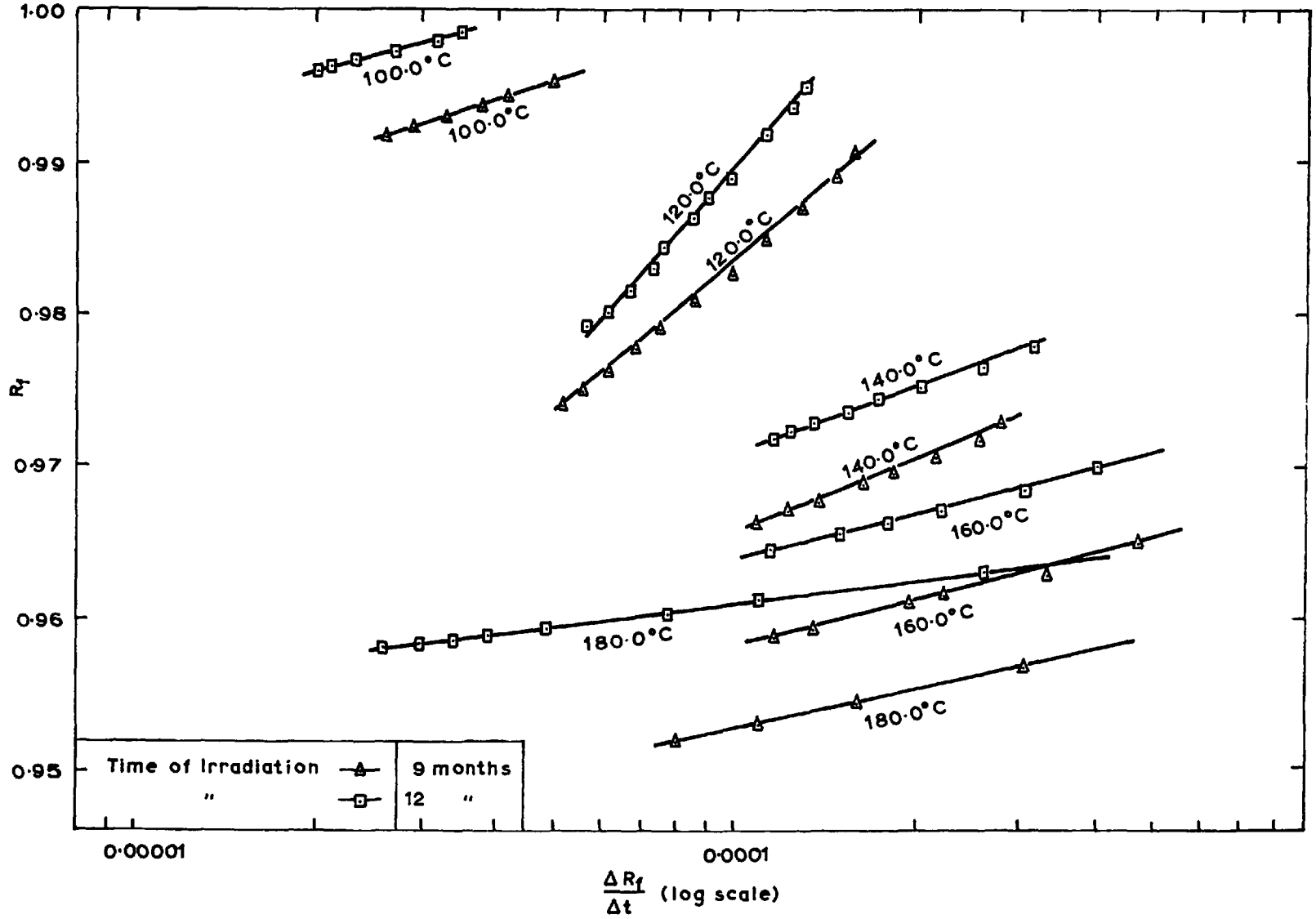


FIG.25 THE RELATIONSHIP BETWEEN R_f AND LOG $\frac{\Delta R_f}{\Delta t}$ FOR IRRADIATED NIOBIUM USING THE DATA OF FIG.23

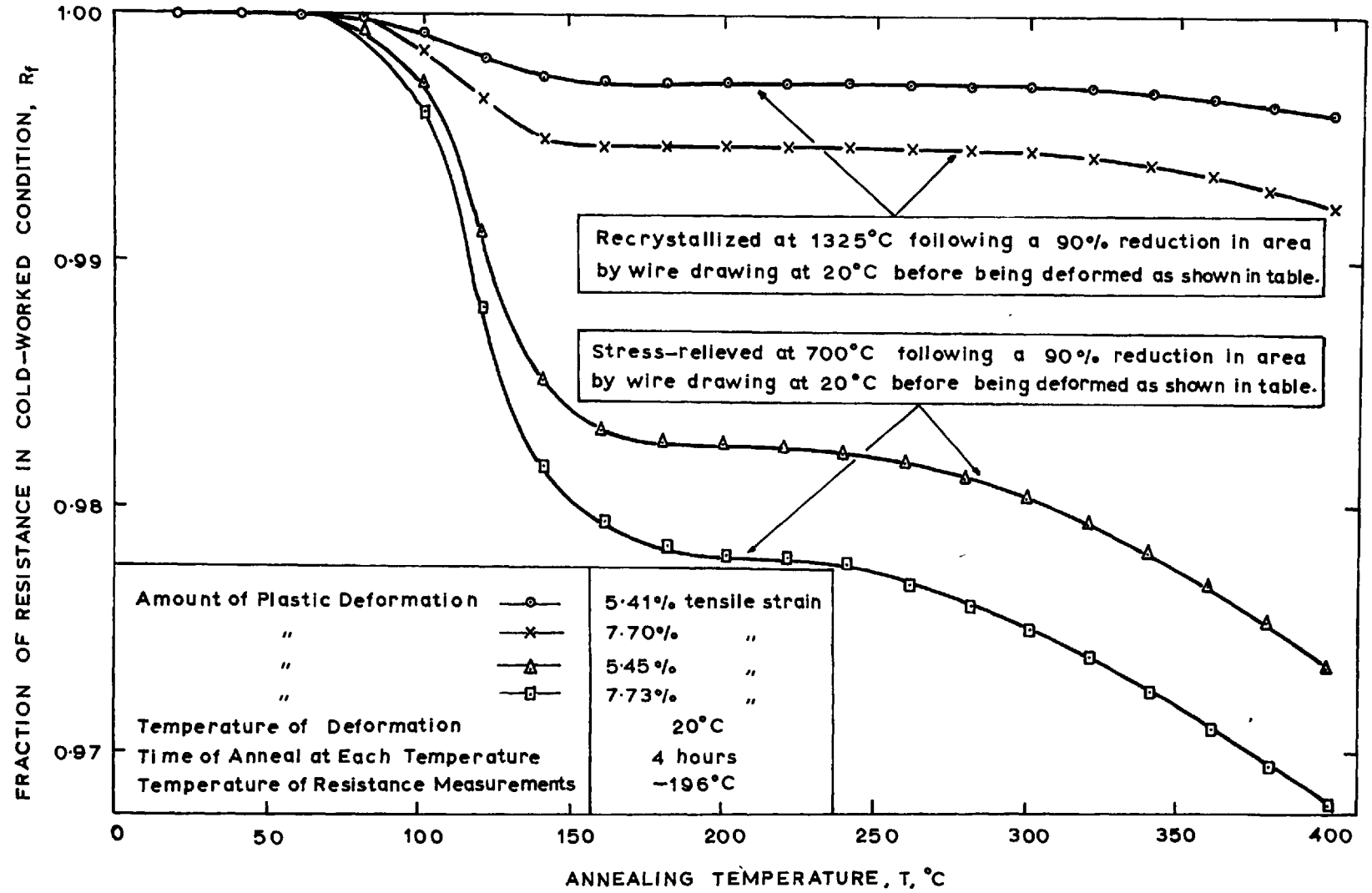


FIG.26 ISOCHRONAL ANNEALING CURVES FOR COLD-WORKED NIOBIUM

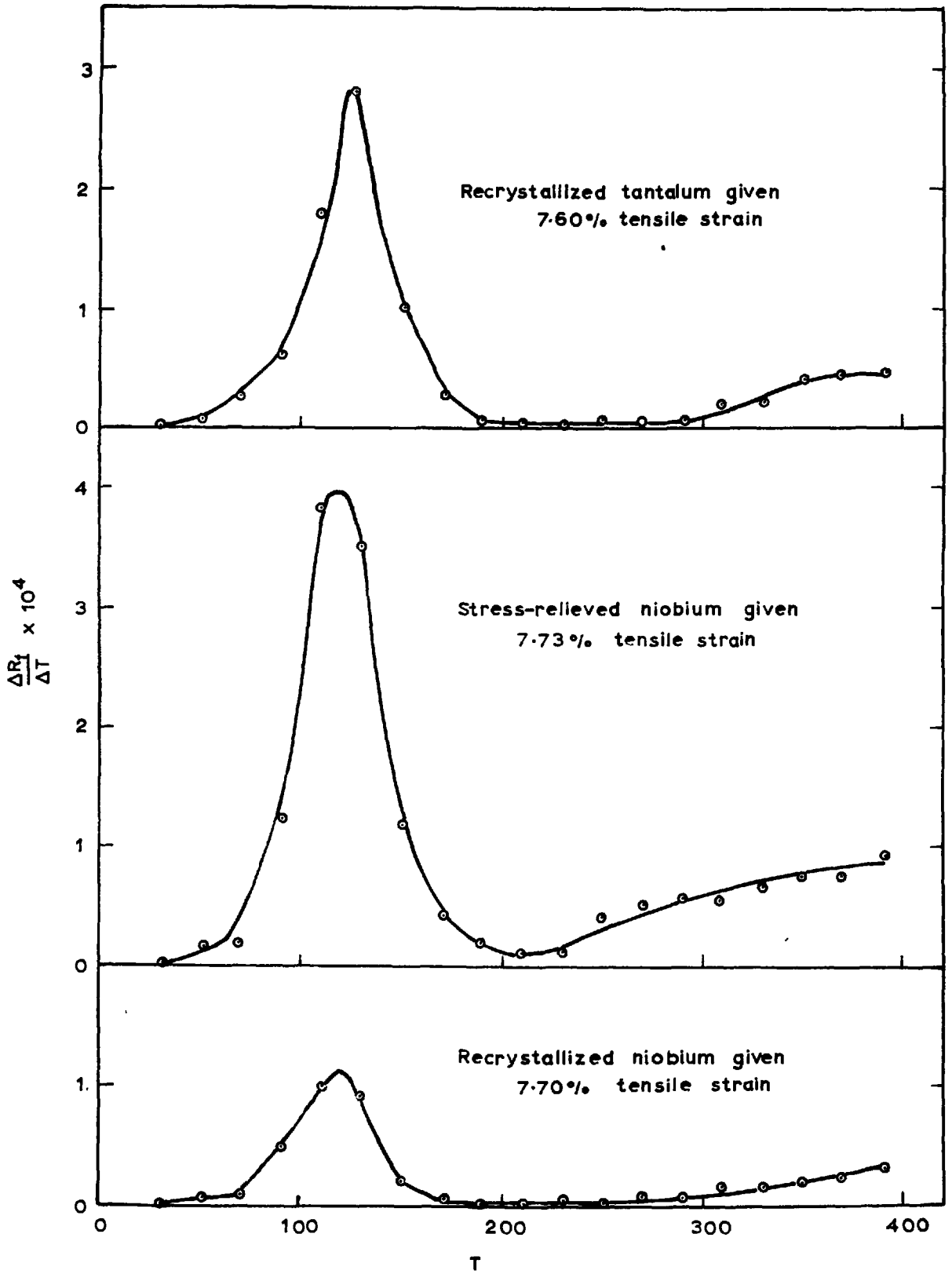


FIG.27 $\frac{\Delta R_f}{\Delta T}$ PLOTTED AGAINST T FOR COLD-WORKED NIOBIUM AND TANTALUM USING DATA FROM FIGS.26&33

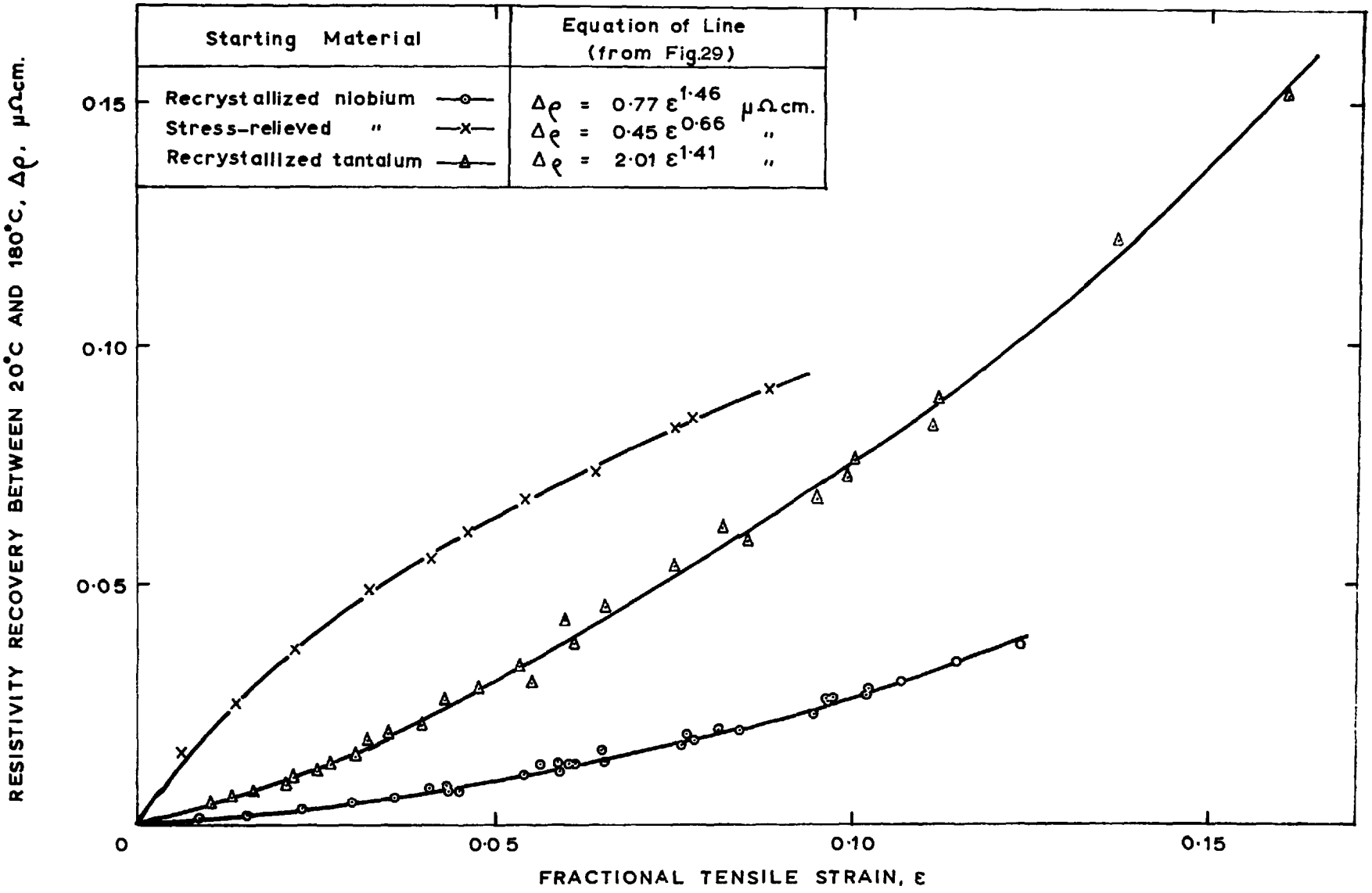


FIG.28 RESISTIVITY RECOVERY BETWEEN 20°C AND 180°C AS A FUNCTION OF TENSILE STRAIN FOR NIOBIUM AND TANTALUM DEFORMED AT 20°C

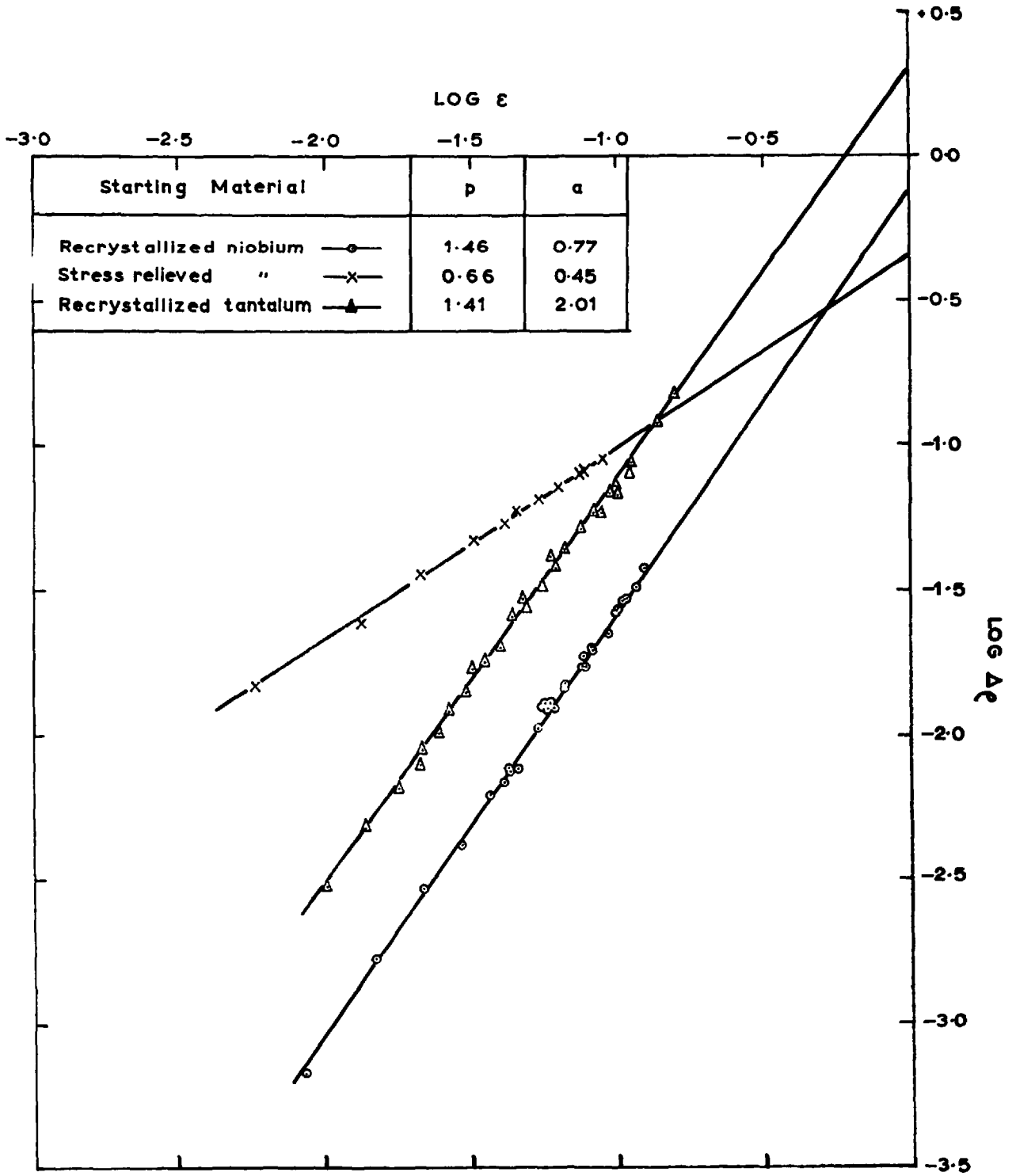


FIG.29 GRAPH SHOWING THE LINEAR RELATIONSHIP BETWEEN LOG $\Delta\rho$ AND LOG ε FOR COLD-WORKED NIOBIUM AND TANTALUM USING THE DATA OF FIG.28. THE RELATIONSHIP BETWEEN $\Delta\rho$ AND ε IS THUS OF THE FORM $\Delta\rho = a\varepsilon^{p}$

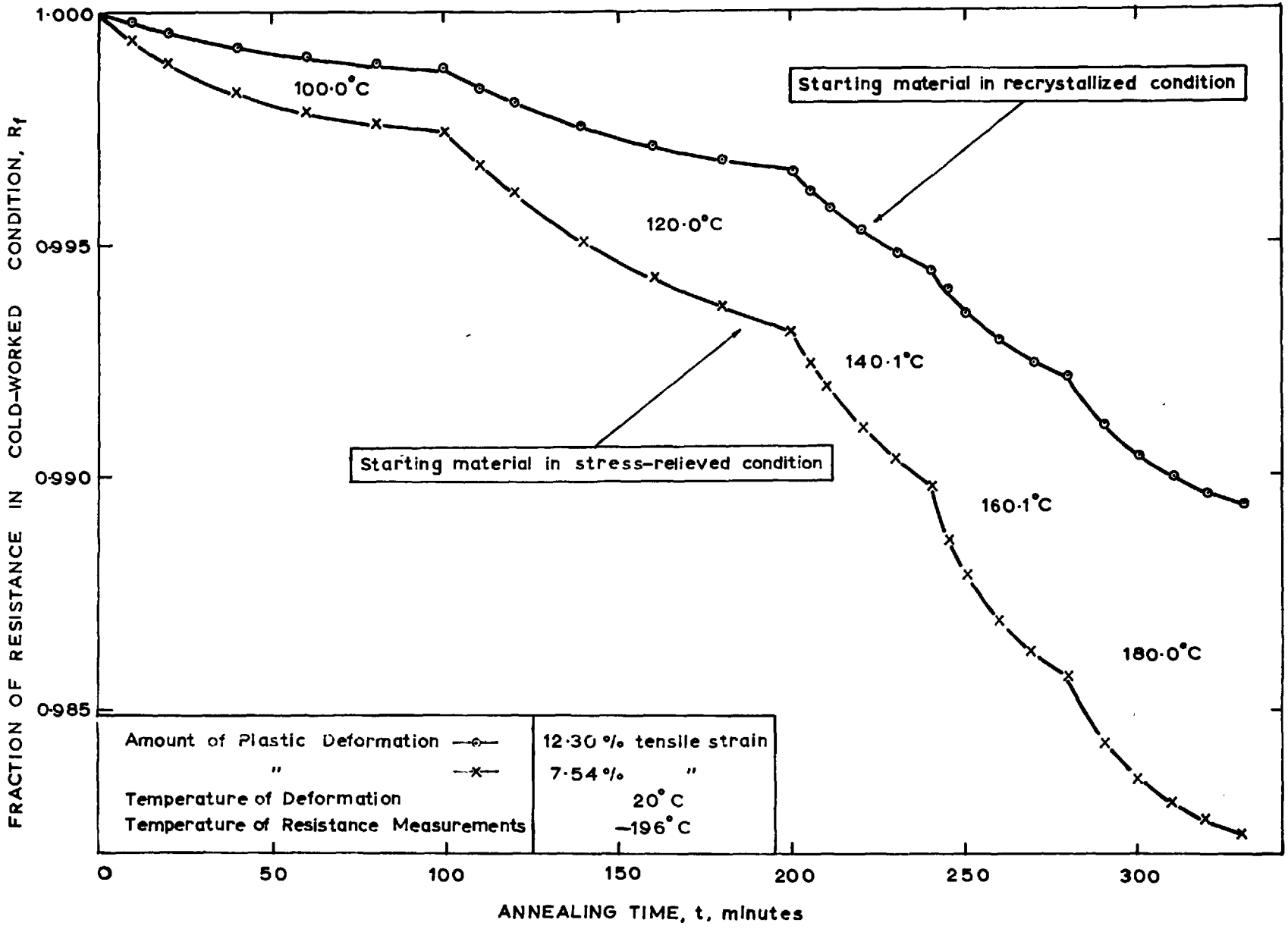


FIG. 30 ISOTHERMAL ANNEALING CURVES FOR COLD-WORKED NIOBIUM

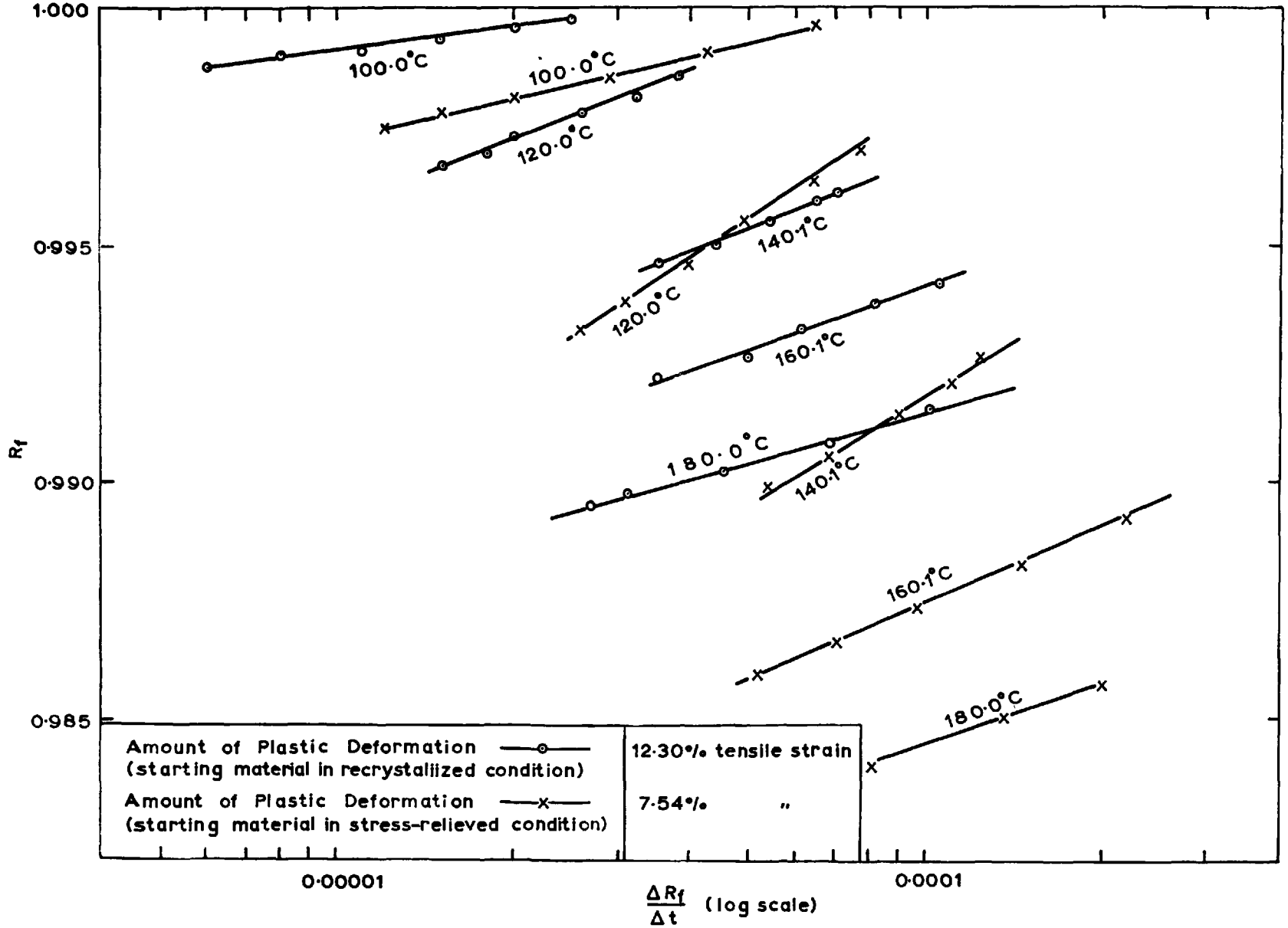


FIG.31 THE RELATIONSHIP BETWEEN R_f AND LOG $\frac{\Delta R_f}{\Delta t}$ FOR COLD-WORKED NIOBIUM USING THE DATA OF FIG.30

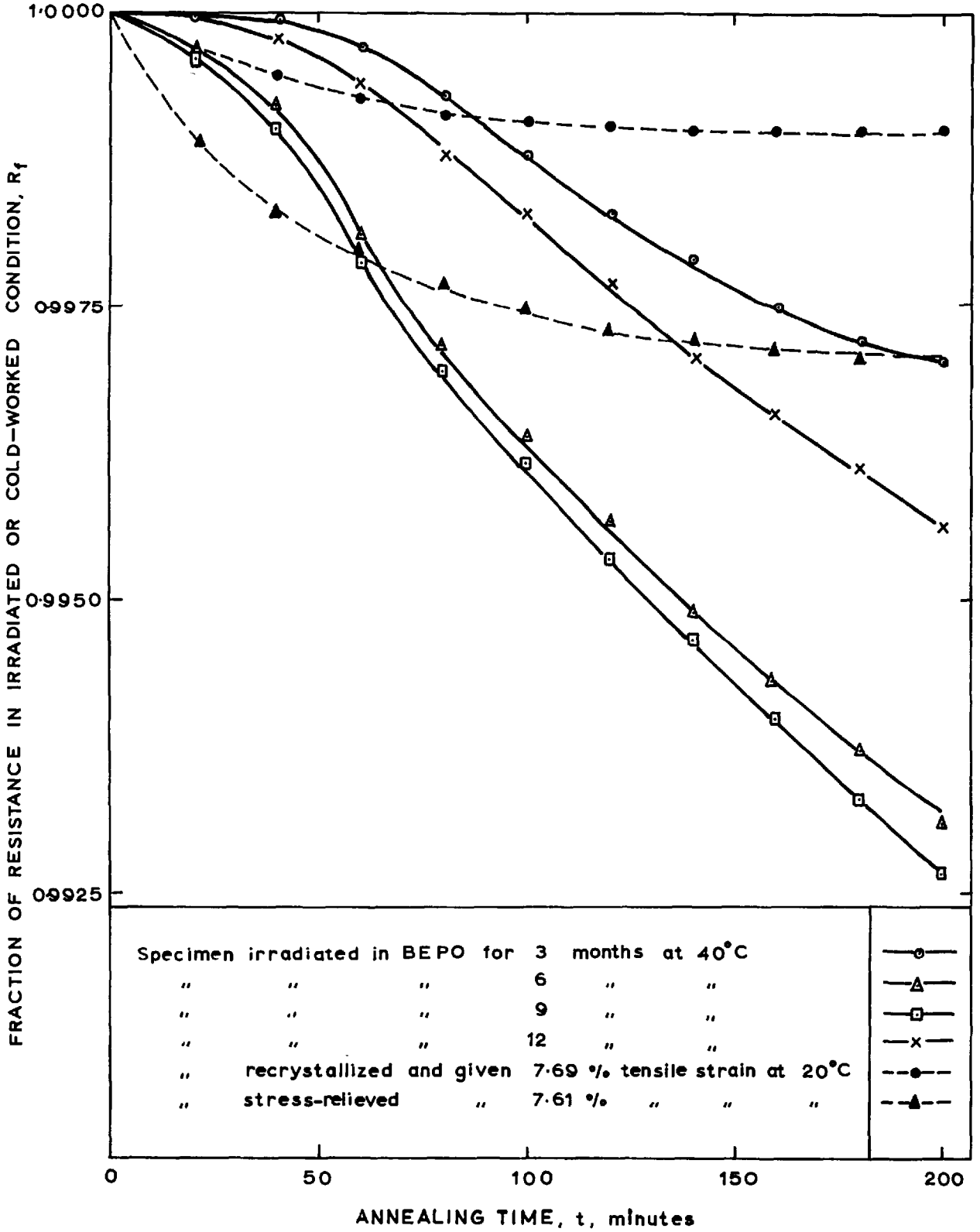


FIG.32 100°C ISOTHERMAL ANNEALING CURVES FOR NIOBIUM SHOWING THE DIFFERENCE IN INITIAL RECOVERY BEHAVIOUR BETWEEN IRRADIATED AND COLD-WORKED SPECIMENS

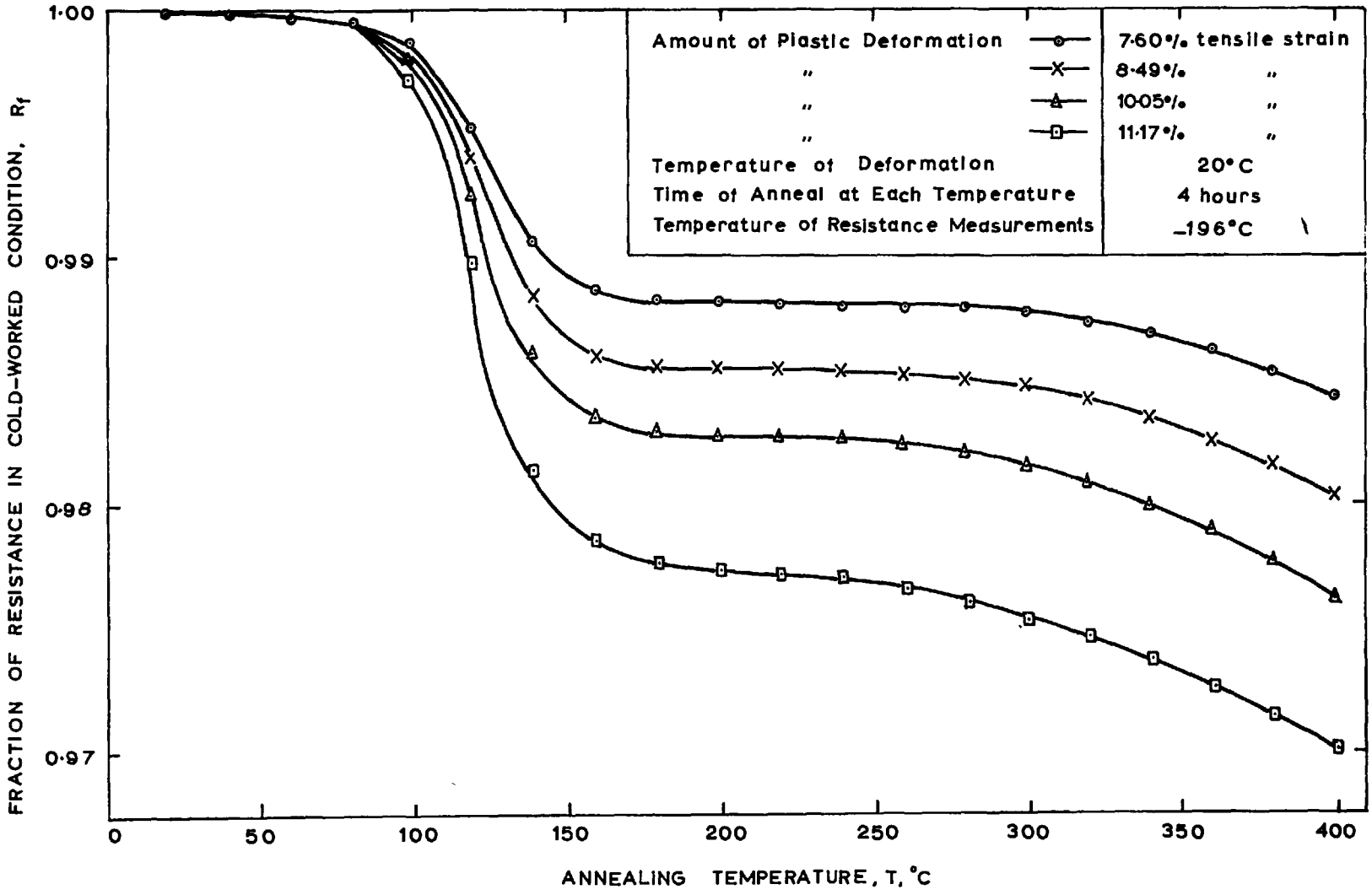


FIG. 33 ISOCHRONAL ANNEALING CURVES FOR COLD-WORKED TANTALUM

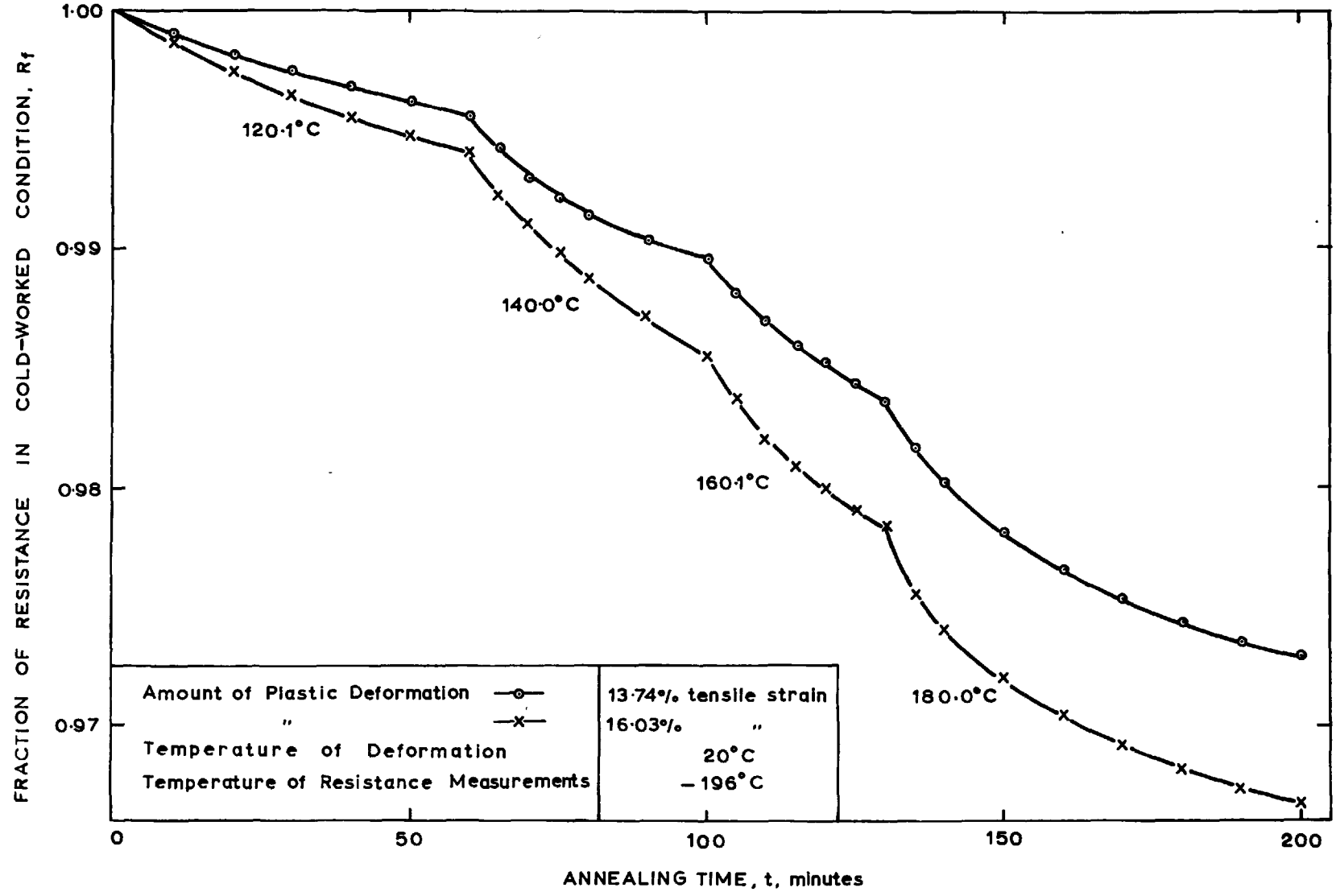


FIG. 34 ISOTHERMAL ANNEALING CURVES FOR COLD-WORKED TANTALUM

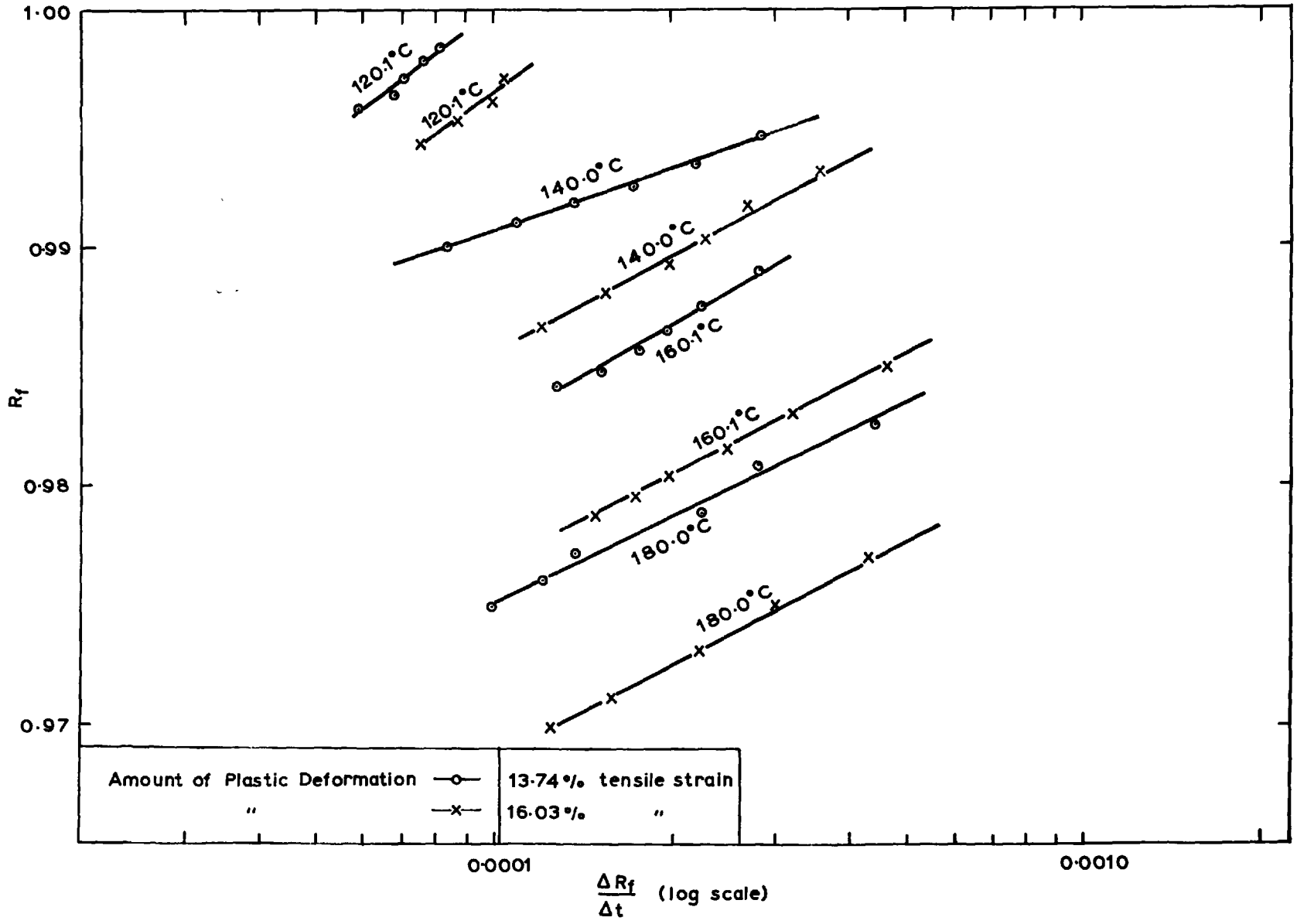


FIG.35 THE RELATIONSHIP BETWEEN R_f AND LOG $\frac{\Delta R_f}{\Delta t}$ FOR COLD-WORKED TANTALUM USING THE DATA OF FIG.34

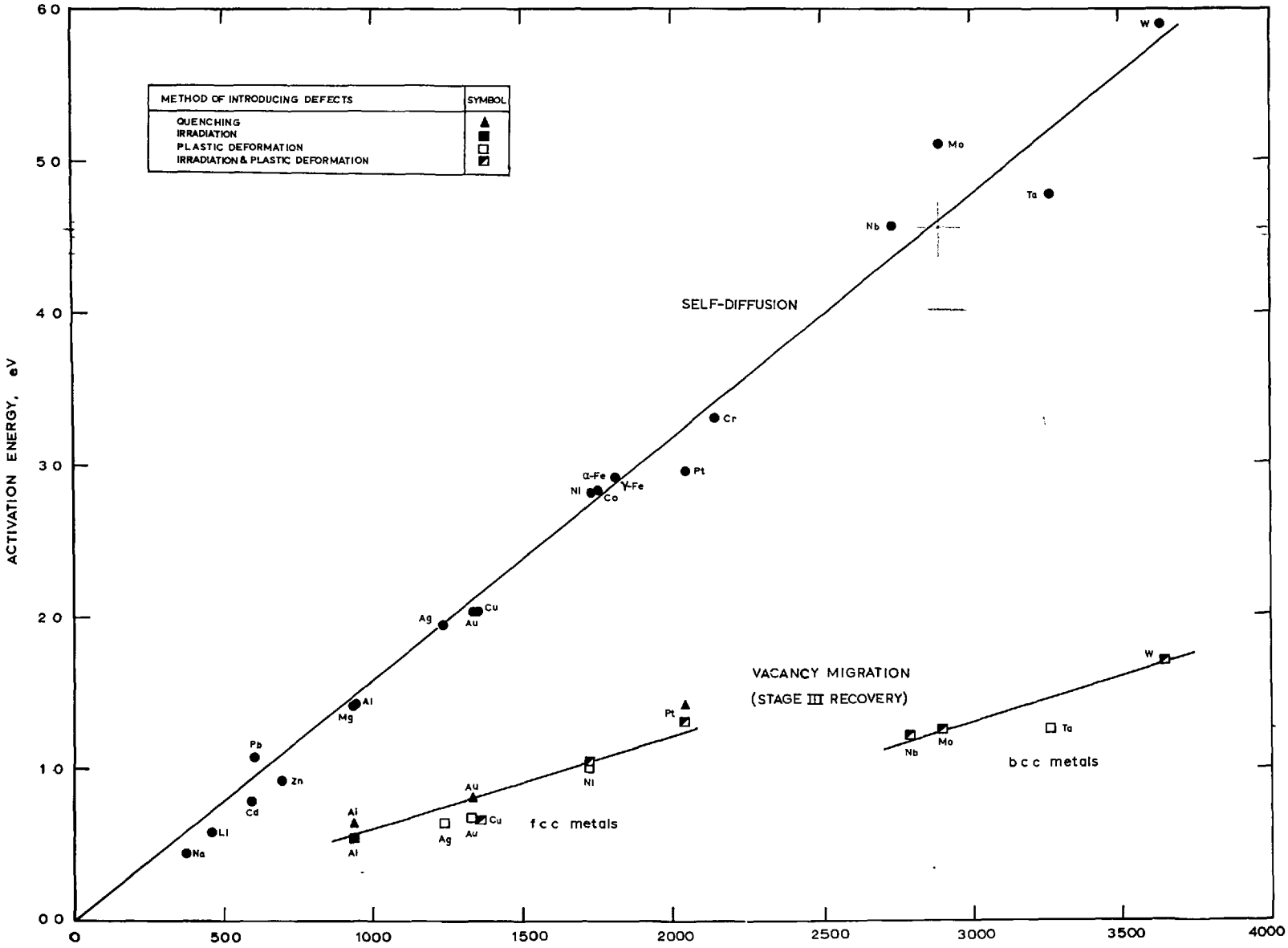


FIG 36 ACTIVATION ENERGIES FOR SELF-DIFFUSION AND VACANCY MIGRATION AS FUNCTIONS OF MELTING TEMPERATURE FOR SOME METALLIC ELEMENTS

4 DISCUSSION

4.1 The Increase in Resistivity of Molybdenum on Irradiation

The increase in resistivity of molybdenum on irradiation can be satisfactorily explained in terms of the presence of lattice defects created as a result of fast neutron collisions. The shape of the damage curve (Figure 13) is similar to that obtained by Kinchin and Thompson[17] although the percentage and absolute changes in resistivity are not directly comparable since in the earlier work resistance measurements were made at $0^{o}C$ and irradiations were carried out in a hollow uranium cylinder where the neutron flux and energy spectrum were somewhat different from those used in this investigation. The fact that the curve shows deceleration suggests that a decrease in the rate of accumulation of damage occurs as the irradiation proceeds. One explanation for this is that although interstitial atoms and vacant lattice sites are probably created in equal numbers only the interstitials are mobile at the irradiation temperature. It is generally agreed that interstitials become mobile at much lower temperatures than do vacancies. At low doses the vacancies cannot compete effectively with dislocations and impurity atoms, which act as sinks and traps for the interstitials, with the result that there is an almost linear increase in the number of vacancies and hence an almost linear increase in resitivity. At high doses, however, the rate of mutual annihilation of vacancies

and interstitials increases with the result that there is a decrease in the rate of accumulation of vacancies and thus a decelerating resistivity versus dose curve. An alternative and possibly more likely explanation is that at both low and high doses few interstitials are annihilated at dislocations and little mutual annihilation of vacancies and interstitials occurs but that interstitial cluster formation and growth takes place at an ever increasing rate as the irradiation proceeds. Dexter's[118] calculations on the resistivities of spherical clusters of from 10^2 to 10^4 vacancies in copper suggest that the resistivity of a number of vacancies is less when they are clustered together than when they are distributed singly. If this result can be applied to interstitials, even though they are more likely to form penny-shaped clusters, then a decrease in the rate of increase in resistivity would be expected if interstitial cluster formation and growth occurred. A further decrease would be expected if the larger discs of interstitials were able to form dislocation loops. The mutual annihilation of vacancies and interstitials would not be favoured if the two species of defect were formed some distance away from each other. This would be the case if focussing collisions played an important role in the damaging process. The experimental evidence for cluster formation in irradiated metals, discussed in 1.4.2 and 1.5.1, is now considerable and the importance now given to focussing collisions in radiation damage theory would seem to make this explanation the more probable one.

Since there are no theoretical estimates of the electrical resistivities of point defects in the body-centred cubic transition metals it would be hazardous to estimate from the results obtained the number of defects present after an irradiation, particularly as the annealing processes that occur at the irradiation temperature may result in the formation of defect clusters. It would be equally hazardous to estimate the electrical resistivities of vacancies and interstitials from the changes in resistivity observed because of the uncertainty in the numbers of defects created in displacement spikes and in the numbers and distribution of those defects that remain after annealing processes at the irradiation temperature.

4.2 The Resistivity Recovery of Irradiated Molybdenum and Niobium

The annealing spectra obtained for irradiated molybdenum and niobium are very similar to those obtained for molybdenum by Kinchin and Thompson[17] except that the small peak observed in molybdenum at about 280°C is not quite so obvious in the earlier work. For both molybdenum and niobium the symmetrical nature of the major peak, the relatively small temperature range over which it extends, the constant activation energy of the recovery process and, in the case of molybdenum, the magnitude of the recovery, about 55 per cent of the increase in resistivity due to irradiation, all point to a recovery process involving a fundamental point defect. It has been established experimentally that a major recovery process occurs in quenched, irradiated and cold-worked face-centred cubic

metals such that E_m/E_d is approximately 0.4, where E_m is the activation energy of the recovery process and E_d is the self-diffusion activation energy of the metal concerned. This recovery process, or Stage III recovery as it is usually termed, is generally attributed to the migration of vacant lattice sites. The published data upon which this observation is based are given in Table 18, which also gives the vacancy formation energy, E_f, for several metals as determined by quenching experiments. It can be seen that in most cases the value of $E_f/E_d + E_m/E_d$ is near to unity which should be the case if E_f and E_m really do refer to single vacancies and if self-diffusion in these metals is by a vacancy mechanism. Stage III recovery in the body-centred cubic transition metals yields a value of about 0.3 for E_m/E_d (Table 18) so that if this recovery stage can again be attributed to vacancies and if self-diffusion in these metals is also by a vacancy mechanism then it can be said that for the body-centred metals the vacancy migration energy is a smaller proportion of the self-diffusion energy. This difference between metals of the two crystal structures can also be seen if E_m is plotted as a function of melting temperature (Figure 36). The b.c.c. metals lie on a straight line which is parallel to and about 0.5 eV below a straight line through the f.c.c. metals. Shaw's[53] recent calculations on the migration energies of vacancies in the body-centred transition metals (Table 6) agree reasonably well with the experimentally determined activation energies for Stage III recovery. The sum of the theoretical formation and migration

energies for each metal also agrees reasonably well with the experimentally determined value of the self-diffusion activation energy (Table 17). This correlation between theory and experiment would seem to support the view that Stage III recovery in the body-centred cubic transition metals is due to vacancy migration.

The fact that the resistivity change, $\Delta\rho$, during Stage III recovery for both molybdenum and niobium passes through a maximum when plotted as a function of irradiation time (Figure 17) is an unexpected and at first sight a surprising result. One consequence of the explanation given earlier for the saturation effect observed in the damage curve is that the concentration of vacancies increases almost linearly with dose. If these vacancies are simply annihilated at existing sinks such as dislocations and interstitial clusters, an almost linear $\Delta\rho$ versus dose curve should be observed. However, the situation may be similar to that described for the interstitials. After a high dose, the vacancies may cluster in preference to disappearing at existing sinks. Thus, because of the resistivity of the clusters, less recovery would be observed than on annealing after a low dose, when perhaps most of the vacancies disappear completely. The number of jumps to annihilation associated with Stage III recovery, 10^2 to 10^3 at 50 per cent recovery, is also not that expected for a random array of vacancies migrating to and being annihilated at the dislocation network of the material. This would be of the order of 10^7 as discussed in 1.3. The formation or presence of clusters could give rise to a low number of jumps but apart from this, because of the rather high impurity contents

of the materials used in this investigation, it is quite likely that the measured number of jumps is considerably different from the true number. From equation (29) we know that

$$j_{app} = j\,(n + e^{-B/kT})/(n + e^{-B/kT} + c)\,, \qquad (29)$$

where j_{app} and j are the apparent and true number of jumps respectively, n is the concentration of vacancies and c is the concentration of traps which bind the vacancies with an energy B. Unfortunately with pile irradiations on rather impure materials it is virtually impossible to assign definite values to n, c or B. It may be significant that the number of jumps for niobium is a factor of about 10 lower than that for molybdenum. The impurity content of the niobium is ten times greater than that of the molybdenum, excluding the tantalum in the niobium (Table 8). Since there is little difference between niobium and tantalum as regards atomic size and chemical properties it is reasonable to suppose that a tantalum atom would not provide a very effective trapping centre in the niobium lattice. If n and $e^{-B/kT}$ were both small compared with c, the factor of 10 difference between the numbers of jumps could be accounted for by the factor of 10 difference in the impurity contents.

Although in most cases the isothermal annealing curves were incomplete in that they were not continued until no further recovery occurred, the plots of R_f against log. $R_f/\,t$, both for irradiated and cold-worked specimens, give good straight line relationships, except in the initial stages of recovery of

irradiated niobium. This would seem to justify the use of equation (35) to describe the temperature dependence of the rate of resistivity recovery during Stage III.

From the conclusion arrived at in 1.2, that the concentrations of point defects created by irradiation in molybdenum and niobium should be similar, the difference between the magnitudes of the resistivity recovery during Stage III may be an indication of the difference between the resistivities of vacancies in the two metals. For comparable irradiation times the resistivity recovery in niobium is 1.5 times greater than it is in molybdenum so that the resistivities may differ by this amount also.

The small peak at 280°C in molybdenum could be what is usually described as Stage IV recovery. This has been observed in quenched, irradiated and cold-worked metals but it is always small compared with Stage III and is not always reproducible. Seeger[20] believes that Stage IV is due to vacancy migration and that Stage III is due to interstitials. Another possibility is that during Stage III vacancies are trapped at impurity atoms and that during Stage IV they are released from these traps and migrate to and are annihilated at dislocations or other sinks. Yet another possibility is that during Stage IV a particular size of defect cluster becomes mobile, perhaps a tri- or quadri- vacancy, produced by irradiation or during Stage III.

The continuous recovery in both metals from 280 to 400°C and in molybdenum from 400 to 900° is obviously not due to a

simple process. There are several possibilities as to its cause. It could be due to the release of point defects from deeper and deeper traps, to the break-up of clusters of defects, to the collapse of clusters to form dislocation loops or to the relaxation or regrouping of dislocations, even though the temperatures involved are well below those required for normal dislocation climb. The fact that recovery in the case of molybdenum is incomplete, particularly for the specimens irradiated for 3 months (Table 12), even after annealing at 900°C, indicates that the dislocation structure of the material is altered as a result of irradiation or subsequent annealing, or both. Even prolonged annealing above the recrystallization temperature, in this case about 900°C, need not necessarily reduce the resistivity to the pre-irradiation value since the dislocation structure after recrystallization depends very much on the dislocation structure of the damaged material. For example, it is well known that when a cold-worked metal is recrystallized the resulting grain size depends very sensitively on the degree of cold-work.

4.3 The Resistivity Recovery of Cold-Worked Niobium and Tantalum

The fact that the annealing spectra obtained for cold-worked and irradiated niobium are very similar suggests that the annealing processes in both types of material are the same. The symmetrical nature of the major peak, the relatively small temperature range over which it extends and the constant activation energy again

point to an annealing process involving a fundamental point defect. It is suggested, therefore, that the same defect, the lattice vacancy, is responsible for the major recovery process in both irradiated and cold-worked niobium. The similarity between the annealing spectra of cold-worked niobium and tantalum also suggests that the major recovery process in this material is also due to this species of point defect. The fact that the resistivity recovery in Stage III is very much less in the cold-worked than it is in the irradiated material is in agreement with the general observation that irradiation is the more effective method of producing point defects. The similar shape of the resistivity recovery, $\Delta\rho$, versus tensile strain curves for recrystallized niobium and tantalum (Figure 28) suggests that the two metals are behaving in a similar way as regards the generation of point defects. If the difference between the magnitudes of the recovery for comparable strains is due only to the difference between the resistivities of vacancies in the two metals and not to any difference in concentrations then the resistivity of vacancies in tantalum is greater than that in niobium by a factor of about 2.5. If it is assumed that a linear relationship exists between

and the number of defects removed from the lattice, and that all the vacancies produced by plastic deformation are only removed from the lattice during Stage III recovery, then the relationship between concentration of defects produced and amount of plastic deformation does not fit any of the theories listed in 1.2.2. This is not very surprising, however, since not one of

the theories takes into account such things as thermal annealing and the annihilation of point defects by the passage of dislocations over slip planes containing them. Plastic deformation of both niobium and tantalum at room temperature would result in the immediate migration of any interstitials that are generated. If the ratio of vacancies to interstitials produced did not change with amount of cold-work, and if little mutual annihilation occurred, then anytheoretical relationship should still hold qualitatively. However, it is perhaps too much to expect these conditions to be satisfied. The difference in the shape of the $\Delta\rho$ versus tensile strain curves for recrystallized and stress-relieved niobium suggests that the initial dislocation density effects not only the concentration of defects produced for a given amount of strain, as would be expected, but also alters the rate of production so that both accelerating and decelerating curves are obtained. It is possible that an initial dislocation density exists which would produce a linear relationship between $\Delta\rho$ and tensile strain. This could account for the results obtained by Peiffer[49] on plastically deformed molybdenum.

As in the irradiated material, the number of jumps to annihilation associated with Stage III recovery is rather low. The fact that it is the same for stress-relieved and recrystallized material where the dislocation densities must differ by at least a factor of 10 suggests that a considerable amount of vacancy-impurity atom interaction is taking place. However, the absence

of an incubation period at the commencement of recovery and the more nearly exponential form of the 100°C isothermal annealing curves (Figure 32) are evidence that, compared with irradiated material, recovery in cold-worked specimens is a much simpler process. This may be due to the smaller concentrations of point defects involved and the more important part played by fixed sinks in the form of dislocations. As in the case of irradiated material it is not possible to discuss the number of jumps in a more quantitative way because of the difficulty in assigning definite values to the concentrations of defects and traps and the binding energies involved.

The most probable explanation for the continuous recovery between 300 and 400°C in the recrystallized niobium and tantalum and between 200 and 400°C in the stress-relieved niobium is that relaxation and regrouping of dislocations is taking place. The fact that the recovery is greatest and occurs at a lower temperature in the stress-relieved material would seem to support this view since it should contain the highest dislocation density.

CONCLUSIONS

The investigation may be summarized in the following conclusions:

(i) The increase in electrical resistivity, $\Delta\rho$, of molybdenum due to irradiation in BEPO at 40°C can be described by the equation

$$\Delta\rho = 0.071\ t^{0.54}\ \mu\Omega\text{cm.},$$

where t is the irradiation time in months. The neutron flux during irradiation was estimated to be in the region of 10^{11} fast (>1 MeV) neutrons $cm.^{-2}sec.^{-1}$ This is similar to a relationship found earlier under somewhat different irradiation and measuring conditions by Kinchin and Thompson[17]. It is suggested that interstitial cluster formation and growth during irradiation could account for this behaviour.

(ii) About 55 per cent of the extra resistivity due to irradiation anneals out in the temperature range 100 to 200°C with an activation energy of 1.25 ±0.08 eV. The number of jumps to annihilation associated with this recovery is of the order of 10^3. All these results are independent of neutron dose. The resistivity recovery, $\Delta\rho$, during the process passes through a maximum when plotted as a function of irradiation time. By analogy with the recovery of quenched, irradiated and cold-worked face-centred cubic metals, which have received the greatest attention in the past, it is proposed that the recovery between

100 and 200°C is due to the migration and annihilation of vacant lattice sites created during irradiation. The low number of jumps for the process can be explained in terms of the trapping of vacancies by impurity atoms and the maximum in the resistivity versus dose curve is thought to be due to the formation, during annealing, of vacancy clusters when a high supersaturation exists, that is, after a high neutron dose.

(iii) A small recovery peak, observed at about 280°C, could be attributed to the release of trapped point defects or to the migration of a particular size of defect cluster. Continuous recovery, observed between 300 and 900°C, is probably caused by the relaxation or regrouping of dislocations. The dislocation structure of a material may be altered considerably by the annihilation of point defects at existing dislocations and by the formation of dislocation loops due to the collapse of point defect clusters. A modified dislocation structure is also indicated by the fact that recovery is incomplete even ater annealing at 900°C, the probable recrystallization temperature of the material.

(iv) The annealing spectra of niobium specimens irradiated under the same conditions show a major recovery process between 80 and 180°C with an associated activation energy of 1.22 ±0.02 eV. In this case the number of jumps to annihilation is of the order of 10^2. Continuous recovery between 250 and 400°C

is also observed. The similarity between the annealing spectra of niobium and molybdenum suggests that similar annealing processes are taking place in both metals. In the case of niobium the lower number of jumps and the absence of a small peak in the region of 280°C might be due to its higher impurity content. The resistivity changes in niobium are greater than those in molybdenum by a factor of about 1.5 which may mean that the same difference exists between the resistivities of vacancies in the two metals.

(v) Recrystallized niobium and tantalum plastically deformed in tension at room temperature behave very similarly when annealed. A major recovery process is observed in both metals between 80 and 180°C with an activation energy of 1.22 ±0.02 eV in niobium and 1.25 ±0.02 eV in tantalum. The number of jumps to annihilation associated with these processes is of the order of 10^3. The relationship between the resistivity recovery, $\Delta\rho$, between 80 and 180°C and the fractional plastic tensile strain, ϵ , is found to be

$$\Delta\rho = 0.77\,\epsilon^{1.46}\ \mu\Omega\text{cm. for niobium}$$

and

$$\Delta\rho = 2.01\,\epsilon^{1.41}\ \mu\Omega\text{cm. for tantalum.}$$

The annealing spectrum for cold-worked niobium with a higher initial dislocation density is similar to that for recrystallized material but for comparable strains the resistivity recovery is much greater, although after heavy deformation it tends to

saturate, the corresponding relationship being

$$\Delta\rho = 0.45\,\varepsilon^{0.66}\ \mu\Omega\text{cm}.$$

None of these relationships can be fitted to existing theories of point defect production during plastic deformation. The major recovery processes in the irradiated and cold-worked niobium are very similar and it is suggested, therefore, that both these processes and that in tantalum are due to the migration and annihilation of vacant lattice sites created, in the case of cold-worked specimens, by the movement of dislocations. The difference, by a factor of 3, between the resistivity changes in the recrystallized niobium and tantalum could mean that the same difference exists between the resistivities of vacancies in the two metals. The substantial recovery observed above about 250°C in the more heavily cold-worked specimens is almost certainly due to the relaxation and regrouping of dislocations, a great number of metastable arrays of dislocations having been produced during plastic deformation.

(vi) The results obtained in this and other investigations on niobium, molybdenum, tantalum and tungsten indicate that the activation energy for vacancy migration, or Stage III recovery, in the body-centred cubic transition metals is a smaller proportion of the self-diffusion activation energy than it is in the face-centred cubic metals. Since for all metals, irrespective of crystal structure, a linear relationship exists between

melting temperature and self-diffusion energy, this means that it requires relatively more energy to create but relatively less energy to move a vacancy in the body-centred lattice. This presupposes, of course, that self-diffusion in these metals is by a vacancy mechanism, (it is fairly well established that this is the case in the face-centred metals), and that an analogy between Stage III recovery in metals of different crystal structure is admissible. Recent calculations by Shaw[53] on the formation and migration energies, E_f and E_m, of the vacancy in the body-centred cubic transition metals suggest that these assumptions are correct, since the calculated values of E_m and $E_f + E_m$ agree reasonably well with the experimental values of E_m and E_d, the self-diffusion energy which, of course, should be equal to the sum of E_f and E_m if a vacancy mechanism is operative.

SUGGESTIONS FOR FUTURE WORK

A quantitative interpretation of the experimental data provided by this investigation is made difficult for several reasons. Firstly, the nature and extent of the damage produced by pile irradiations are not known with any certainty; secondly, the theory of point defect production by plastic defprmation is in a very unsatisfactory state; thirdly, the relatively high irradiation and deformation temperatures employed enabled a considerable amount of thermal annealing to take place and, fourthly, the effect, on the migration of point defects, of the high concentrations of impurity atoms present can only be treated qualitatively. Some of the more important experimental and theoretical studies which would assist interpretation and also provide fundamental data on point defects in the body-centred cubic transition metals are listed below:

(i) Experiments on the electron irradiation of very pure metals at liquid helium temperatures would make available valuable information on the displacement energies of atoms and the electrical resistivities of vacancy-interstitial atom pairs.

(ii) Quenching experiments on very pure metals, if performed satisfactorily, would make possible the determination of the formation and migration enrgies and the electrical resistivities of vacancies, although the concentrations present would only be known within an uncertain entropy factor. As mentioned in the discussion, a certain

amount of controversy exists as to whether Stage III recovery in cold-worked and irradiated face-centred cubic metals is due to vacancies or interstitials. This situation exists because no one has yet performed, on a metal for which there is a reasonable amount of theoretical knowledge, such as copper or gold, satisfactory recovery experiments on quenched, irradiated and cold-worked material. The most reliable quenching experiments have been performed on gold, for which no satisfactory irradiation experiments have been carried out and no one has yet successfully quenched copper, which has received by far the greatest attention both from the theoretical and from the irradiation and deformation points of view. Until these critical experiments have been performed it will be impossible to say, with complete certainty, that Stage III recovery is due to vacancies, as is generally believed. This situation will also exist for the body-centred transistion metals until quenching experiments have been carried out. In these metals, however, there is the added difficulty that it is by no means certain that a large difference exists between the formation energies of vacancies and interstitials, which would ensure an overwhelming preponderance of vacancies at high temperatures. In addition to the usual resistivity measurements, therefore, it would be profitable to carry out both high and low temperature density and lattice parameter determinations, which would help in the interpretation of such experiments.

(iii) The plastic deformation of very pure metals at temperatures low enough to freeze in all the lattice defects produced would enable

a comparison to be made between theory and experiment as to the concentrations of point defects and dislocations generated during plastic flow. The difficulty of separating the effects due to dislocations from those due to point defects could be overcome by carrying out recovery experiments and also by making both electrical resistivity and magnetoresistivity measurements, as suggested by van Bueren[10]. The latter property is only effected by the presence of defects that produce anisotropic strain fields, such as dislocations and possibly interstitial atoms.

(iv) It would be profitable to repeat the experiments described in (i), (ii) and (iii) on material containing controlled amounts of impurities in order to elucidate the role played by impurity atoms during the migration of point defects.

(v) The interpretation of all the above experiments would be greatly assisted by reliable theoretical calculations on the physical properties of fundamental point defects and point defect clusters. Some of the more important of these would be the determination of the formation and migration energies and the electrical resistivities of single vacancies and interstitials and the binding energies of some vacancy-impurity atom and interstitial-impurity atom pairs.

ACKNOWLEDGEMENTS

The author is indebted to Dr. A. A. Johnson who first suggested the problem and who throughout the investigation provided many valuable and stimulating discussions. The continual interest and encouragement of Professor J. G. Ball are also gratefully acknowledged.

The work was carried out during the tenure of a D.S.I.R. Research Studentship and was financed in the initial stages by the U.S. Navy Department and subsequently by the U.K. Atomic Energy Authority and the Central Electricity Board. Irradiation facilities were provided by Dr. H. M. Finniston and Mr. N. H. Hancock of A.E.R.E., Harwell.

REFERENCES

1. DEKKER, A.J., "Solid State Physics", Macmillan & Co. Ltd., 1958.
2. SEITZ, F., Advances in Physics 1952, 1, 43.
3. HASIGUTI, R.R., Jnl. Phys. Soc. Japan 1953, 8, 798.
4. DAMASK, A.C. and DIENES, G.J., Acta Met. 1959, 7, 818.
5. SEEGER, A.K., 2nd U.N. Int. Conf. Peaceful Uses Atomic Energy, 1958.
6. COTTRELL, A.H., "Dislocations and Mechanical Properties of Crystals", John Wiley & Sons, 1957.
7. FRIEDEL, J., "Dislocations", Gauthier-Villars, 1956.
8. MOTT, N.F., Trans. A.I.M.E. 1960, 218, 962.
9. COTTRELL, A.H., "Vacancies and Other Point Defects in Metals and Alloys", Institute of Metals, 1958.
10. VAN BUEREN, H.G., "Imperfections in Crystals", North-Holland Publishing Co., 1960.
11. MOTT, N.F., Phil. Mag. 1953, 44, 742.
12. SEEGER, A.K., "Dislocations and Mechanical Properties of Crystals", John Wiley &Sons, 1957.
13. KINCHIN, G.H. and PEASE, R.S., Reports on Prog. in Phys. 1955, 18, 1.
14. SEITZ, F. and KOEHLER, J.S., Solid State Physics 1956, 2, 305.
15. DIENES, G.J. and VINEYARD, G.H., "Radiation Effects in Solids", Interscience Publishers, Inc., 1957.
16. LUCASSON, P.G. and WALKER, R.H., General Discussion on Radiation Effects in Inorganic Solids, Faraday Society, Paris, 1961.
17. KINCHIN, G.H. and THOMPSON, M.W., Jnl. Nuc. Energy 1958, 6, 275.
18. LOMER, W.M., Prog. in Metal Physics 1959, 8, 255.
19. COTTRELL, A.H., Met. Revs. 1956, 1, 479.
20. SEEGER, A.K., Proceedings of the Lattice Defects in Noble Metals Conference, Atomics International Report No. NAA-SR-3250, 1958.
21. LOMER, W.M., General Discussion on Radiation Effects in Inorganic Solids, Faraday Society, Paris, 1961.
22. PIERCY, G.R., Phil. Mag. 1960, 5, 201.
23. LOMER, W.M. and COTTRELL, A.H., Phil. Mag. 1955, 56, 711.
24. VINEYARD, G.H., General Discussion on Radiation Effects in Inorganic Solids, Faraday Society, Paris, 1961.

25. DAMASK, A.C., DIENES, G.J. and WEIZER, V.G., Phys. Rev. 1959, 113, 781.

26. BAUERLE, J.E. and KOEHLER, J.S., Phys. Rev. 1957, 107, 1493.

27. KIMURA, H., MADDIN, R. and KUHLMANN-WILSDORF, D., Acta Met. 1959, 7, 145.

28. FRANK, F.C., Symposium on Plastic Deformation of Crystalline Solids, C.I.T. and O.N.R., Pittsburgh, 1950.

29. KUHLMANN-WILSDORF, D., Phil. Mag. 1958, 3, 125.

30. SILCOX, J. and HIRSCH, P.B., Phil. Mag. 1959, 4, 72.

31. HIRSCH, P.B., SILCOX, J., SMALLMAN, R.E. and WESTMACOTT, K.H., Phil. Mag. 1958, 3, 897.

32. SMALLMAN, R.E. and WESTMACOTT, K.H., Jnl. Appl. Phys. 1959, 30, 603.

33. MAKIN, M.J., WHAPHAM, A.D. and MINTER, F.G., Phil. Mag. 1961, 6, 465.

34. WILSDORF, H.G.F., Phys. Rev. Letters 1959, 3, 172.

35. SILCOX, J.,

36. SILCOX, J., Private communication, 1961.

37. SHEININ, S.S. and KERRIDGE, J.F., Private communication, 1961.

38. GEISS, W. and VAN LIEMPT, J.A.M., Zeit. Physik 1927, 41, 867.

39. THOMPSON, M.W., Phil. Mag. 1960, 5, 278.

40. ADAM, J. and MARTIN, D.G., Phil. Mag. 1958, 3, 1329.

41. GRAY, D.L. and CUMMINGS, W.V., Acta Met. 1960, 8, 446.

42. GRAY, D.L., Acta Met. 1959, 7, 431.

43. CHAUDHURI, K.D., MENDELSSOHN, K. and THOMPSON, M.W., Cryogenics 1960, 1, 47.

44. MAKIN, M.J. and MINTER, F.J., Acta Met. 1959, 7, 361.

45. MAKIN, M.J. and GILLIES, E., Jnl. Inst. Met. 1957, 86, 108.

46. WRONSKI, A., Private communication, 1961.

47. DAUTREPPE, D., MOSER, P. and PAULEVE, J., General Discussion on Radiation Effects in Inorganic Solids, Faraday Society, Paris, 1961.

48. MARTIN, D.G., Acta Met. 1957, 5, 371.

49. PEIFFER, H.R., Jnl. Appl. Phys. 1958, 29, 1581.

50. NEIMARK, L.A. and SWALIN, R.A., Trans. A.I.M.E. 1960, 218, 82.

51. SCHULTZ, H., Zeit. Naturforschung 1959, 14a, 361.

52. BROOKS, H., "Impurities and Imperfections", A.S.M., 1955.

53. SHAW, B.J., University of London M.Sc. Thesis, 1960.

54. MEHL, R.F., SWANSON, M. and POUND, G.M., Acta Met. 1961, 9, 256.

55. VASIL'EV, V.P. and CHERNOMORCHENKO, S.G., Zav. Lab. 1956, 22, 688; D.S.I.R., L.L.U., RTS1491.

56. BROOM, T., Advances in Physics 1954, 3, 26.

57. BROOM, T. and HAM, R.K., "Vacances and Other Point Defects in Metals and Alloys", Institute of Metals, 1958.

58. JOHNSON, A.A., University of London Ph.D. Thesis, 1960.

59. CHALMERS, B. and QUARREL, A.G., "The Physical Examination of Metals", Edward Arnold Ltd., 1960.

60. HOLCOMB, D.F. and NORBERG, R.E., Phys. Rev. 1955, 98, 1074.

61. GUTOWSKY, H.S., Phys. Rev. 1951, 83, 1073.

62. NACHTRIEB, N.H., WEIL, J.A., CATALANO, E. and LAWSON, A.W., Jnl. Chem. Phys. 1952, 20, 1185.

63. SLICHTER, C.P., Conference on Defects in Crystalline Solids, Physical Society, Bristol, 1954.

64. NAUMOV, A.N. and RYSKIN, G.Y., Zhuv. Tekhn. Fiziki 1959, 29, 189; Met. Abs. 1959, 26, 899.

65. WAJDA, E.S., SHIRN, G.A. and HUNTINGTON, H.B., Acta Met. 1955, 3, 39.

66. OKKERSE, B., Acta Met. 1954, 2, 551.

67. NACHTRIEB, N.H. and HANDLER, G.S., Jnl. Chem. Phys. 1955, 23, 1569.

68. MILLER, P.H. and BANKS, F.R., Phys. Rev. 1942, 61, 648.

69. SHIRN, G.A., WAJDA, E.S. and HUNTINGTON? H.B., Acta Met. 1953, 1, 513.

70. LIU, T. and DRICKAMER, H.G., Jnl. Chem. Phys. 1954, 22, 312.

71. JAUMOT, F.E. and SMITH, R.L., Trans. A.I.M.E. 1956, 206, 137.

72. SHEWMON, P.G., Trans. A.I.M.E. 1956, 206, 918.

73. SPOKAS, J., University of Illinois Thesis, 1957.

74. KRUEGER, H. and HERSH, H.N., Trans. A.I.M.E. 1955, 203, 125.

75. TOMIZUKA, C.T. and SONDER, E., Phys. Rev. 1956, 103, 1182.

76. NACHTRIEB, N.H., PETIT, J. and WEHRENBERG, J., Jnl. Chem. Phys. 1957, 26, 106.

77. GERTSRIKEN, S.D. and TSITSILIANO, B.D., Physics of Metals and Metallography 1958, 6, 80.

78. KURTZ, A.D., AVERBACH, B.L. and COHEN, M., Acta Met. 1955, 3, 442.

79. MAKIN, S.M., ROWE, A.H. and LECLAIRE, A.D., Proc. Phys. Soc. 1957, 70,545.

80. MEAD, H.W. and BIRCHENALL, C.E., Trans. A.I.M.E. 1957, 209, 874.

81. OKKERSE, B., Phys. Rev. 1956, 103, 1246.

82. NOWICK, A.S., Jnl. Appl. Phys. 1951, 22, 1182.

83. KUPER, A., LETAW, H., SLIFKIN, L., SONDER, E. and TOMIZUKA, C.T., Phys. Rev. 1954, 96, 1224 and correction 1955, 98, 1870.

84. BURGESS, H. and SMOLUCHOWSKI, R., Jnl. Appl. Phys. 1955, 26, 491.

85. HOFFMAN, R. E., PIKUS, F.W. and WARD, R.A., Trans. A.I.M.E. 1956, 206, 483.

86. NIX, F.C. and JAUMOT, F.E., Phys. Rev. 1951, 82, 72.

87. MEAD, H.W. and BIRCHENALL, C.E., Trans. A.I.M.E. 1955, 203, 994.

88. KIDSON, G.V. and ROSS, R., "Radioisotopes in Scientific Research", Vol. 1, Pergamon Press Ltd., 1958.

89. BOKSHTEIN, S.Z., KISHKIN, S.T. and MOROZ, L.M., Metalloved. i Obrabotka Metallov 1957, 2, 2; Abs. Jnl. Met. 1957, abs. no. 15, p. 7.

90. GRUZIN, P.L., Izvest. Akad. Nauk S.S.S.R. 1953 (Tekhn.), 383; Abs. Jnl. Met. 1958, abs. no. 108, p. 45.

91. IVANOV, L.I., MATEEVA, M.P. and KULIKOV, J.S., Akad. Nauk S.S.S.R., Inst. Met. im. A.A. Baikova 1956, 11; Chem. Abs. 1958, 52, 9700i.

92. BORG, R.J. and BIRCHENALL, C.E., Trans. A.I.M.E. 1960, 218, 980.

93, BOKSHTEIN, S.Z., KISHKIN, S.T. and MOROZ, L.M., Zav. Lab. 1957, 23, 316; D.S.I.R., L.L.U., RTS 1490.

94. GRUZIN, P.L., PAVLINOV, L.V., TYUTYUNNIK, A.D. and FEDEROV, G.B., Issledovaniya po Zharoprochn. Splavam, Akad. Nauk S.S.S.R., Inst. Met. im. A.A. Baikova 1959, 5, 155.

95. RESNICK, R. and CASTLEMAN, L.S., Trans. A.I.M.E. 1960, 218, 307.

96. EAGER, R.L. and LANGMUIR, D.B., Phys. Rev. 1953, 89, 911.

97. GRUZIN, P.L. and MESHKOV, V.I., "Problems of Metallography and the Physics of Metals", Chapman & Hall, 1959.

98. BRADSHAW, F.J. and PEARSON, S., Phil. Mag. 1957, 2, 570.

99. PANSERI, C. and FEDERIGI, T., Phil. Mag. 1958, 3, 1223.

100. DESORBO, W. and TURNBULL, D., Phys. Rev. 1959, 115, 560.

101. MCREYNOLDS, A.W., AUGUSTYNIAK, W., MCKEOWN, M. and ROSENBLATT, D.B., Phys. Rev. 1955, 98, 418.

102. QUERE, Y., Compt. Rendu. 1960, 251, 367.

103. MANINTVELD, J.A., Nature 1952, 169, 623.

104. BRADSHAW, F.J. and PEARSON, S., Phil. Mag. 1957, 2, 379.

105. AIROLDI, G., BACCHELLA, G.L. and GERMAGNOLI, E., Phys. Rev. Letters 1959, 2, 145.

106. ECCLESTON, R.R., Jnl. Appl. Phys. 1952, 23, 1400.

107. OVERHAUSER, A.W., Phys. Rev. 1953, 90, 393.

108. ECCLESTON, R.R., Acta Met. 1953, 1, 679.

109. MEECHAN, C.J. and BRINKMAN, J.A., Phys. Rev. 1956, 103, 1193.

110. TAKAMURA, J., Kinsoku-Butsuri (Metal Physics) 1956, 2, 112; referred to by Cottrell[9].

111. NICHOLAS, J.F., Phil. Mag. 1955, 46, 88.

112. SOSIN, A. and BRINKMAN, J.A., Acta Met. 1959, 7, 478.

113. BRADSHAW, F.J. and PEARSON, S., Phil. Mag. 1956, 1, 812.

114. ASCOLI, A., ASDENTE, M., GERMAGNOLI, E. and MANARA, A., Jnl. Phys. Chem. Solids 1958, 6, 59.

115. BACCELLA, G.L., GERMAGNOLI, E. and GRANATA, S., Jnl. Appl. Phys. 1959, 30, 748.

116. SMITHELLS, C.J., "Metals Reference Book", Butterworths Scientific Publications, 1955.

117. ARGENT, B.B. and MILNE, J.C., Jnl. Less Common Metals 1960, 2, 154.

118. DEXTER, D.L., Phys. Rev. 1956, 103, 107.

119. PAXTON, H.W. and GONDOLF, E.C., Arch. Eisenhüttenweisen 1959, 30, 55.

120. BOGDANOV, N.A., Izvest. Akad. Nauk S.S.S.R., Met. i Topl. 1960, (Tekhn.), 99; Met. Abs. 1961, 28, 835.